REPUBLIC OF TURKEY

YILDIZ TECHNICAL UNIVERSITY

GRADUATE SCHOOL OF NATURAL AND APPLIED SCIENCES

SYNTHESIS OF IONIC LIQUID CRYSTAL DENDRIMERS AND INVESTIGATION OF THEIR MESOMORPHIC PROPERTIES

HARUN NEZİH TÜRKÇÜ

PhD. THESIS

DEPARTMENT OF CHEMISTRY

PROGRAM OF ORGANIC CHEMISTRY

2015

Istanbul

REPUBLIC OF TURKEY

YILDIZ TECHNICAL UNIVERSITY

GRADUATE SCHOOL OF NATURAL AND APPLIED SCIENCES

Synthesis of Ionic Liquid Crystal Dendrimers and Investigation of Their Mesomorphic Properties

A thesis submitted by Harun Nezih Türkçü in partial fulfillment of the requirements for the degree of **PHILOSOPHY OF DOCTORATE** is approved by the committe on 10.04.2015 in Department of Chemistry, Organic Chemistry Program.

Thesis Adviser

Prof. Dr. Metin TÜLÜ
Yıldız Technical University

Approved by Examining Committe

Prof. Dr. Metin TÜLÜ
Yıldız Technical University ----------

Prof. Dr. Belkıs BİLGİN-ERAN
Yıldız Technical University ----------

Assoc Prof. Mehmet Altun
Istanbul University ----------

Prof. Dr. Tarık EREN
Yıldız Technical University ----------

Prof. Dr. Yeşim HEPÜZER GÜRSEL
Istanbul Technical University ----------

This study was financially supported by Yıldız Technical University Scientific Research Project Coordination Department (BAPK) with Project no: 2013-01-02-DOP02.

ACKNOWLEDGMENTS

I would like to express my gratitude to my supervisor Professor Metin Tülü and Professor Belkız Bilgin Eran for their supervision and help. In addition, I owe a debt of gratitude to Dr. Hale Ocak for her tedious work on POM and other stuff.

I would like to add special thanks to Yıldız Technical University Scientific Research Project Coordination Department (BAPK) for financial supporting my thesis with the project no: 2013-01-02-DOP02.

In addition, I would like to thank my lab-mates, Ali, Zafer, Mustafa and Mehmet. Moreover, I am indebted to my friends, Sönmez, Cemil, Erkan, Taner, Emre, Recep, Baki and Can.

I am particularly indebted to my wife, my mother and my Father.

TABLE OF CONTENTS

LIST OF SYMBOLS

^{13}C NMR	Carbon Nuclear Magnetic Resonance Spectroscopy
DSC	Differential Scanning Calorimetry
^{1}H NMR	Proton Nuclear Magnetic Resonance Spectroscopy
FT-IR	Fourier Transform-Infrared Spectroscopy
J	Joule
mg	Milligram
min.	Minutes
ml	Milliliter
nm	Nanometer
POM	Polar Optical Microscopy
ppm	Parts per million
TGA	Thermal Gravimetric Analysis

LIST OF ABBREVIATIONS

C8	4-(Octyloxy) benzoic acid
C12	4-(Dodecyloxy) benzoic acid
C8-BP	4-(4-Octyloxyphenyl) benzoic acid
C10*BP	4'-(3S)-3, 7-dimethyloctyloxy-4-biphenylcarboxylic acid
C12-BP	4-(4-Dodecyloxyphenyl) benzoic acid
DAB	Diaminobutane
DCC	N,N'-dicyclohexycarbodiimide
EDA	Ethylene diamine
G	Generation
LCD	Liquid Crystalline Dendrimer
MA	Methyl acrylate
MW	Microwave
N	Nematic
PAMAM	Poly(amido) amine
PPI	Polypropylene imine
S-CBA	S-4-Citronellyoxy benzoic acid
SmA	Smectic A
SmC	Smectic C
SmX	Smectic X

LIST OF FIGURES

LIST OF TABLES

ABSTRACT

SYNTHESIS OF DENDRITIC IONIC LIQUIDS

Harun Nezih Türkçü

Organic Chemistry Division
Department of Chemistry
PhD.Thesis

Adviser: Prof. Metin Tülü

Dendrimers are highly branched, multi-functional and monodispersed macromolecules. Due to their unique properties, many application fields utilize them. The field of liquid crystalline, which has become dominant in our modern life for a couple of decades, has started to utilize dendrimers at the level of research interest. In the literature, by changing interior architecture of dendrimer or addition of pro-mesogenic or non-mesogenic units onto the exterior of dendrimer, various studies have been performed.

In our study, new sets of dendritic ionic liquids have been synthesized. When synthesizing them, amine terminated PAMAM, PPI, trimesic acid core amidoamine dendrimers have been firstly synthesized or purchased. In addition, various types of pro-mesogenic alkoxy-benzoic acids are attached onto periphery of dendrimer via electrostatic interaction. Longer and shorter alkoxy chains of acids are investigated.

Ionic synthesis is checked by FT-IR and NMR spectroscopy. Mesomeric characterization is performed by POM and DSC studies. The great majority of these

salts have gained large mesomeric range. To see the difference between ionic and covalent attachment onto the periphery of dendrimer, PPI based new macromolecules have been synthesized. These molecules are characterized by FT-IR, NMR, POM and DSC.

Keywords: PAMAM, PPI, Dendrimer, Liquid Crystal, Liquid Crystalline Dendrimers.

ÖZET

DENDRİTİK İYONİK SIVILARIN SENTEZİ

Harun Nezih Türkçü

Organik Kimya Anabilim Dalı
Kimya Bölümü
Doktora Tezi

Danışman: Prof. Metin Tülü

Dendrimerler çok dallı, çok fonksiyonlu ve tek saçılmalı (monodisperse) büyük moleküllerdir. Kendine ait özellikleri sebebiyle, pek çok uygulamam alanı bu yapılardan faydalanmıştır. Son dönemde gündelik hayatımızda önem kazanan sıvı kristal alanında da dendrimerler araştırma seviyesinde kullanılmaya başlanmıştır. Literatürde dendrimerin iç mimarisini değiştirme ile ve mezojenik olan veya mezojenik olmayan yapıları dendrimerin dış yüzeyine ekleme üzerine çeşitli çalışmalar yapılmıştır.

Bizim çalışmamamızda, yeni dednritik iyonik sıvı kristaller sentezlenmiştir. Bunların sentezi esnasında, amin sonlu PAMAM, PPI ve trimesik asit çekirdekli amidoamin dendrimerler satın alındı veya sentezlendi. Bunun dışında, çeşitli promezojenik alkoksi benzoik asitler dendrimerin dış cephesine elektrostatik etkileşimle bağlanmıştır.

İyonik sentez FT-IR ve NMR ile takip edilmiştir. Mezomerik karakterizasyon ise POM ve DSC çalışmaları ile yapılmıştır. Sentezlenen tuzların büyük bir kısmı geniş mezomerik aralığa sahiptir. Dendrimerin yüzeyine iyonik ve kovalent bağlanma arasında ki farkı görmek için, PPI temelli yeni makromoleküller sentezlenmiştir. Bu moleküllerin karakterizasyonu ise FT-IR, NMR, POM ve DSC ile yapılmıştır.

Anahtar Kelimeler: PAMAM, PPI, Dendrimer, Sıvı Kristal, Sıvı Kristal Dendrimerler

CHAPTER 1

INTRODUCTION

1.1 Literature Review

Studies on Liquid Crystalline Dendrimers (LCDs) have been started to become popular since early 1990s. Dendrimers have become good opportunity on the Liquid Crystal field [1] like many other fields [2] such as medical, environmental, electronics optoelectronics and material Sciences. Properties of dendrimers such as well-defined structure and wide varieties of functionality are the main reasons of the popularity [3]. Another advantage of dendrimers is amplifying of function of a single molecule by ordered macromolecular entities [4]. Particularly, by even small changes in the exterior part of the dendrimer but also interior parts, mesomorphism can be managed at the extent of great variety [5].

Silicon containing [6-7], PAMAM [8-9], PPI [10-14], polyether [15-16] and polyester [17-18] based dendrimers were commonly used for LC field. In addition, specific dendrimers containing mesomeric parts as repeating units become an example [19]. Generally, when dendrimers offer stable scaffold, mesomeric building blocks as terminal unit become determined to what type of mesophase appears. The system, composed of these two parts, is incompatible due to different chemical nature. For this reason, this macromolecular arrangenment is sometimes called block molecules. In addition, this state brings microsegregated chemical environments. By this way, fruitful

and versatile molecular engineering arise when synthesizing dendritic liquid crystalline molecules.

Due to presence of amide bonds in the PAMAM causing more hydrogen bonding possibility, ther interior of PAMAM is more rigid compared to PPI [20]. This situation causes more thermodynamically stable in the favor of PAMAM. Similarly, other types of dendrimers as a scaffold play a different role in the system.

Regarding nature of mesogenic unit, such as polarity, functional group, including aromatic moiety or not, shorter or longer haydorcarbon chains (alkyl or alkoxy), various types of mesomorphism were demonstrated. Although mesogenic parts are generally carboxylic acid derivatives, sometimes sulfate ended groups can be a good candidate for these studies [21].

Calamatic (rod-like) mesogenic units bring dendrimer into being liquid crystalline dendrimer having nematic, smectic or cholesteric mesomorphism (calamatic) [22-23]. However, disc-like mesogenic units bring the same molecules into being dicotic liquid crystalline dendrimers. For example, an aromatic moiety attached to one-chain hydrocarbon chain (alkyl or alkoxy) can develop calamatic type mesophases. Depending on the longevity of hydrocarbon chain, mesophase phase can be nematic or smectic. By introducing chiral point(s) in attached unit [24-25], liquid crystalline dendrimer can gain smectic C*. In addition, codendrimer synthesized by various rate of different types of mesogenic part can alternate form one calamatic type mesophase to another [25-26]. If an aromatic moiety with two or three terminal chains [27], liquid crystalline dendrimer have discotic type mesomorphism such as cubic, columnar hexagonal, columnar rectangular etc. In addition, exceptions are observed by increasing of generation of dendrimer. An aromatic moiety with only one terminal chain can gain columnar type mesomorphism. However, generally, the generation of dendrimer is not play a deciding role for mesomorphism type and range. If one desires to learn the function of dendrimer in those systems, main role is attributed to scaffold or port habiting many mesomeric molecules due to its inherent multifunctionality.

Generally, an attached unit has mesomeric property. A dendrimer having possibility of binding many molecules can multiply this mesomeric property to higher state. However,

an attached unit like alkanoic acids without mesomeric property can demonstrate mesomorphism by reacting dendrimers [28]. This is explained by microsegregation phenomena which is widely utilized and established for synthesizing of liquid crystalline dendrimers.

Between 1990 and 2000s, liquid crystalline dendrimers were synthesized by covalent route [29-30]. Since 2000s, due to practical advantages, ionic pathway has been commonly used for synthesizing LCDs [30-31]. For this practical pathway, choosing appropriate dendrimer and mesogenic units (sometimes even non-mesogenic units) play an important issue. By the way, tedious synthetic procedures, purification steps are ignored.

For dendritic systems, promesogenic units are strictly congested in the three dimensional geometry of the system. Other conventional liquid crystalline molecules cannot have properties of dendritic liquid crystalline molecules. Microsegregation is phenomena to explain the source of LC state. There are two parts, hard and soft which are separated from each other. Hard part is resulted from dendrimer due to its own hydrogen bonding or other close intra-molecular attractions in the core and branch fragments. Soft part is coming from alkyl chain of mesogenic or non-mesogenic unit. Shibaev [33] summarized that while dendrimer part contributes to entropic factor due to spatial distribution a dendrimer in space, the bundle of rod-like mesogens contribute enthalpy factor by anisotropinng phase. Later, he added in the same article that the structure formation should be resulted from microsegregation by self-assembling of rod-like mesogenic units. Tschierske [34] demonstrated that increasing of fluorine content in alkyl chain of pentaerythritol tetrabenzoates caused intramolecular contrast resulting in microsegregation. In his study, non-fluorinated hydrocarbon derivative has just monotropic, fluroinated and semi-flurinated ones have wide range enantriopic columnar hexagonal mesophase. By increasing incompatibility (increasing of polar fluorine content), mesophase stabilization is only logical reason for expalanation of wide range of mesomorphism. Mezzenga [21] expressed that $C_x > C_8$ is required to observed long-range microsegregation allowing columnar and lamellar mesomorphism for his sulfate molecules.

1.2 Objective of Thesis

This dissertation focuses on sysnthesizing macromolecular dendritic ionic liquid composed of dendrimers as cationic part and mesogenic aromatic benzoic acid derivatives as anionic part. This thesis is concentrated mainly on ionic interaction of these tow counterparts. Also, covalently connected dencritic macrosystems is another issue of this thesis. Investigation of mesomeric properties of synthesized dendritic ionic and covalent molecules is the most important part of this study by POM and DSC interpretations.

1.3 Hypothesis

Practical advantage of ionic synthesis can allow synthesizing versatile dednritic ionic liquids without any difficulties. Dendrimers, as a member of supramolecular family, have multiplier effect due to multifunctionality. By utilizing this property, by multipliying mesomeric property of anionic part, wide and stable mesomeric range macromolecules can be developed. In addition, phase transitions of dendritic ionic liquids can be tailored to optimal range by using appropriate promesogenic molecule with lower isotropization point.

CHAPTER 2

GENERAL INFORMATION

2.1 Introduction to Dendrimers

Dendrimers are hyperbranced repetitive macromolecules. Etymology of the word "Dendrimer" is rooted from the composition *dendron* and *meros*. In Greek language, *dendron* means "tree" and *meros* refers to "part". The other less pronounced names of dendrimers are "*arborols*" and "*hyperbranced polymers*". Similarly, the meaning of "arborol" refers to "tree" in Latin dictionary. Actually, the three dimensional shape of dendrimer structures quite resembles a tree with many branches. The tree-like macromolecules are mainly generated from addition of molecules with functional groups into a small molecule (inner core) with functional groups and the extension of the molecule by the same logic step by step. Historically, in 1978, Vögtle and his coworkers firstly synthesized cascade macromolecules. In 1985, Tomalia and Newkome independently introduced symmetric different types of cascade dendritic macromolecules. In the years that followed, dendrimers have found wide area in polymer science [35-37]. Unaccountable number of papers and books has been published [38]. Upcoming years, the exponential increasing of curiosity on dendrimers is expected. In addition, commercial dendrimers have been sold in market such as poly(amidoamine) (PAMAM or Starburst^{TM}), polypropyleneimine (PPI), phosphorous dendrimers. The reason behind the curiosity and vigorous work is unique properties of

dendrimers. The main ones can be counted as monodispersity, maximized telechelic (reactive end groups) property, globular, compact, regular structure. In addition, structure control and solubility in both aqueous and non-aqueous solvents are other advantages.

2.2 Physicochemical Properties of Dendrimers

Macromolecular phenomena established its basis around 70 years ago. Scientists have classified synthetic polymer family according to three types (linear, cross-linked and branched polymers). These traditional polymers cannot be synthesized in the structural control manner. Hence, those macromolecules are highly polydispersed. Around 30 years ago, dendrimers are accepted as a member of macromolecule family as depicted [36] in Figure 1.Owing to structural control synthesis of dendrimers, they have quite distinctive and different properties than other members of macromolecules. These properties are monodispersity, compact size, multifunctionality at periphery and lower hydrodynamic volume [35-40].

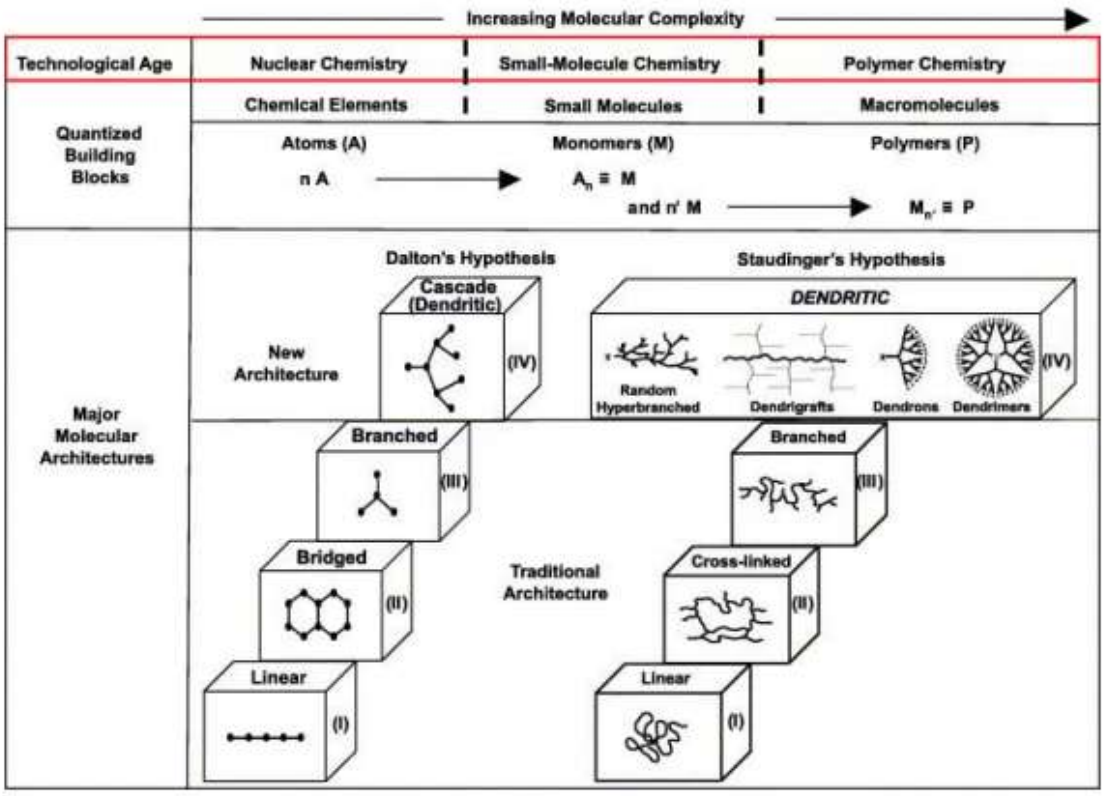

Figure 1: A comparison complexity as a function of molecular architecture, strategy, quantized building blocks and technological age.

When dendrimers compared to proteins, molecular dimensions of both are comparable. In addition, electrophoretic properties and responsive behaviors of dendrimers against pH, temperature, ionic strength associates dendrimers as artificial proteins. Nowadays, numerous studies have been performed mimicking for proteins [35, 41-42]. However, proteins become more compact than dendrimers. For example, as shown in Table 1, when ovalbumin and G4 PAMAM have close diameter sizes, medium size ovalbumin has three times more molecular weight than G4 PAMAM. Similar case is observed for β- Lipoprotein which has about 2.7 times molecular weight than G10 PAMAM, despite two have similar dimensions. Moreover, while the cavities are more common in dendrimer interiors, high dense media is observed in the protein. In addition, covalently fixed and large number of branching points in dendrimer architecture make dendrimer less flexible compared to structures of proteins. Whereas dendrimers have homogenous interior, the interior of proteins have hydrophobic and hydrophilic regions which are usually unexpectable [35, 41-42].

Table 1: Several examples of dendrimer&protein in terms of size and molecular weight

Name	Diameter	Molecular Weight
A Medium Size Dendrimer (G4 PAMAM)	4.5nm	14,215
A Medium Size Protein (Ovalbumin)	5nm	43,000
A Large Protein (β-Lipoprotein)	~15-16nm	2,663,000
A Large Dendrimer (G10 PAMAM)	13.5nm	934,720

Despite more detailed structural descriptions for dendrimers, there are three main structural parts, which are core, interior, and surface, as described [35] in Figure 2.

Core: The core of dendrimer is a starting functionalized molecule, such as ethylene diamine (EDA), 1,4-diaminobutane (DAB), aromatic groups like trimesic acid. The core of dendrimer, especially by increasing of generation, has been separated from the surface groups and created its own microenvironment.

Interior: It is composed of shells and homostructural from center to periphery. This part is dominantly spherical and hydrophobic. The creation of microenvironment is similar to core part as generation of the dendrimer increases.

Surface: The functional terminal groups (amine, carboxylic acids etc.) are settled in the outer shell of dendrimers. The chemistry of surface part is different from interior and core part. For example, the polarity of functional groups makes a polar surface and then the molecule becomes a proccessable in aqueous environment.

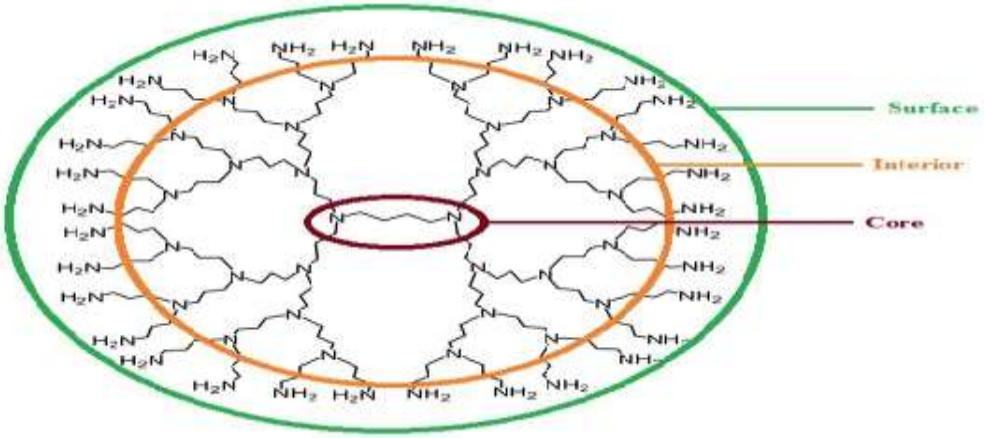

Figure 2: Core, Interior, Surface Regions of diaminobutane based PPI dendrimer

In addition, the term *generation* is used to describe dendrimer designs. The layer is called generation between consecutive two branching points (focal point). In the core part, there is no focal point, and then it is named as G0. In the fourth generation, there are four focal points and called G4. Figure 3 depicts five generations (from G0 to G4) of PPI dendrimer. Moreover, half generations (carboxylate ended) and full generations (amine ended) of PAMAM dendrimer are represented in Figure 4.

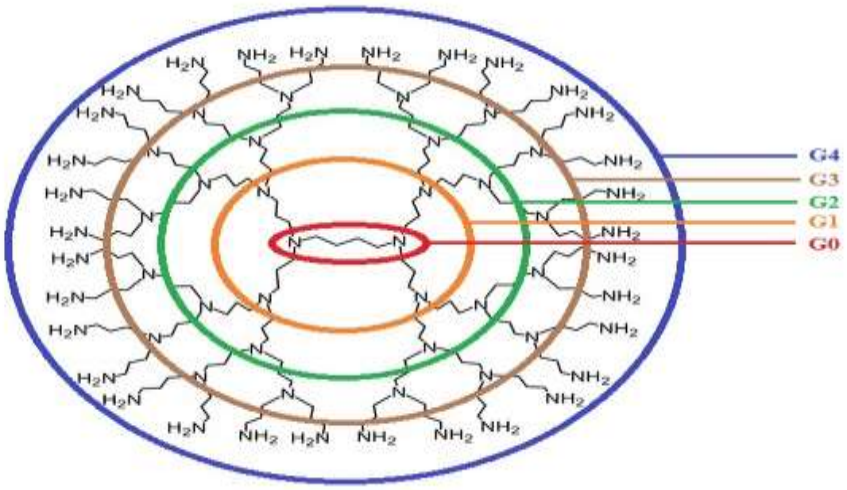

Figure 3: G0-G4 generations of PPI dendrimer

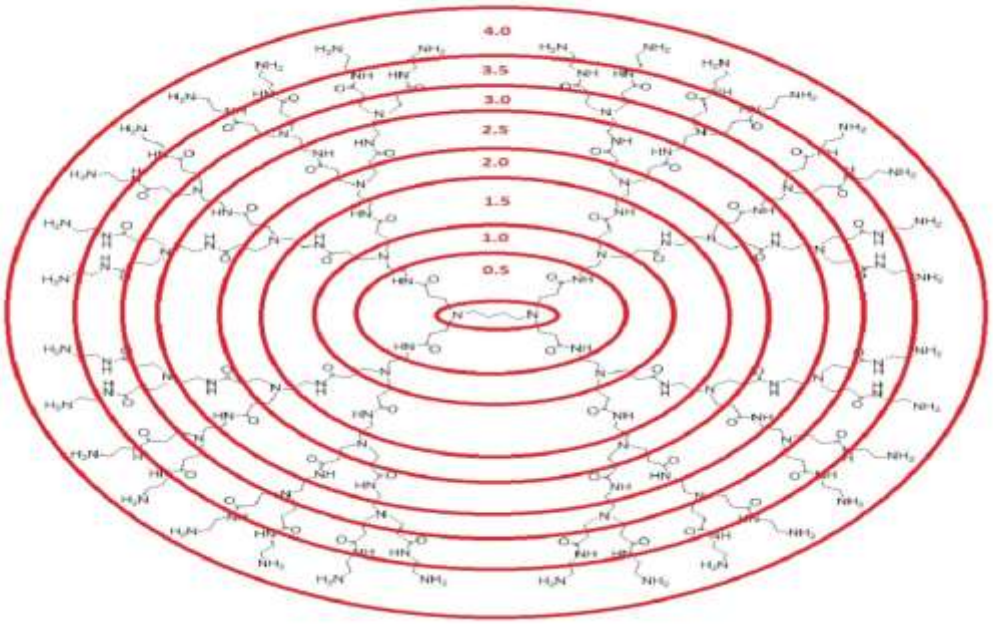

Figure 4: Half and full generations of PAMAM dendrimer

2.3 Synthesis of Dendrimers

Divergent Method: Synthesis begins with a core molecule terminated functional groups and then propagates to outer shell by addition of reactant with functional groups [43-45]. This method is commonly (commercial and research based) used for synthesizing of PAMAM and PPI dendrimers. For synthesizing PAMAM dendrimers, using Michael addition reaction, methyl acrylate is added in to amine terminated molecule such as ethylene diamine. Next step is addition of amine terminated molecule into ester ended molecule. Iteratively, higher generations are built from core to outer shell layer by layer. In PPI dendrimers, repetitive double alkylation reaction of the amine ended groups with acrylonitrile by Michael addition is other example of divergent synthesis. Although this method is very common, the purification of byproducts is more difficult due to high number of extra addition of reactants and imperfect final dendrimers.

Convergent Method: Synthesis begins at outer shell and propagates to inner core [46-47]. In this methods, reactive site remains as low as possible. The core part of dendrimer is deactivated until joining of two dendritic fragments at final step. This method allows better control of dendritic units and lower rate of imperfect dendrimers. These advantages bring better monodispersity compared to divergent type synthesis. However, steric hindrance along the core at final reaction prevents the popular usage of this method. Schematic representation of two methods [48] is shown in Figure 5.

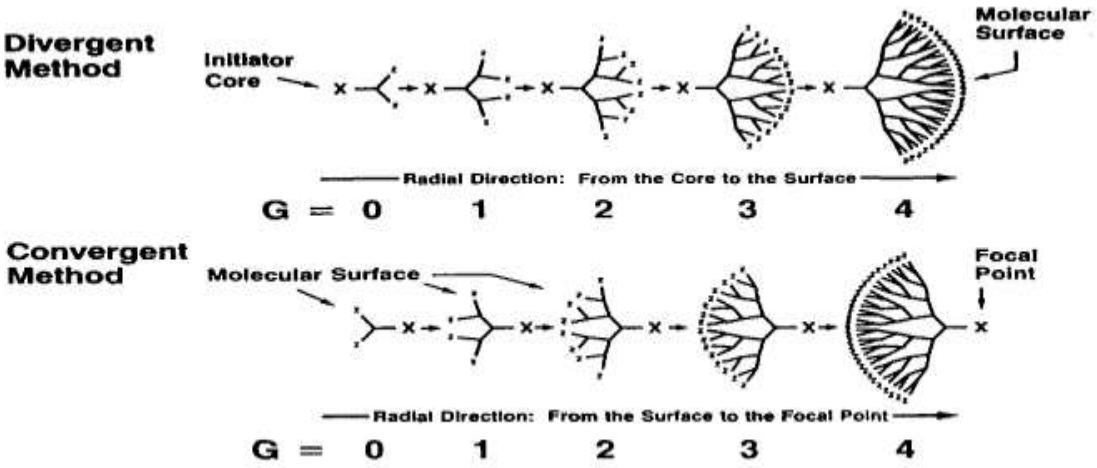

Figure 5: Divergent and convergent methods of dendrimer synthesis [48]

2.4 Application Fields of Dendrimers

Sensors: Dendrimers have started to play an important role in sensor field at the state of academic curiosity more than ten years. A couple of examples of application of dendrimers in the sensor field are expressed below. Fabricating of CdS-PAMAM Quantum-Dots onto gold surface by electrodeposition gives successful results for detecting dopamine [49]. For nitrite detection, Ag-PAMAM electrode is used [50]. Au-PAMAM modified surface is used as an imminosensor for detecting cancer biomarker [51]. PPI based films deposited on indium tin oxide (ITO) plates are used for pH sensor [52]. Au-PPI nanoparticles are used for determining vapor of toluene, 1-propanol and water. Especially, increasing generation of PPI dendrimer gives better results for toluene and 1-propanol due to better solvation of solvents [53].

Drug Delivery: Dendrimers are novel carriers of active substances to reach them to desired address which is low pH region cancer cells love. In drug carrier systems, dendrimer as a host is desired to release anticancer drugs when contacting an acidic media. A bundle of research studies is given below how dendrimers are powerful tool. Practically insoluble niclosamide molecule is converted to aqueous soluble complexes via interaction with amine terminated PAMAM. This study shows that these complexes are much more stable and controllable than cyclodextrin [54]. Novel pH responsive PEG attached PAMAM based dendrimers are used for encapsulation and delivery of 5-fluorouracil which is used for tumor therapy [55]. Doxorubicin-PAMAM attached liposomes have better incorporation and low release ratio of doxorubicin molecule. This work illustrates that this liposome-complex has promising results to cure cancer cells [56]. Beclometasone dipropionate, hydrophobic anti-asthma drug, is interacted with different generations of PAMAM via hydrogen bonding in the cavities or surfaces of dendrimer. Nebulizer studies concluded that the sustainable release of stable complexes is significantly observed [57]. As a last example, indomethacin is loaded into the PEGylated PAMAM dendrimers having thermosensitive properties enabling more controlled release. In this study, PEGylation is another issue to improve dendrimer-drug complexes in terms of undesired toxicity and short circulation time of blood [58]. More than thousands of papers have been published about drug-dendrimer nanocarriers.

Magnetic Resonance Imaging (MRI): This new emerging area of dendrimers has started to attract scientists. A brief of examples is mentioned shortly. Encapsulating Gd-chelates, having contrasting agents, by glycerol modified PPI dendrimers is studied. In

this study, choosing of suitable lipophilic chelate accommodates well hydrophobic core of PPI [59]. Polyester based biodegradable dendrimers are synthesized to target tumor in magnetic resonance. Synthesized molecules have significantly high contrast rate for imaging. In addition, degradability of these molecules at physiological pH range is a significant advantage [60].

Environmental Concerns: Like fields mentioned above, dendrimers have found themselves as collector of contaminants in the environmental technologies. A couple of examples are briefly mentioned below. Stable dispersion properties of PAMAM dendrimers on aromatic and aliphatic hydrocarbons are shown. PAMAM binds crude oil mixtures in water solvent [61]. Discharging of Cu(II) ions from water is succeeded by using PAMAM supported ultrafiltration. The changing pH of PAMAM based aqueous solution is enough to remove metal ions [62]. Another study is realized to remove textile dyes using PPI aqueous. While various types of dye are significantly adsorbed in dendrimer in acidic conditions, those released from PPI at pH=12 [63].

Until now, examples of some fields contributed by dendrimer have been mentioned. Those fields above are not full coverage of dendrimer and dendritic hyperbranced macromolecules incorporated. However, it seems enough to describe versatility of dendrimers.

At this point, liquid crystalline dendrimers, which is relatively new and scientific curiosity area, maybe going to be application area for forthcoming years, has to be mentioned in detail as the subject of this thesis. However, before entering introducing liquid crystalline dendrimers, a brief introduction about liquid crystal (LC) is going to be presented.

2.5 Introductive Information about Liquid Crystal

The term liquid crystal expresses an intermediate state which has fluidity like a liquid and anisotropy like a solid. Reinitzer and Lehmann firstly observed liquid crystalline, mesomeric behavior at the end of 19^{th} century. Later, Vorlander, as an organic chemist at the beginning of 20^{th} century, systematically synthesized various liquid crystalline molecules and established the main strategic routes to obtain mesomeric molecules. Until 1960s, studies had continued as mainly research interest. As shown in Figure 6,

after new LC applications were introduced around 1970s, synthesized molecules were exponentially increased [64].

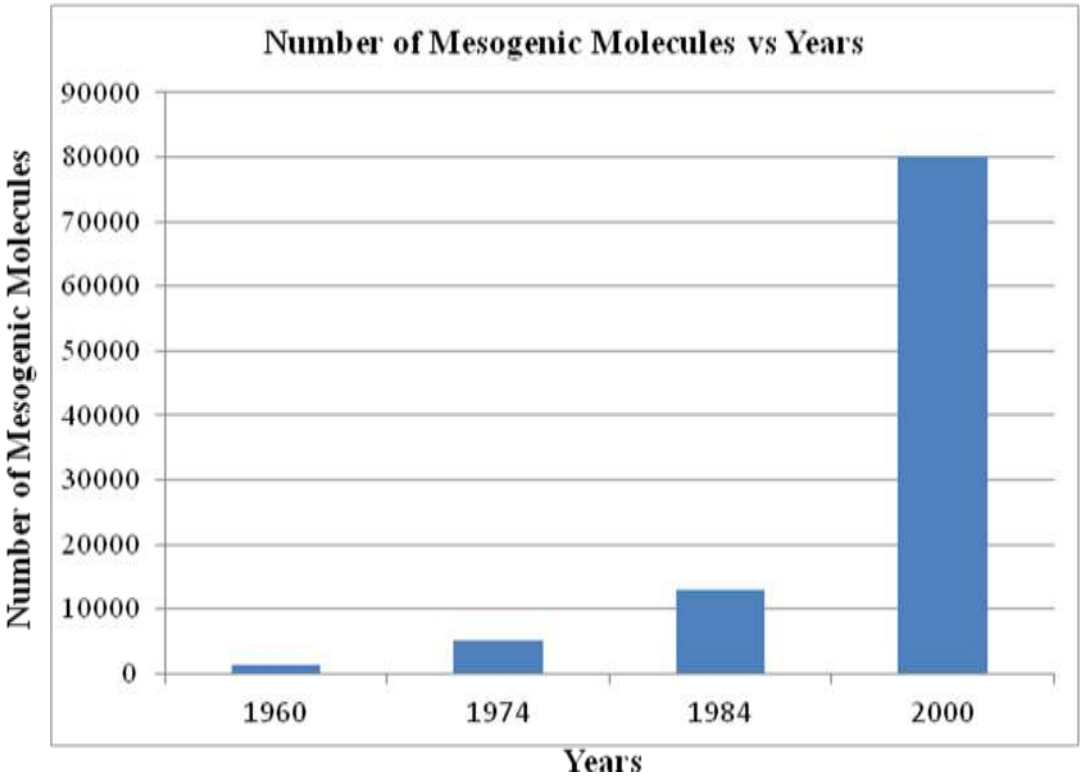

Figure 6: According to years, reported number of mesogenic molecules.

Extrinsically, the formation of mesomeric phase can be realized by an external effect which is solvent or temperature. When lyotropic mesomorphism is formed by presence of solvent, thermotropic mesomorphism is formed by changing temperature. Intrinsically, to demonstrate mesomeric behavior, a molecule has to have geometrically anisotropic conformation which is rod-like or disc-like shape. The components of intrinsic and extrinsic parts must be mutually agreed in a certain degree to observe mesomorphism [64-66].

Lyotropic liquid crystals are made up of two components which are amphiphile (polar end groups and non-polar interior) and water. By increasing water content in the system, various types of mesophase are observed such as lamellar, hexagonal. Since the subject lyotropic liquid crystal is not the issue of this thesis, this short information seems enough [64-66].

Second class of liquid crystal phenomena, thermotropic, has a temperature interval, sometimes delicate, where liquid crystallinity survives. At above the interval, molecule

transforms to liquid state or decomposes. At below the interval, molecule freezes and returns its solid state. Liquid crystal molecules at this temperature range have one or more mesophase [64-66].

Rod-like, *calamatic* molecules, forms three types of thermotropic mesophase, nematic, chlorestic and smectic. The calamatic molecules are main source of LC materials. The typical shape of vast majority of calamatic molecules is shown in Figure 7. There is one or more benzene ring, aliphatic and alkoxy chain. In LC formations, aliphatic unit, flexible part, is separated from rigid core. Number of carbon, *n*, in aliphatic unit plays a critical role forming layer formation and lubrication. For example, for alkyloxybenzoic acids, if *n* is lower than 3 or higher than 18, generally, it cannot form liquid crystal [64-66].

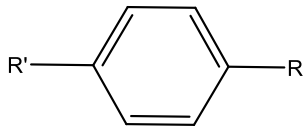

R'	R
C_nH_{2n+1}-	-COOH
C_nH_{2n+1}O-	-NH_2
C_nH_{2n+1}OCO-	-CN
C_nH_{2n+1}OAr-	-NO_2
C_nH_{2n+1}Ar-N=N-	-F
C_nH_{2n+1}Ar-	-CI
C_nH_{2n+1}Ar-CH=N-	-Br
C_nH_{2n+1}Ar-CH=CH-	

Figure 7: A typical structure of a calamatic molecule.

Nematic mesophase is the least ordered and close to the liquid side. It has long-range orientational order but no significant translational order (crystalline order). Figure 6 shows an example of nematic scheme. As shown in Figure 6, molecules are aligned with *n director* in one dimension (1D) at considerable degree of extent. However, there are some fluctuations in *"anisotropic"* order. The S factor describes the degree of parallel alignment, "*"anisotropic order"*. $S=1/2<3\cos^2\theta-1>$

Θ measures the angle between orientational director, *n* shown in Figure 6, and any molecule in the system. The brackets represent average value. If all Θ values of all molecules become zero, S value is going to be significantly high. It means system is going to be highly anisotropic. This rule applies all molecules with Θ=90 which again leads to highly anisotropic state. However, if each molecule has a different angle from

each other, anisotropicity of the system reduces. In this perspective, S value of nematic phase is higher than a liquid and lower than a smectic phase which is going to be described below [64-65].

Cholesteric mesophase, as shown in Figure 8, is similar to nematic phase. In addition, it is optically active and helicoidal shape which are absent in nematic. The spiral shape can be formed by addition of cholesteric substance or addition of chiral but non-LC molecules into nematic system. However, the selective reflection of circular dichroism of cholesteric substance is significantly higher than that of a chiral material. Another issue is that arrangement of molecules in a cholesteric mesophase tends to be changing of director axis in each layer. In this mesophase, molecules do not have long range positional order which is clear property of smectic phase [64-66].

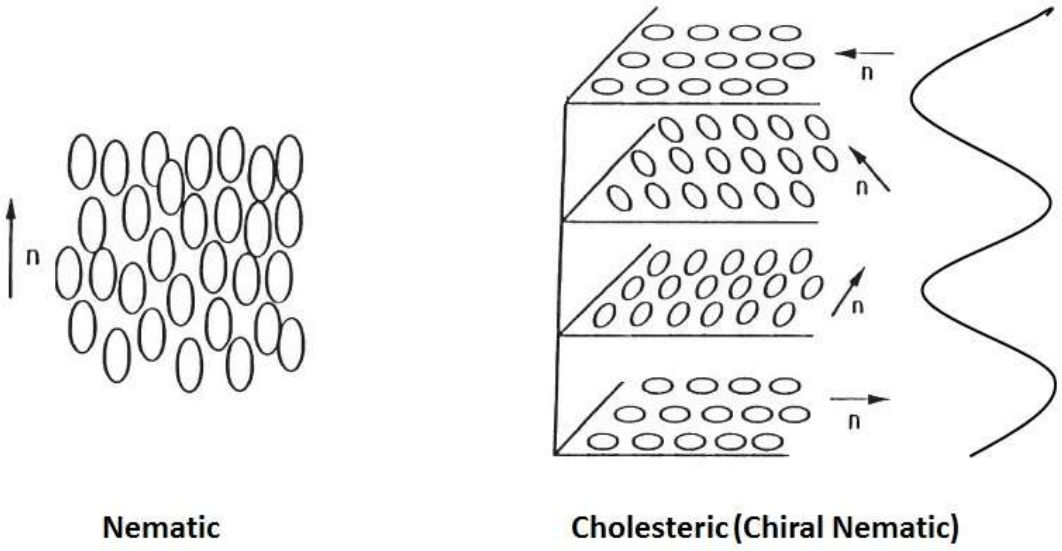

Figure 8: Represenation of nematic and cholesteric phase.

Smectic phases, rooted from "cleaning" in Latin, have lots of variety. Some of them are crystalline such as SmB, SmE, SmG, SmH, SmJ and SmK. They have weak interactions within layers but three dimensional (3D) positional order proven by X-ray studies. Thus, it is called soft crystal. Some of them are very rare hexatic smectic mesophases such as SmB_{HEX}, SmF, SmI. While there is no positional order between layers, there is up to 200 A^0 long-range two dimensional positional order within each layer. Most common smectic liquid crystalline phases are SmA and SmC. Those mesophases have

both orientational order and short positional order (ordered in each layer). Layers are stratified and this state is called lamellar. However, there is no order in lateral distribution (in-plane there is just 10 A^0 order observed, keeping in mind, 10 A^0 is the full length of a typical mid-size linear molecule). For this reason, layers are identified as liquid, and SmA/SmC is sometimes in literature called as "*liquid layer smectics*". Another conclusion is that hexatic smectic LCs demonstrate more intense anisotropicity than positionally-ordered smectic LCs (SmA/SmC). Due to liquidity in layers for SmA and SmC phases, molecules can flow from one layer to another by partial degree of freedom. SmA phase has optical uniaxial domain and less ordered class of smectics. The layer thickness of SmA, similarly SmC, is sometimes shorter than that of an average molecule. This situation is a clear indication of short positional order. Smectic C phase, tilted and slightly more ordered version of SmA phase, is optically biaxial domain. Another extra property of SmC is that addition of chiral molecules leads to spiralization of layers and this state is named as SmC*[64-66].

Figure 9 shows general description of phase transitions and properties of a calamatic based LC system.

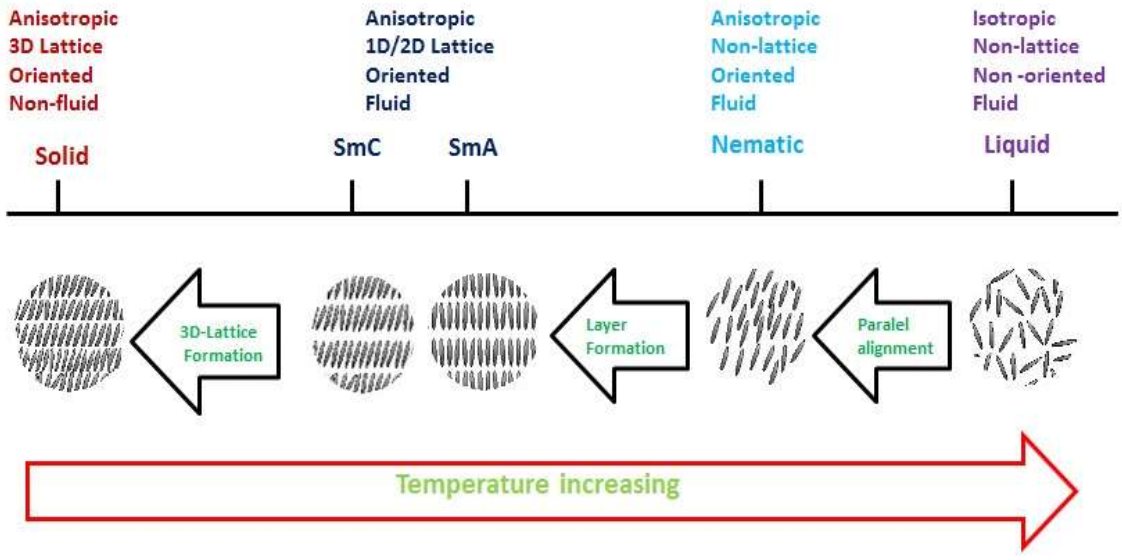

Figure 9: Solid, SmC, SmA, Nematic and Liquid Phases and their basic properties.

Disc-like molecules resemble flat and disc shape as shown in Figure 10. Generally, they have a rigid core such as one or more benzene rings, and a flexible chain for example

aliphatic units. Aliphatic units contributed to the segregation of columns or other structural units by *"greasing or lubrication"* due to amphiphilic interaction. This situation leads to stabilized columns and forms different microenvironments [64-66].

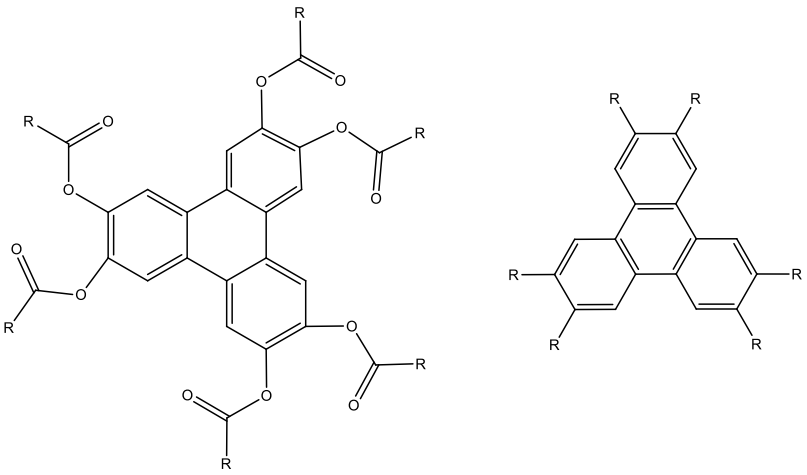

Figure 10: Two representatives for discotic mesogens.

Disc-like molecules form nematic discotic and various columnar mesophases, which are different types of thermotropic LCs as depicted in Figure 11. Except nematic discotic (N_D), three of them (nematic columnar (N_{Col}), columnar rectangular (Col_r), and columnar hexagonal (Col_h)) have two-dimensional positional order. Especially, last three ones have significant anisotropicity [64-66].

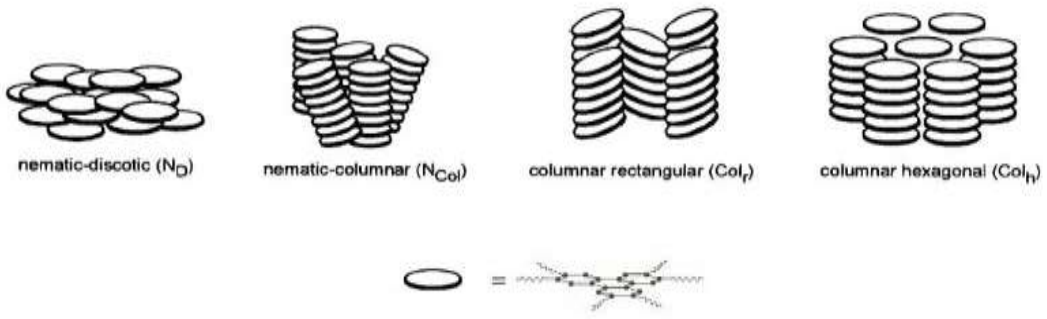

Figure 11: Pictorial drawings of nematic discotic and columnar mesophases.

2.6 Thermotropic Liquid Crystalline Polymers

Upon heating, polymers forms ordered mesophase called thermotropic liquid crystalline polymers (TLCPs). Two subclasses of TLCPs are enantiotropic where mesophase is formed by repetitive heating and cooling loops and monotropic where mesophase is formed by only cooling cycle from liquid form. There are two major thermotropic liquid crystalline polymer classes which are main-chain and side-chain polymers. Two examples from main-chain TLCPs are poly-(hydroquinone terephthalate) and poly-(hydroxyl benzoic acid) shown in Figure 12. These two polymers are quite rigid, and their clearing point is just below decomposition temperature.

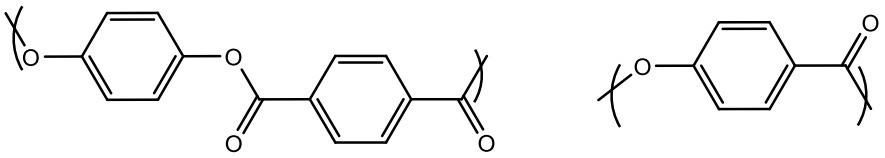

Figure 12: (Left) Poly-(hydroquinone terephthalate); (Right) Poly-(hydroxyl benzoic acid).

Decreasing of rigidity and transition temperatures can be realized by a couple of ways. First one is to add flexible sequences such as $(\text{-CH2-})_n$, $(\text{-CH}_2\text{O-})_n$, $(\text{-Si(CH}_3)_2\text{O-})_n$. Second one is to substitute aromatic units laterally to distort symmetry. Last one is to copolymerization by adding mesogenic units. Side-chain TLCPs are synthesized by addition of mesogenic groups via flexible part into existing polymer backbone. In this addition, flexible sequences such as $(\text{-CH2-})_n$, $(\text{-CH}_2\text{O-})_n$ are required to remove steric hindrance which prevents mesophase formation, because mesogenic units as pendant groups couple each other in the manner of bonding without flexible units. On the other hand, polymer itself plays as an internal lubricator or plasticizer. This case is similar to liquid crystalline dendrimers where the core and interior part of dendrimer lubricate the system. The structure of mesogenic units determines the type of mesophase of the polymer. If rod-like mesogenic unit is attached to polymer backbone, polymer itself is going to have nematic, cholesteric or smectic mesophase. If discotic mesogenic part is coupled to macromolecular, polymer forms columnar mesophase. Similarly, chiral

mesogenic unit produces a polymer with chiral mesophase like SmC*. This case is valid for dendrimers as the member of polymer family [66-67].

2.7 Textures of Thermotropic Liquid Crystalline Polymers

Under microscope, textures of mesomeric polymers are different from that of mesomeric molecules. Properties such as specific textures, fast classification of mesophases and perfectly ordered mesophases are peculiar to polymer. However, various difficulties and limitations are common. The multiphase domain, polydispersity other various properties peculiar to polymer prevent full characterization of phases especially smectic phases in some cases and leads to hesitancy for determining phase. To have better clarification, annealing of polymers overnight is required. However, it cannot solve problem completely in some cases [66].

2.8 Smectic Phases of Thermotropic Liquid Crystalline Polymers

Textures of smectic phases of polymers are commonly obscure due to the reason mentioned above. On the other hand, various textures are similar to focal conic and fan shaped textures of average mesomeric molecules. There are two focal conics which are ellipse and hyperbola in a focal conic zone. From clearing point to the formation of smectic phase, firstly battonets of smectics are encountered and focal conic appears on continuing of cooling. These focal conics can produce fan-shape textures in thin layer. This is sort of a focal conic arrangement where ellipse and hyperbola cannot be differentiated. In addition, several studies illustrate homeotropic and Schlieren textures. To sum up, each texture is peculiar to each LC polymeric system [66].

2.9 Liquid Crystalline Dendrimers (LCDs)

Liquid crystalline dendrimers have become considerable research area due to the fact that thermotropic liquid crystals have playing important role in modern life. The popularity of this topic has significantly increased since 2000. Figure 13 shows the number of reported publications relative to years using related keywords in Sci-Finder.

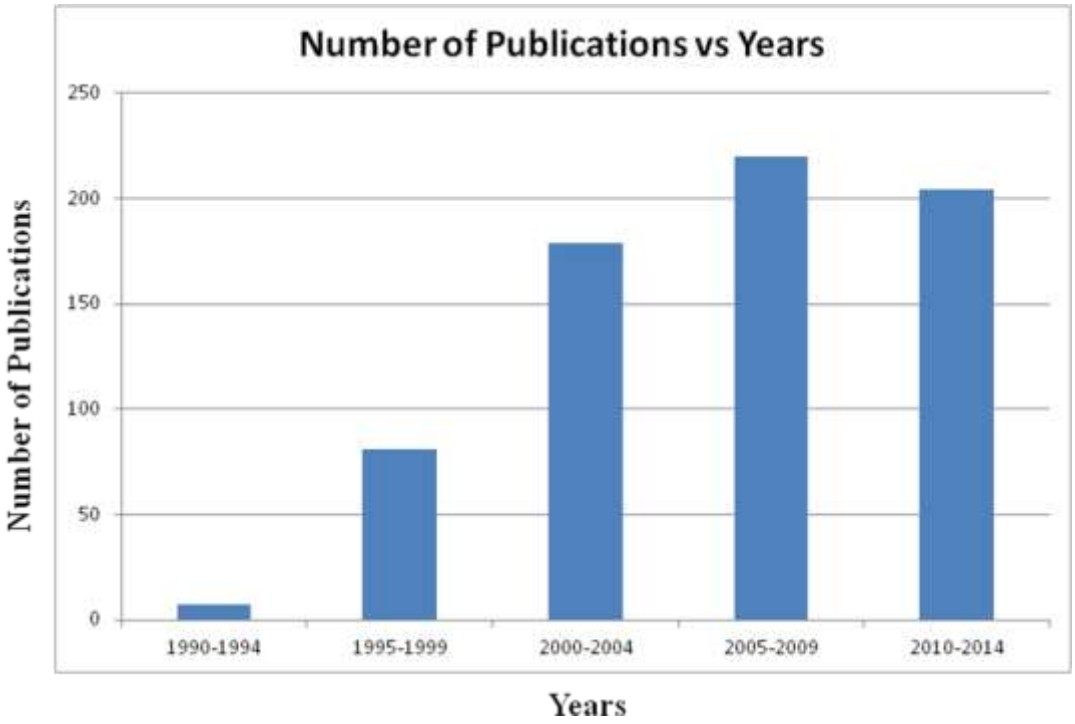

Figure 13: According to years, number of publications in the area of LCDs.

The properties of single molecule can be developed to better state by using well-ordered dendritic matrixes. By manipulating functional groups of dendrimer, mesomeric properties can be tuned at great extent. Two structural categories become common for LCDs. These are main chain and side chain LC dendrimers [68-69], which structurally resembles main chain and side chain LC polymers discussed in the related section above. In the first one, mesogenic unit becomes repeating unit in dendritic scaffold. This type is very rare due to the intrinsic difficulties forming structure. A few examples are introduced by Percec [70], Meier [71], Guillon [72]. Second one is major class of LCDs on which many publications and research efforts are performed. Side chain liquid crystalline systems are composed of two major parts, shown in Figure 14.

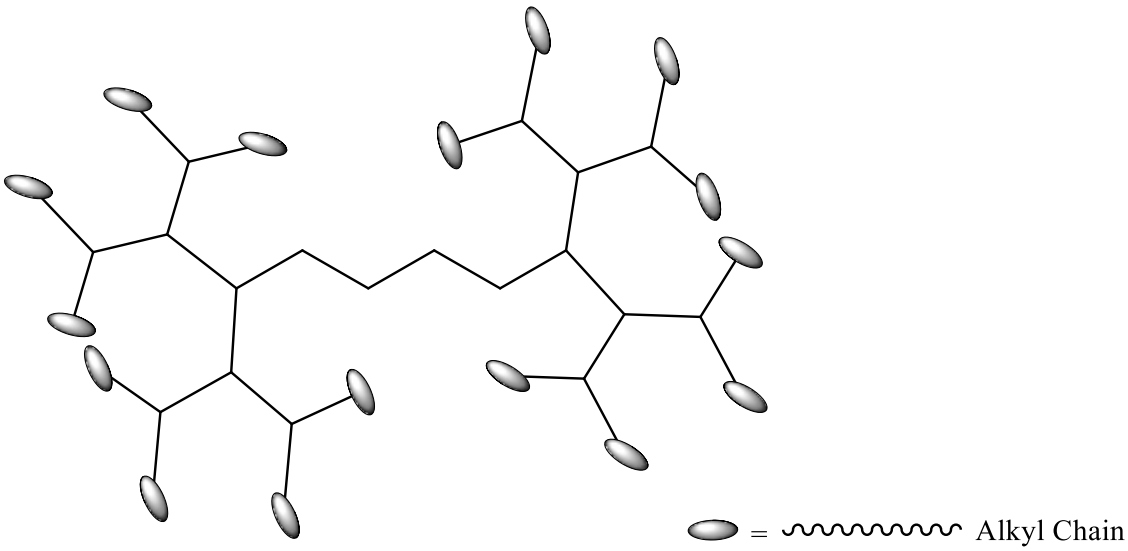

Figure 14: Schematic representation of side-chain LCDs

First one is dendritic core and branches. The dendrimers used in these studies can be listed as polyamidoamine, polypropyleneimine, siloxane, carbosilane etc [68, 69]. Second part is a terminal group which can be commonly mesogenic or seldomly non-mesogenic (such as alkanoic acids). The second part is grafted onto the periphery of first part (dendrimer) via chemical bonding or electrostatic interaction. The attaching of an end group leads to a shift from fully isotropic system of dendritic structure to an anisotropic system [68, 69].

Depending on the length and type of terminal mesogenic unit, nematic, smectic and columnar mesophases are obtained. While short rod promesogenic units favor nematic phase, longer versions of them favor smectic mesophase. If terminal unit has two or more branches, columnar mesophase can be observed. Majority of studies on this area show that LCDs possess lamellar phases which can be described by cylindrical geometric model. In this model, while dendritic molecule has centered on the cylinder, promesogenic units are aligned to parallel each other and located at upper and lower region of cylinder. Then, each cylinder is stacked side by side and up and down. This organization explaining the smectic mesophase is shown in Figure 15 below.

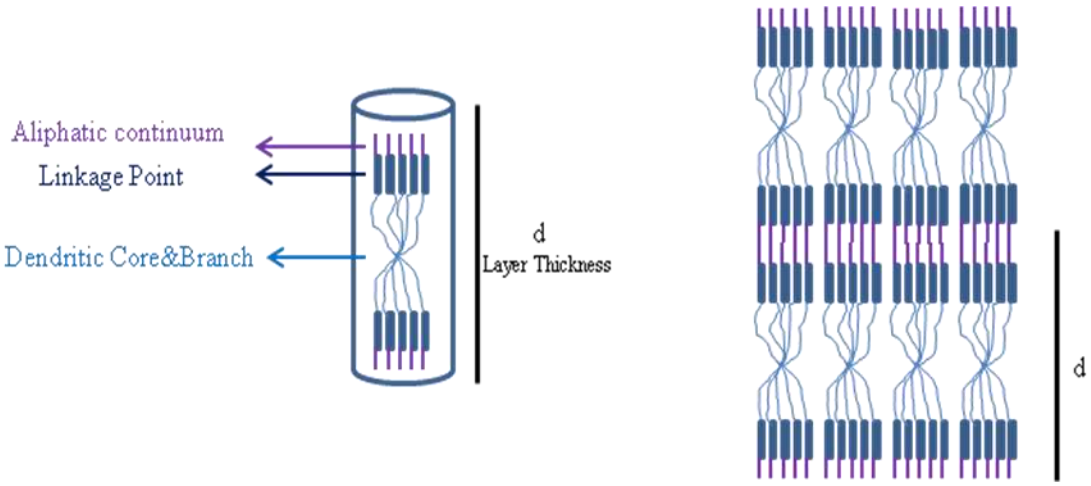

Figure 15: Schematic representation of smectic mesophase of LCDs

The proposed cylindrical figure of LCDs is composed of three major parts, which are dendritic unit, linkage region (amidation, carboxylate bond etc.) and aliphatic (flexible) part. Layer thickness is total measure of these three parts. By increasing of generation of dendrimer, generally, d-spacing does not change appreciably. In the study as an example, d-spacing is only increased from about 52 A^0 for zero generation to about 61 A^0 for fourth generation. However, circular molecular area of cylinder increases from 65 A^2 for zero generation to 1050 A^2 for fourth generation [68]. This can be explained by accommodating much more mesogenic units at periphery due to widening of the structure of the dendrimer along its own circumference.

Covalent linkage of promesogenic units onto the dendritic surface has been highly studied. A bundle from numerous examples is given below to describe what type of mesophase formation occurs how mechanism works. Meijer [73] introduced pentyloxycyanobiphenyl and decyloxycyanobiphenyl into the periphery of various generation of PPI and obtained smectic A mesophase. Decyloxy spacer, longer one, has better mesophase formation and wider temperature range. Lattermann [74] incorporated the 3, 4-bis (decyloxy)benzoyl groups onto the surface of a poly(propylene imine) dendrimer and obtained columnar hexagonal phase.

While Serrano group observed smectic A mesophase [75] by attaching one-chain 4-(4'-decyloxybenzoyloxy) salicylaldehyde into the surface of four generations of PAMAM, they observed columnar mesomorphism [76] by incorporating two-chain 4-(3',4'-

didecyloxybenzoyloxy)-salicylaldehyde into the same dendrimer. Similar comparative observations are reported for diaminobutane based PPI dendrimers [77]. Serrano group, also, performed lateral grafting of pentafluorophenylester to DAB based PPI surface. In this study, nematic and smectic C phases are observed [78]. Series of PAMAM codendrimers were synthesized by alternating number of *one-chain* 4-(4′-decyloxybenzoyloxy) salicylaldehyde and *two-chain* 4-(3′,4′-didecyloxybenzoyloxy) salicylaldehyde. While lamellar phase becomes dominant by high rate *one-chain* codendrimer, columnar mesophase becomes more dominant by high rate *two-chain* codendrimer [79]. By incorporating of discotic triphenylene mesogenic units onto outer surface of PPI dendrimers, while columnar rectangular phase was observed for first generation, columnar hexagonal phase was observed for from second to fifth generation of PPI [80]. Linear azobenzene units attached to the periphery of PPI (16 and 32 amine functional groups) via amidation reaction led to form smectic A mesophase [81].

Ionic thermotropic LCDs have become an important research subject for recent years due to various advantages. Easy preparation is one of the most important advantages due to the simple acid-base reaction. By using this route, tedious synthetic reactions and clean-up works are removed. The formation of mesophase is based on self-assembly of the functional groups of dendrimers by additives. In addition, simple dilution or addition of diluted acid to solvent provides transferring of dendrimer into aqueous solution. Another advantage is that dendrimers can be proccessable in non-polar common organic solvents. By giving several basic examples from literature below, the topic can be much more clearly understood.

Actually, the first studies performed about dendritic ionic system were not generally related about liquid crystallinity. Crooks simply combined fourth generation of PAMAM with dodecanoic acid to make dendrimer proccessable in apolar solvent like heptanes and toluene [72]. In this study, the aim was to transfer hydrophilic methyl orange dye from aqueous solvent to non-aqueous using the binding property of methyl orange to amine terminated PAMAM. The dye performed its phase transfer almost %100 extent at the rate of %10 dodecanoic acid. Another aim was to transfer Pd nanoparticles from aqueous to non-aqueous by using 10-20% dodecanoic acid-G4 PAMAM. The catalytic activity of encapsulated Pd in dodecanoic acid-PAMAM system in toluene solvent is highly effective. In the same year, electrostatic interaction of polyethylene imine with stearic acid and oleic acid by cooling DMF solvent, lamellar

mesophase of comb-like complexes [83]. Later, smectic phases of cholesterol based carboxylic acid-PPI complexes were analyzed. In addition, tertiary protonation of PPI was proved. For low generation of PPI complexes compared to covalent homologues, the lamellar thickness is higher due to the expansion of dendrimeric scaffold by positive charges in the binding sites [84]. Later, Ujiie used the protonation reaction for designing homeotropic smectic A mesophases based on longer alkanoates (*n*=14, 16, 18) by PAMAM ion complexes. However, mesophase formation was not obtained by shorter alkanoates (*n*=10, 12). In the same study, it was interesting to note that the observation of columnar mesophase formation was succeed by extra-added linear stearic acid (*n*=18) by ratio of (carboxylic acid: terminal amine 2.33:1). The proposed explanation is that the protonation of tertiary amine groups arranges the dendrimer in columnar formation [85]. While Serrano [86] group show various lamellar mesophase formation via ionic linkage several types of alkanoic acids for PAMAM and PPI, another study [87] performed earlier could not reach mesomorphism by covalent route for a similar alkanoic acid and PPI. The study [86] show that successive heating cycles cause partial decreasing of transition temperature due the chemical transformation of system and oxidation of amide bond. Another interesting point [86] is that while layer spacing increases by increasing generation of PAMAM-alkanoic acid (*n*=18) complexes, it is independent of generation for PPI-alkanoic acid (*n*=18) complexes. Serrano continued its contributions for LC ionic-dendrimers [88] by addition of mono, di, tri alkoxy connected aromatic groups (promesogenic units) onto the periphery of PPI. While PPI-(4-Ar-OC_{10})$_n$ and PPI-(3,4-Ar-(OC_{10})$_2$)$_n$ for all five generations have smectic A mesophases, PPI-(3,4,5-Ar-(OC_{10})$_3$)$_n$ for all five generations has columnar type mesophases. Various types of mesomorphism [89] (smectic, columnar square, columnar hexagonal, channelled layer phase) were obtained by tailor-style connecting of T-shaped terphenyl core (oligooxyethylene connected) to DAB-based PPI via lateral, end-point linkage. The surfaces of PAMAM and PPI were functionalized [90] by semifluorinated carboxylic acids [$CF_3(CF_2)_7CH_2CH_2COOH$]. All ionic dendrimers have smectic A phase except the fifth generation of PPI showing columnar rectangular mesophase. The similar exception for the fifth generation of PPI was observed by previously mentioned other study [86]. Using 5-(4-cyanophenylazophenyloxy) pentanoic acid, non mesogenic unit, to obtain ammonium salts led to nematic mesophase for all amine ended dendrimers (PAMAM, PPI, polyethylene imine) [91]. The reason for obtaining nematic phase, relatively rare in dendritic systems, is shorter

alkyl chain of the pentanoic acid. In another study [92], evolving from nematic phase to smectic A mesophase was demonstrated by modulating the number of 5-(4-cyanophenylazophenyloxy) pentanoic acid and 2,2-bis-(undecanoyloxymethylene) propionic acid on PPI surface. Switching from nematic to SmA occur by decreasing content of pentanoic acid derivative. In the other study [93], 5-(4-cyanobiphenoxy) pentanoic acid, demonstrating monotropic nematic phase, was combined with various type of amine terminated dendrimers. Ionic complexes produced nematic and smectic C mesophase depending on the dendrimeric scaffold. When attached units were compared between 5-(4-cyanophenylazophenyloxy) pentanoic acid and 5-(4-cyanobiphenoxy) pentanoic acid for similar dendrimeric structures, mesomorphism was observed at even room temperatures by monotropic 5-(4-cyanobiphenoxy) pentanoic acid. Ionic grafting of two different aromatic acids (4-decyloxybenzoic acid and 4-perfluorodecyloxybenzoic acid) onto PPI in different combinations led to form smectic A and modulated smectic A (unusual type smectic A) mesophases [94]. Bent-core ionic dendrimers were synthesized [95] by using bent-shaped aromatic carboxylic acids as anionic part and PPI and PEI as cationic part. While all building blocks (acids, PPI and PEI) are non-mesogenic, ionic complexes show *polar SmC* and Col_{rec} phases in wide temperature. In this study, role of generation of dendrimer, rigidity of bent-core (number of aromatic ring), length of inner spacer (number of carbon between aromatic part and carboxylic acid), length of outer spacer (alkoxy chain) were comparatively investigated. The generation of dendrimer does not have an effect on mesomorphism and phase transitions. Higher number of aromatic ring (n=6) compared to lower one (n=5) presented wider temperature mesophase range while type of mesophase was not affected. Increasing of inner spacer led to lower melting point but no effect on phase type. Length of outer spacer has remarkable effect on range and type of mesophase. While shorter terminal chains led to Col_{rec} and wide mesophase range, longer chains caused polar SmC and short mesophase range. The other acid-base reaction [96] between a hyperbranched amine ended amidoamine based dendritic scaffold and sodiumdodecyl sulfate produced lamellar and columnar rectangular thermotropic mesophases. In this study, by changing of generation of dendrimer, no appreciable change was observed for both types of mesomorphism and lattice parameters.

The key factor choosing dendrimers is weak intermolecular forces in interior of supramolecular system. Relatively comfortable system enables better movement and

interaction of molecules forming mesomeric phase. Further explanation is defined as competition between entropy and enthalpy. More entropic environment is favored by spherical geometry of dendrimer. On the other side, more enthalpy gain is favored by intermolecular interactions of terminal promesogenic units. Mesomeric properties of the system depend on this delicate race [68-69, 97]. Another driving force is microsegregation for the formation of mesophase for ionic LCDs. Like highly popular topic in low molecular weight molecules, various cyclic or other types of macrostructure [98], microsegragation is highly discussed topic and used tool to derive mesophase formation. Microsegregation concept was utilized firstly for non-ionic amphiphilic molecules, calamatic or discotic, and copolymers containing incompatible units. In amphiphilic molecules, polar and apolar regions segregate themselves in microdomain. This segregation cannot be in the scale of macroscopic domains due to the chemical bonding of polar and apolar units. AB-copolymers composed of two chemically different parts have microsegregated domains due to the incompatibility of parts. Due to this segregation, A is more dominant in one microdomain and B is more dominant in other microdomain [98]. Tail-to-tail bilayered self-organization driven by microsegregation is shown for a conventional molecule [99] shown in Figure 16. Polar groups by additional power of hydrogen bonding were collected in the same microdomain, terminal alkyl chains were collected in the other microdomain. Phase transition of smectic and nematic phases were modulated by changing methylene number.

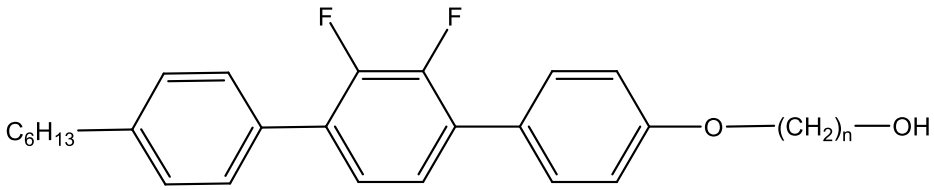

Figure 16: A rod-like molecule studied in [65].

Wendorff [100] demonstrated that smectic A and columnar hexagonal using linear diethylenetriamine and triethylenetriamine derivatives substituted by 3,4-bis(decyloxy)benzoyl represented in Figure 17. Several examples (see Figure 17 B) represented columnar hexagonal mesophase without hydrogen-bonding possibility. Polar amine end of oligoethylene derivative as column core was surrounded by apolar 3,4-bis(decyloxy)benzoyl groups as an example of microsegregation.

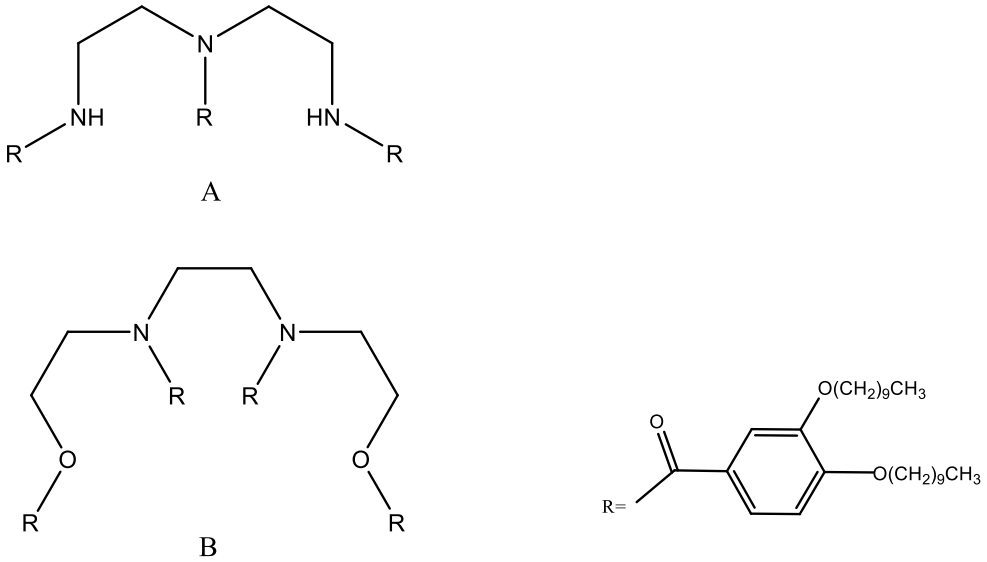

Figure 17: A= Diethylenediamine derivative, B= Triethylenediamine derivative studied in [100].

Tschierske [98] clearly expressed that microsegregation formed by aggregates of lamellar, columnar or spheroidal leads to form smectic, columnar, cubic mesophases respectively in his review paper. Later, this idea was used for formation of mesophase based on dendrimers. By using optimal promesogenic units, calamatic or discotic, smectic A and columnar mesophases were obtained for ionic dendrimers by lateral or end-on substitution [88-89, 95]. (See Figure 18 for the study in [88]). By positive role of microsegregation, the dendrimers can be a tool to create LC materials by using even non-mesogenic end groups [85-86, 91]. As shown in Figure 19, non-mesogenic 5-(4-cyanopheny-lazophenyloxy) pentanoic acid was used to create nematic mesophase by PAMAM, PPI and PEI dendrimers. Microsegregation arises from the presence of incompatible units in the supramolecular system. Dendrimers with polar functional groups and apolar groups like long alkyl or alkoxy aromatic or non-aromatic chains provide microsegregated regions. The reason for microsegregation is a significantly different chemical nature of inner side (dendritic core and branch) from the outer side (terminal groups). While dendritic core becomes hard part, alkyl end unit is called soft part. In this commonly microsegregated system, while inner part plays role as a scaffold, terminal group determines what type of mesophase forming. By contribution of hydrogen bonding, interaction of polar groups (like hydroxyl or ammonium groups), microsegregation becomes reinforced. If attached terminal units are short chain, the units are accepted as coupled into system. If grafted terminal groups are generally long alkyl or alkoxy chains, the terminal groups are accepted as decoupled from

hyperbranched polymer and microsegregation occurs. Especially, for too crowded dendritic systems, microsegregation becomes only way to obtain LC phase due to the limited mobility. By managing microsegregation, various types of mesophases can be obtained. On the contrary, by designing or choosing appropriate molecules, microsegregation can be used to remove or weaken LC phase [68]. Structure-property relationship is heart of this work and enables wide versatility by taking into account all parameters, intermolecular forces, entropy-enthalpy balance, chemical incompatible segments (microsegregation).

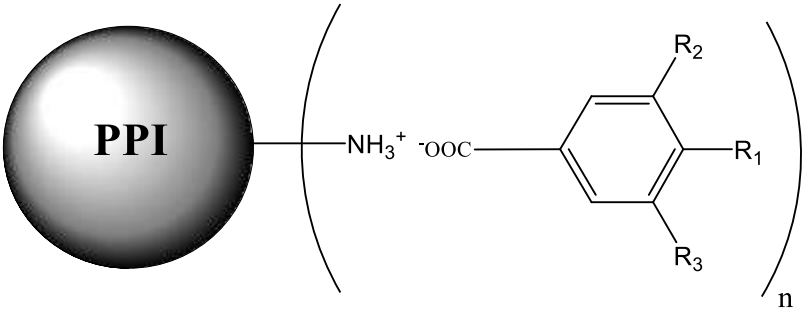

1) R_1= —$OC_{10}H_{21}$; R_2&R_3 = —H

2) R_1&R_2= —$OC_{10}H_{21}$; R_3 = —H

3) R_1&R_2&R_3= —$OC_{10}H_{21}$

Figure 18: In the study [88], SmA for 1 and 2; Colh for 3.

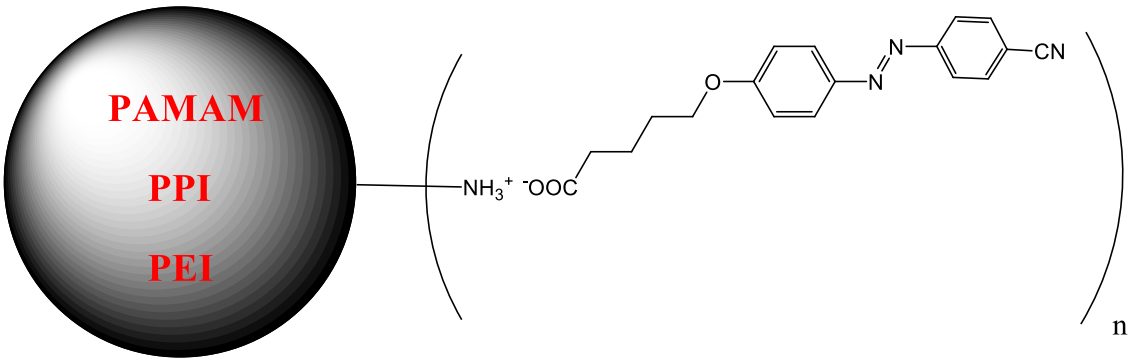

Figure 19: In the study [85], Nematic phase by 5-(4-cyanopheny-lazophenyloxy) pentanoic acid, non-mesogenic building block.

2.10 Microwave Chemistry

Microwave assisted reactions have become important in the various branches of the chemistry. Microwave is an electromagnetic wave ranging from 1 mm to 1 m wavelength. The frequencies corresponding to those wavelengths are from 0.3 to 300 GHz. The region of microwave is between infrared and radio waves. Microwave energy is composed of two components like all electromagnetic waves. While two components are electric and magnetic field, only electric component is used for chemical synthesis. Length of the microwave in the laboratory scale synthesis is around 12,2 cm (2450Mhz) [101].

At 1970s, microwave technique was stated to use in firstly inorganic chemical reactions. Later, after 1990s, it was started commonly to utilize in the area of organic chemistry by introduction of commercial microwave equipment into market. Main and obvious advantage of microwave chemistry is shortened reaction times. Another advantage is the using of lower amount of solvent. For this reason, microwave technique has become popular in pharmaceutical chemistry requiring the synthesis of enormous amount of new molecules [101].

To compare the conventional organic synthesis local heating of reaction media and temperature gradient, microwave technique allows only heating of solvent, reactant and reagent uniformly (see Figure 20). By this way, less decomposition and less side products appear. The reaction rate is determined by the formula $k = Ae^{-Ea/RT}$. For conventional reactions, due to gradient heating, temperature is defined as bulk. For microwave systems, energy is transferred to molecules in the time interval of 10^{-9}s, molecule tries to relax around 10^{-5}s. This situation makes molecules superheated (see Figure 20) by instantaneous temperature increment. The instantaneous temperature of microwave system is higher than bulk temperature of conventional system. By this way, high continuous instantaneous temperature makes high reaction rate, k. This leads to increase in reaction rate up to 1000 fold [101-102].

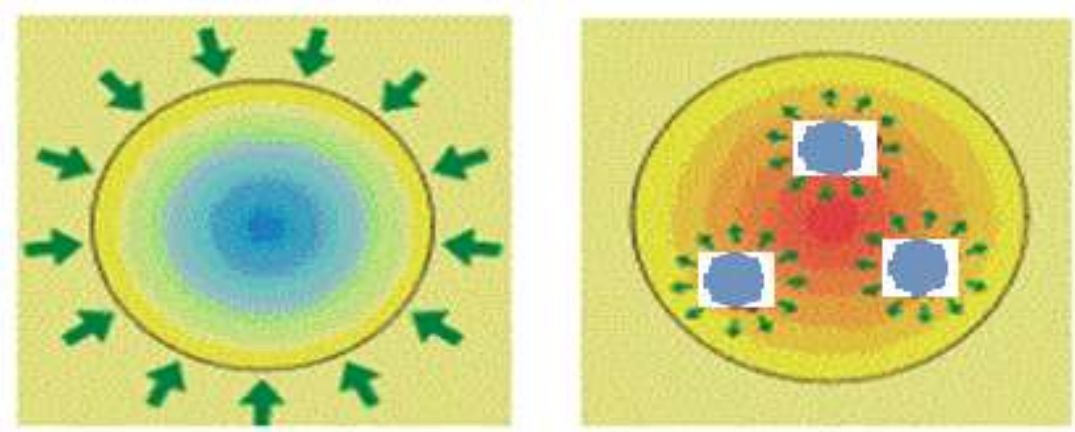

Figure 20: Conventional heating (Left), Microwave heating (Right)

Instantaneous heating by microwave energy is explained by two routes, dipole polarization and ionic conduction. By moving back and forth, polar molecules, having dipole regions, try to align their dipole with changing of electric field of microwave. Similarly, for ionic conduction, ions try to align their own position with electric field by moving. Heat is resulted from these movements [101-104].

Solvent selection is one of the most important tools to manage duration of reaction and whether the product is formed or not. As explained in dipole polarization, polar solvents, having ability to be aligned by microwave heating, absorbs more microwave irradiation. Absorption of energy can be checked by dielectric constant, dielectric loss and tangent loss (delta). Dielectric constant, ε', refers to a substance retaining electrical potential energy under electric field. Dielectric loss, ε", is related to conversion of electrical energy to thermal energy. High dielectric loss, ε", means high thermal conversion. The formula is expressed as $\tan \delta = \varepsilon''/\varepsilon'$. High dielectric loss brings high tangent loss. For this reason, efficient thermal conversion of microwave irradiation is followed by high dielectric loss and tangent loss. As described in Table 2, ethanol, DMSO, formic acid, methanol and isobutanol are more suitable for MW assisted reactions due to high dielectric loss and tangent loss. Chloroform, acetonitrile, ethyl acetate, THF, DCM and hexane are not good solvents for this type of study. To sum up, polar solvents are obviously better choice compared to apolar solvents for MW applications [102, 104].

Table 2: Dielectric constant, Dielectric loss and tan δ of solvents at 2.45 GHz [102, 104]

Solvent	Dielectric constant (ε')	Dielectric loss (ε'')	tan δ
Ethanol	24.3	22.866	0.941
DMSO	45.0	37.125	0.825
Formic Acid	58.5	42.237	0.722
Methanol	32.6	21.483	0.659
Isobutanol	15.8	8.248	0.522
Water	80.4	9.889	0.123
Chloroform	4.8	0.437	0.091
Acetonitrile	37.5	2.325	0.062
Ethyl acetate	6.0	0.354	0.059
THF	7.4	0.348	0.047
DCM	9.1	0.382	0.042
Hexane	1.9	0.038	0.020

Another point boiling point of solvent is not an issue to choose solvent, because solvents are readily boiled by around 150-200W in very short time period.

CHAPTER 3

EXPERIMENTAL

3.1 Materials

Methyl acrylate, ethylenediamine, tetrahydrofuran (THF), chlordoform, dichloromethane (DCM), methanol, ethanol are purchased from Merck. Solvents are analytical grade. THF is dried before use. N,N'-dicyclohexycarbodiimide (DCC) and 1-hydroxybenzatriazole (1-HOBt), trimesic acid are purchased from Fluka. DAB-*4*, DAB-*8*, DAB-*16* and DAB-*32* polypropylene-imine dendrimers were purchased from SyMO-Chem (Netherland) and used without further purification.

3.2 Techniques

The CEM Focused Microwave™ Synthesis System (CEM Corporation, Model Discover, North Carolina, USA) is used for amidoamine synthesis. Power output is from 0 to 300 watts by 1-watt increments and temperature range covers from 25 to 250 ^{0}C.

The IR spectra (4000–400 cm^{-1}, resolution 4 cm^{-1}) were recorded with a Perkin Elmer Spectrum One in ATR. The characterization of the materials is based on ^{1}H-NMR and ^{13}C-NMR (Bruker Avance 400 MHz spectrometer, in $CDCl_3$ solutions, with tetramethylsilane as internal standard). Transition temperatures are recorded by a Mettler FP-82 HT hot stage and control unit combined by a Leica polarizing

microscope. DSC-thermograms are recorded by Perkin Elmer Pyris 6, heating and cooling rate: 10^{o}C/min. TGA studies are performed using Exstar SII TG/DTA 7200.

3.3 Dialysis

Dialysis (ultrafiltration) is performed to remove impurities, excess reagents, excess reactants and low molecular weight uncompleted products when synthesizing dendrimers. Dialysis membranes (Liquid-phase polymer-based retention (LPR) ultrafiltration membranes) with the molecular cut of size (MWCO) 500, 1000, 3000 Da are purchased from Millipore. Dialysis cell is Amicon 8000 Stirred Cell supplied from Millipore.

As shown in Figure 21, dialysis system is composed of couple of units. The substance desired to be purified is placed in dialysis unit (cell) after solving water, methanol or ethanol. Other solvents are not suitable for dialysis. By pressure, nitrogen tank transfer solvent to dialysis unit and pressurize the dialysis unit. According dialysis membranes, lower molecular weight molecules are transported to waste container.

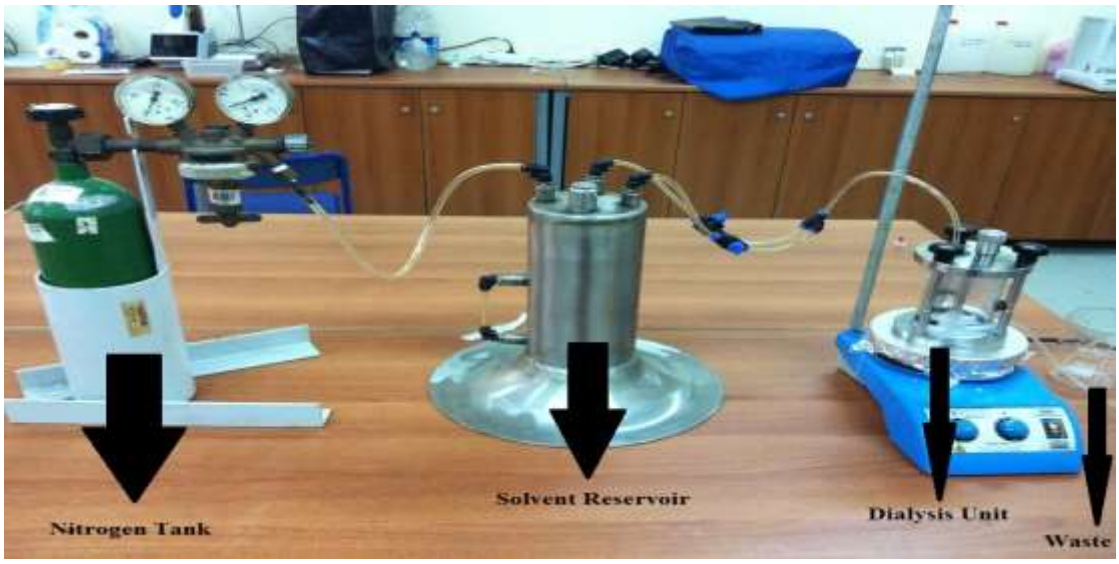

Figure 21: Dialysis System

CHAPTER 4

RESULTS AND DISCUSSION

4.1 PAMAM Based Dendritic Ionic Liquids

To synthesize PAMAM based dendritic ionic liquids, PAMAM dendrimers as cationic part and alkoxy benzoic acids as anionic part and mesomeric unit are needed. Preparation and description of these materials are explained in below.

4.1.1 PAMAM Dendrimers

Tülü Research group has made lots of efforts and contributions on amidoamine type synthesis. One of them is PAMAM which is commonly used in thermotropic LC synthesis.

4.1.2 Synthesizing PAMAM Dendrimers

In this study, firstly we synthesized poly(amidoamine) PAMAM dendrimers. When synthesizing those dendrimers, we used the microwave technique [105]. Four generations (from G0 to G3) were synthesized. Figure 22-25 represents the steps synthesizing of PAMAM generations. For the half generations (G0.5, G1.5, G2.5), excess amount of methyl acrylate was added to amine ended groups. After 24 hours waited, solvent and methyl acrylate was removed by rotary evaporator. Then, whole generations (G0.0, G1.0, G.2.0, G3.0) were synthesized using excess amount of ethylene diamine and little amount of methanol is added to corresponding ester ended generations. Reaction is performed for 40 minutes under reflux using CEM Microwave

at 200W. Dialysis is used for removing excess ethylenediamine and other fragments. The products for full generations are yellowish oil.

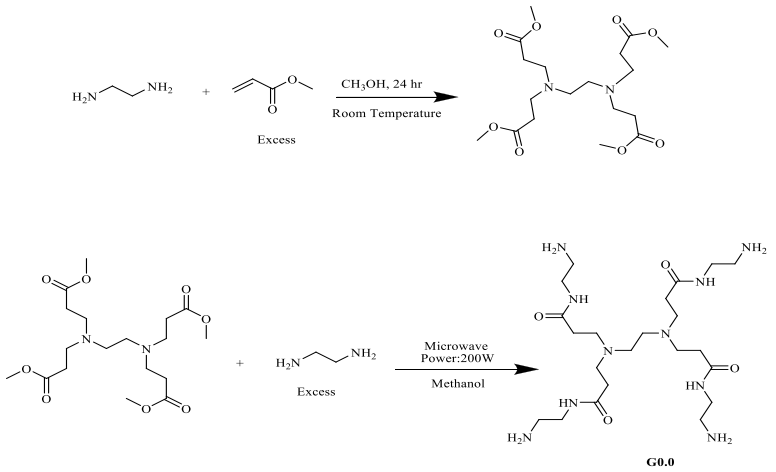

Figure 22: Synthesizing of G0.0 PAMAM dendrimer

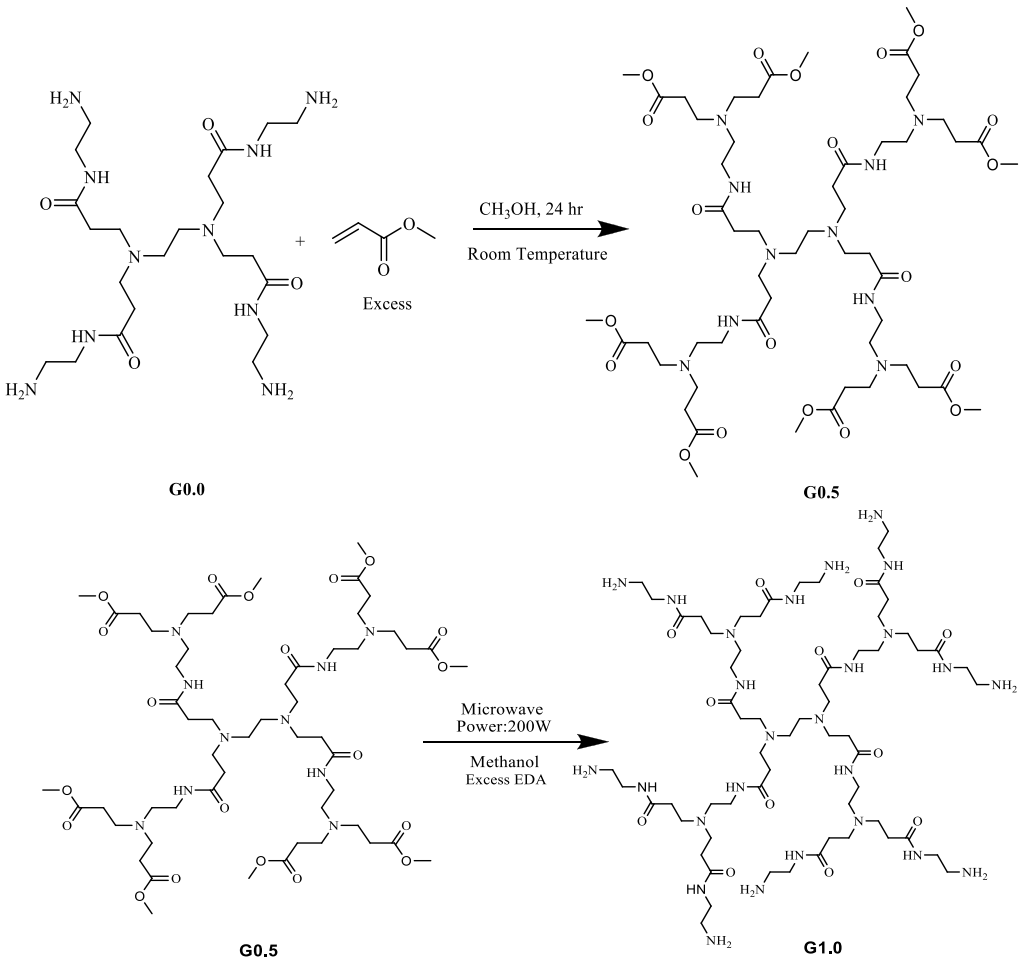

Figure 23: Synthetic route for G1.0 PAMAM dendrimer

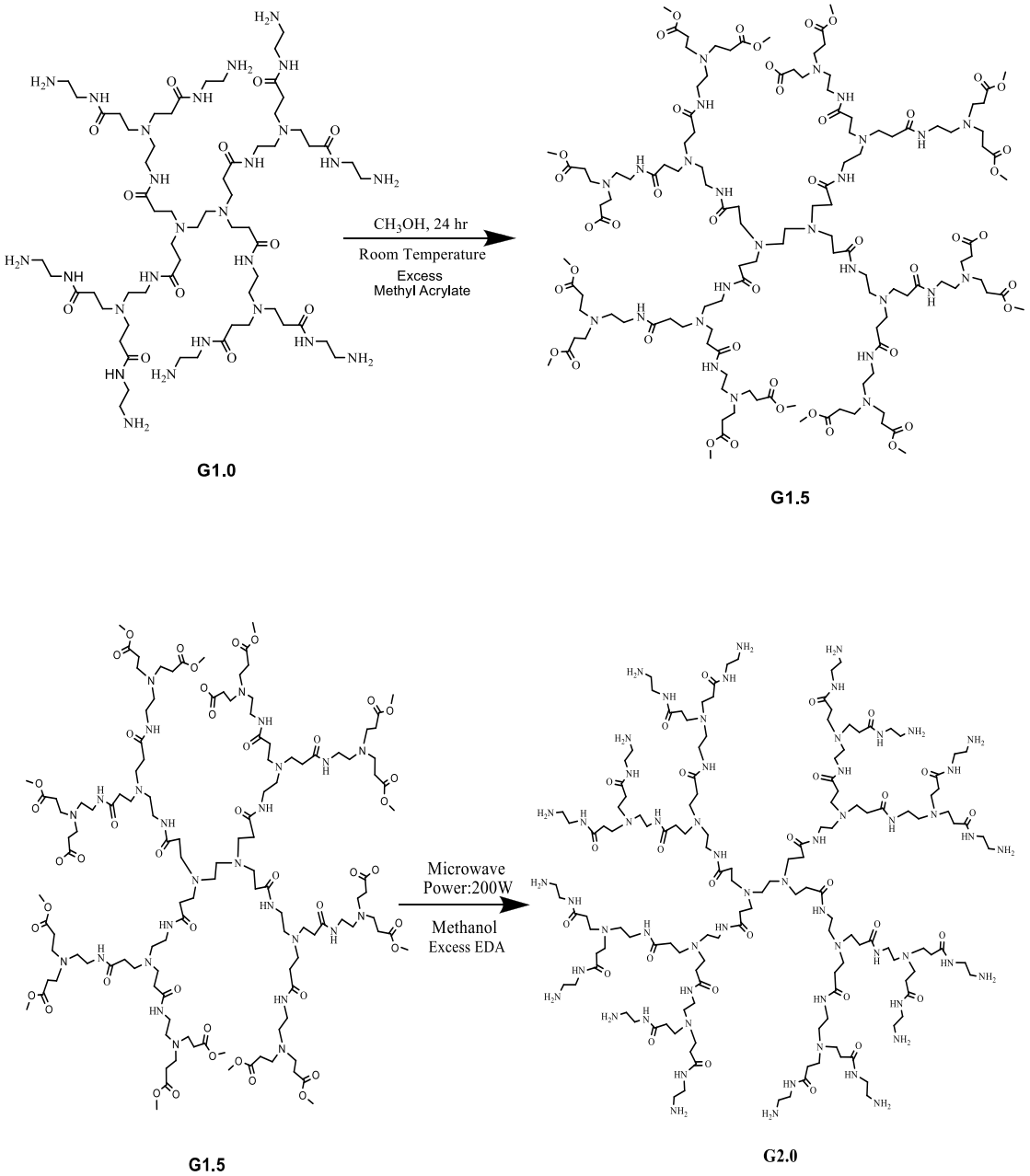

Figure 24: Synthetic route for G2.0 PAMAM dendrimer

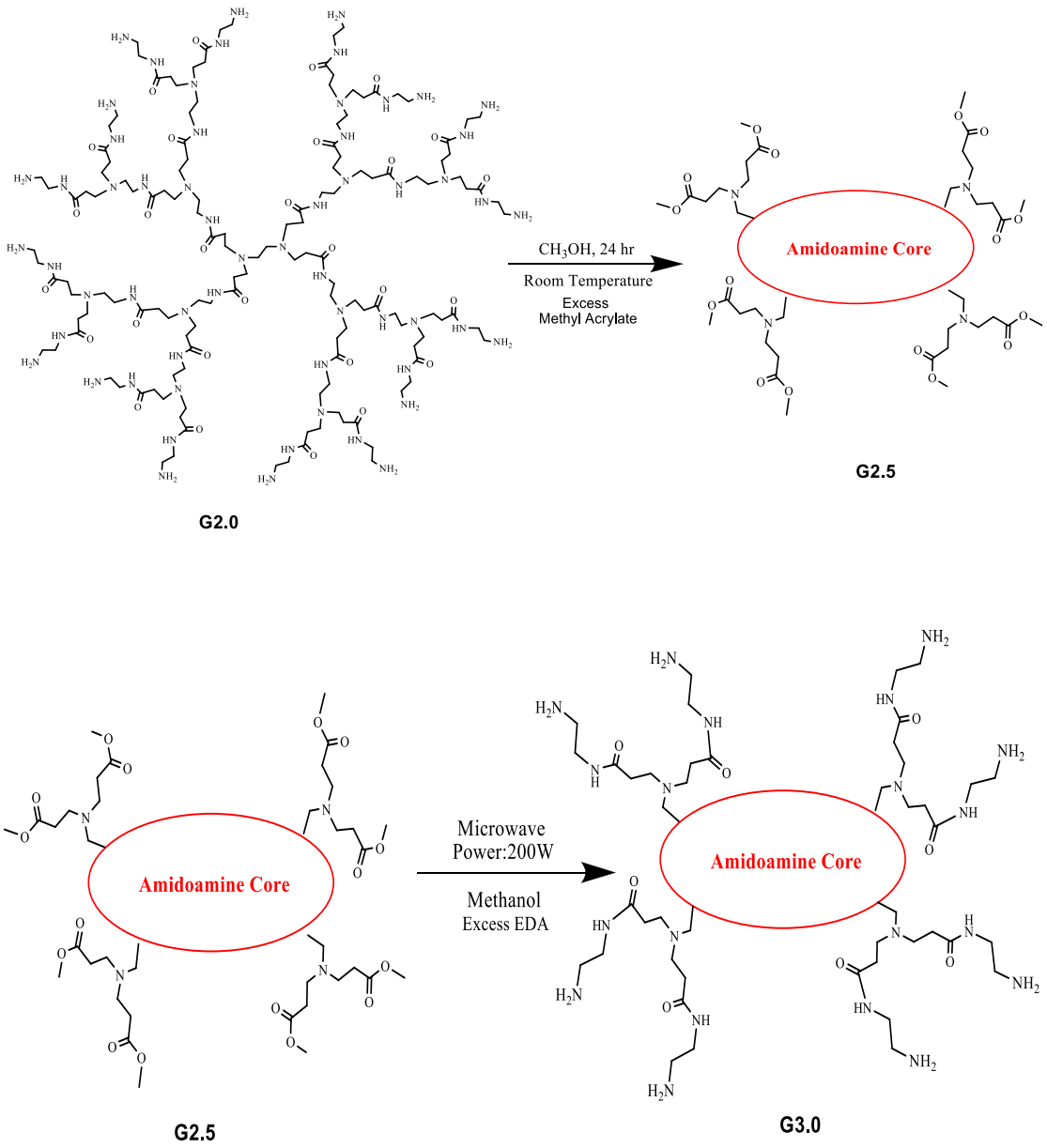

Figure 25: Synthetic route for G3.0 PAMAM dendrimer

4.1.4 Characterization of PAMAM Dendrimers

To realize structural characterization, as shown in Figure 26, the formation of half generations by disappearance of amine peaks at 3300 cm^{-1} and appearance of sharp ester peak at 1730cm^{-1} were checked. In addition, amide formation was followed by observing the appearance at 1645cm^{-1} and disappearance of ester peak at 1730cm^{-1}.

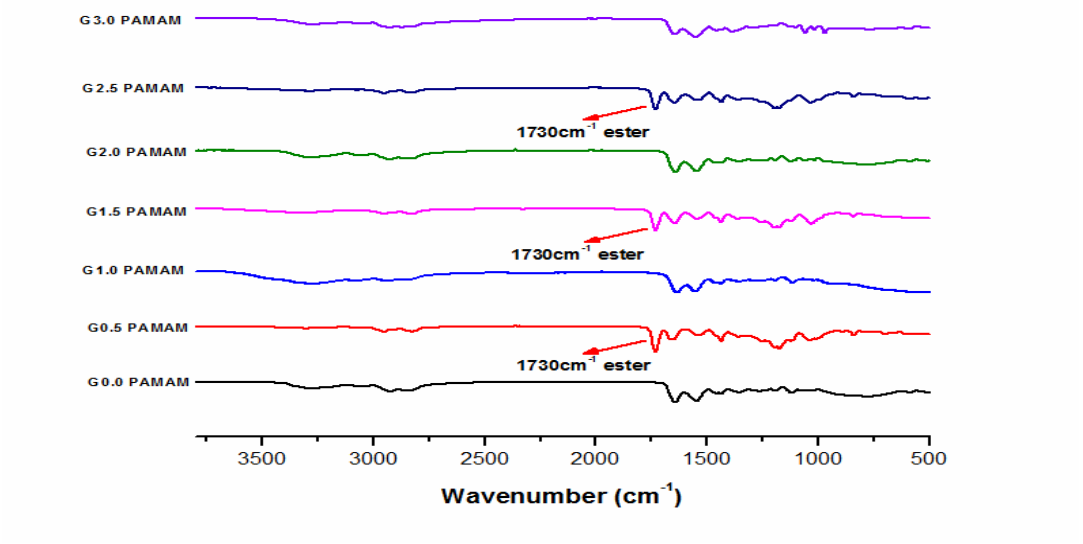

Figure 26: FT-IR Spectra of half and full generations of PAMAM

^{13}C NMR is another good tool to confirm polyamidoamine formations. As depicted in Figure 27, typical outer core amide peak at 177ppm is a characteristics of G1.0-G3.0PAMAM.

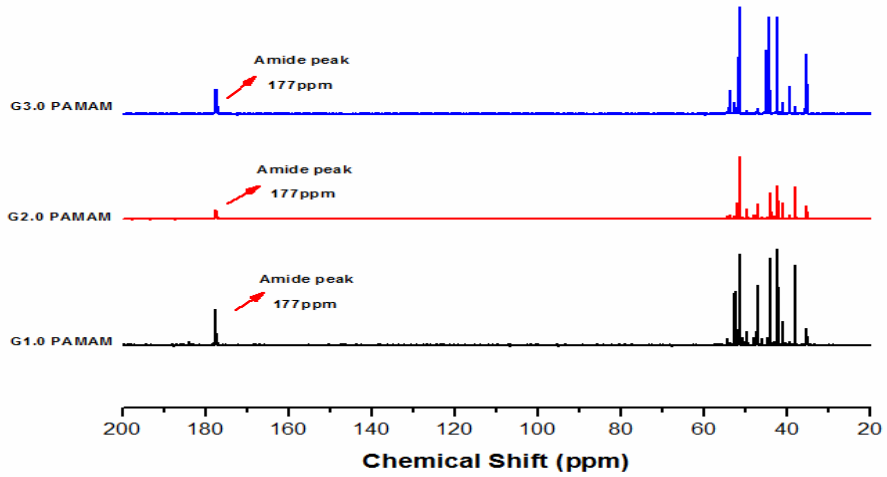

Figure 27: ^{13}C NMR Spectra of G1.0-G3.0 PAMAM (D_2O Solvent)

4.1.5 Mesomeric Units as Anionic Part

To synthesize EDA based PAMAM dendritic ionic liquids, various types of benzoic acids were chosen as mesogenic units. Those molecules were given us by Eran

Research group. Those molecules are shown below Figure 27. The shortest alkoxy chain is composed of 8 carbon and the longest one has 12 carbon. All of them have shown LC property and their isotropization point is significantly high.

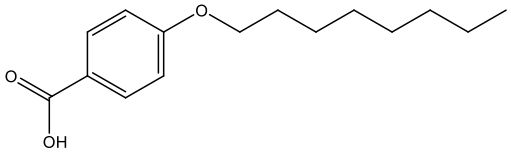

4-(Octyloxy) benzoic acid **(C8)**

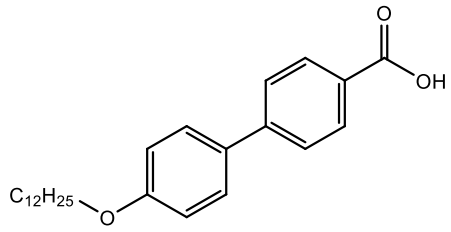

4-(4-Dodecyloxyphenyl) benzoic acid **(C12-BP)**

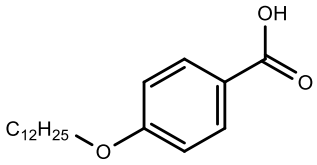

4-(Dodecyloxy) benzoic acid **(C12)**

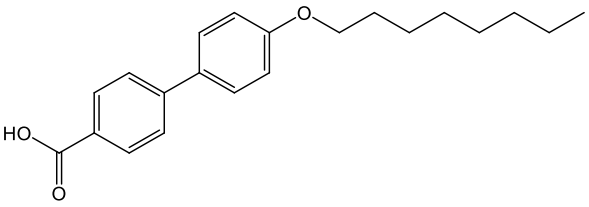

4-(4-Octyloxyphenyl) benzoic acid **(C8-BP)**

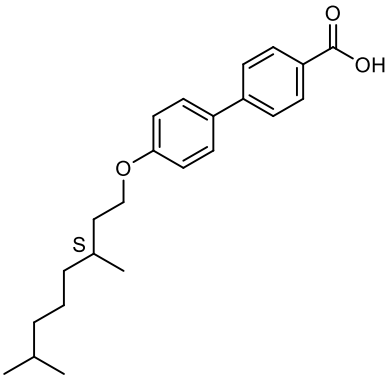

4’-(3S)-3,7-dimethyloctyloxy-4-biphenylcarboxylic acid **(C10*BP)**

Figure 28: Structures, names and abbreviations of alkoxy benzoic acid derivatives used in our studies.

4.1.6 Synthesizing PAMAM based Dendritic Ionic Liquids

Those benzoic acid molecules shown above Figure 28 were reacted with each amine end groups of PAMAM dendrimers with respect to one to one rate by using ultrasonication for 15 minutes in dry tetrahydrofuran solvent shown in Figure 29. Later, tetrahydrofuran was evaporated through rotary evaporator. Structural characterization is performed by FT-IR, ^{1}H NMR and ^{13}C NMR.

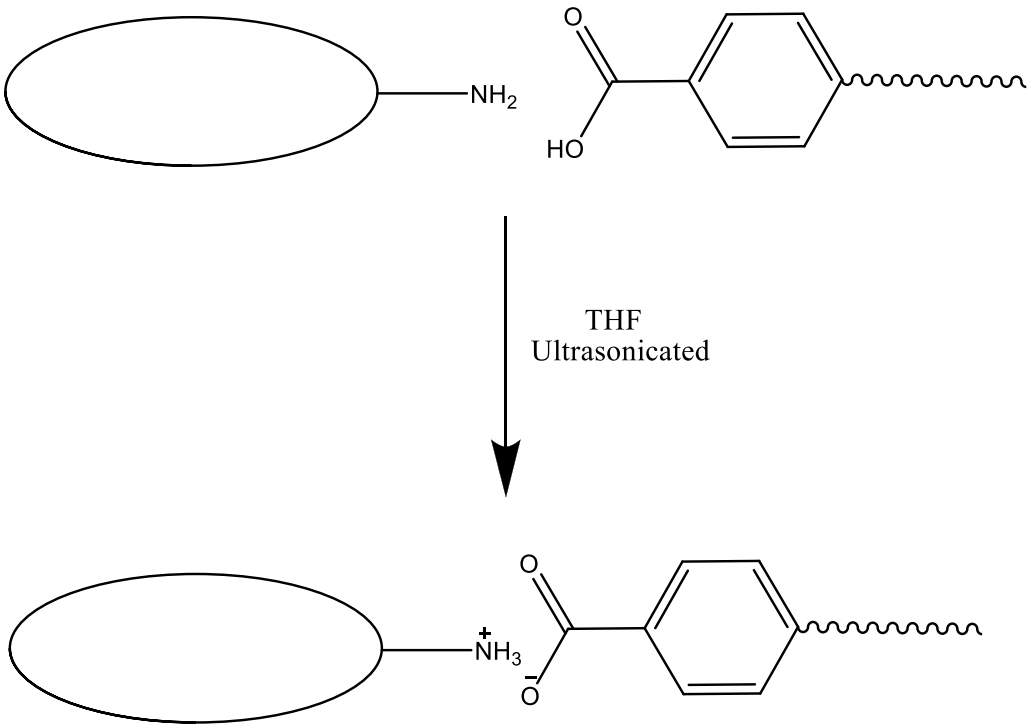

Figure 29: Schematic representation of salt formation between dendrimer and benzoic acid.

4.1.7 C8-PAMAM, C8BP-PAMAM and C12BP-PAMAM Ionic Liquids

Firstly, three salts were synthesized according to Figure 29 shown above. Two of them have short chain (8 carbon) mesomeric units and one of them has long chain (12carbon), biphenyl but achiral mesomeric unit. Structural characterization of these salt groups was performed by FT-IR. Figure 30-32 confirm ion formation by disappearing amine peaks, carbonyl group and appearing carboxylate peaks.

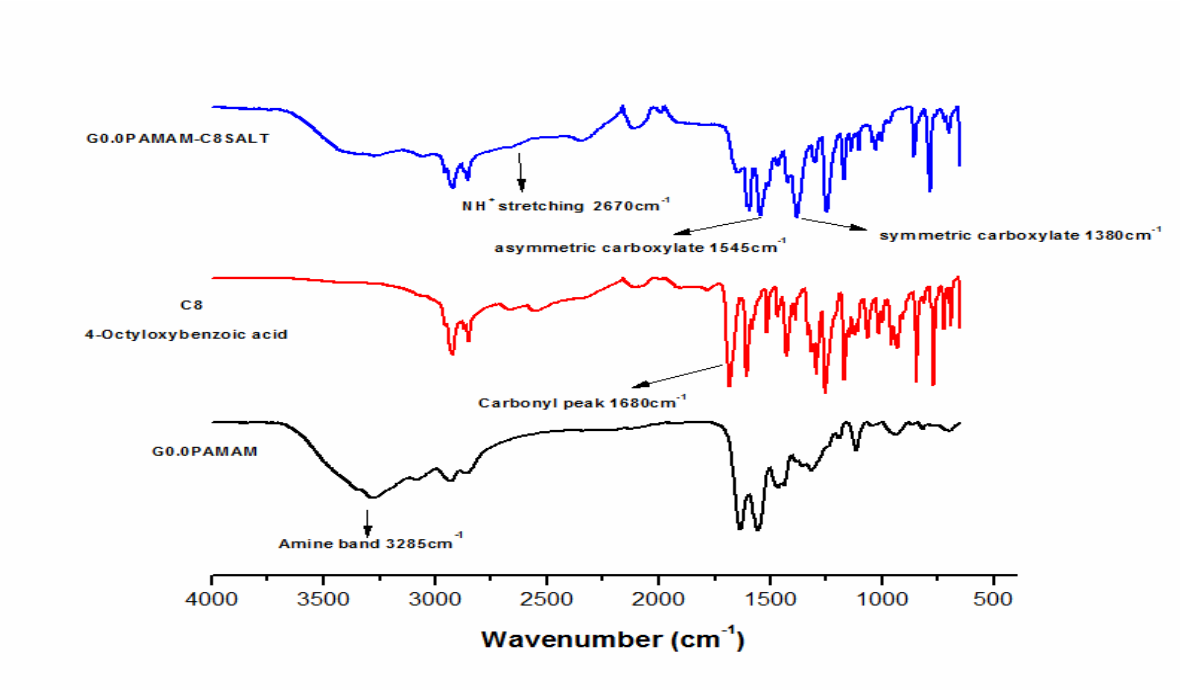

Figure 30: FT-IR Spectra of G0.0 PAMAM, C8, G0.0 PAMAM-C8 Salt

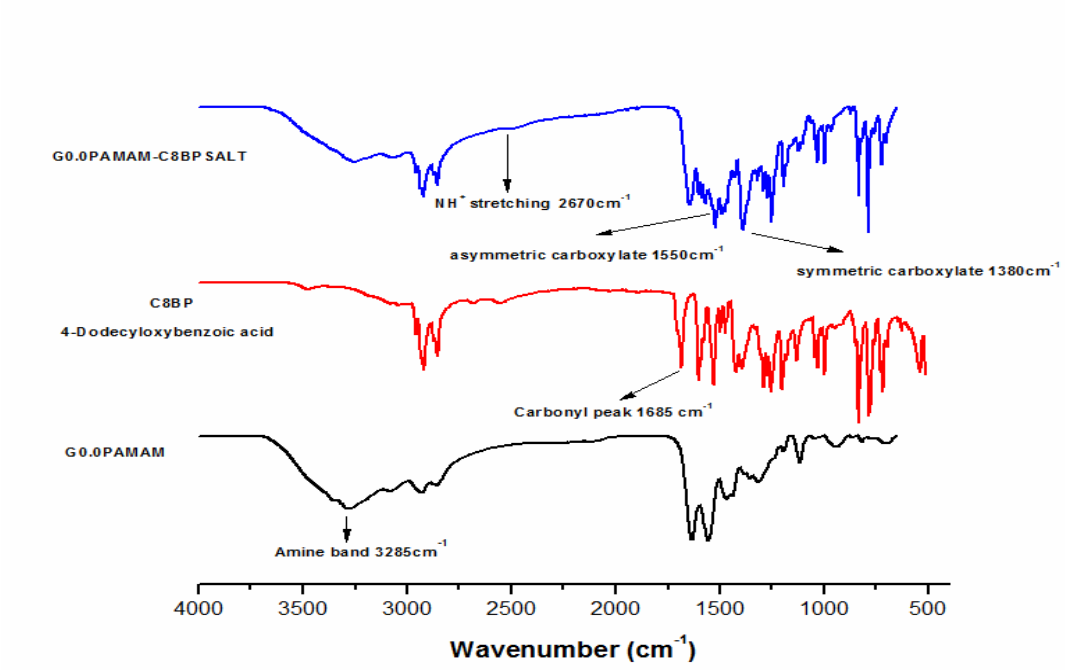

Figure 31: FT-IR Spectra of G0.0 PAMAM, C8BP, G0.0 PAMAM-C8BP Salt

In Figure 30, disappearing amine band of PAMAM at 3285 cm^{-1} and carbonyl group of C8 acid at 1680 cm^{-1} is clear evidence of reaction. Symmetric carboxylate peak at 1380cm^{-1}, suits well with literature*, another proof for confirming reaction. Asymmetric carboxylate peak* at 1545cm^{-1} overlaps with amide II (ca1550cm^{-1}). This overlaps

enhances the peak intensity at 1550cm^{-1} band becoming stronger than 1650cm^{-1} band composed from amide I group.

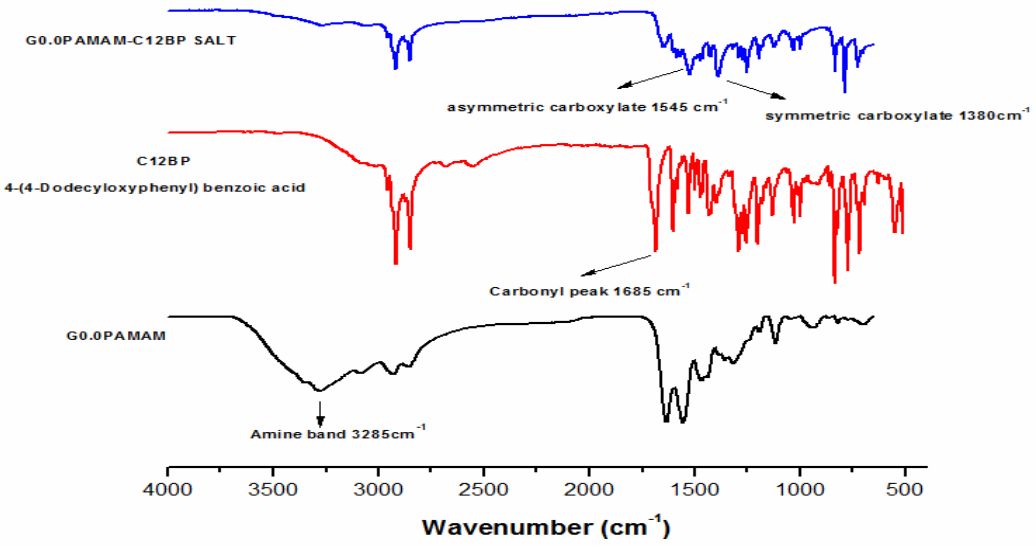

Figure 32: FT-IR Spectra of G0.0 PAMAM, C12BP, G0.0 PAMAM-C12BP Salt

When we look at Figure 31&32 for biphenyl based ones, symmetric carboxylate peak at 1380cm^{-1} coincides with vibrations resulting from C8BP and C12BP acids. Although the coincidence, distinctiveness of carboxylate peak partially retains. For G0.0 PAMAM-C12BP salt, 1550cm^{-1} band (amide II + asymmetric carboxylate) is stronger than 1640-1650cm^{-1} band (solely amide I).

We studied liquid crystal properties of those ionic dendritic liquids using Polarized Optical Microscopy (POM), Differential Scanning Calorimetry (DSC). Firstly, we are going to show 4-(4-Octyloxyphenyl) benzoic acid-PAMAM and 4-(4-Dodecyloxyphenyl) benzoic acid-PAMAM, 4-(Octyloxy) benzoic acid-PAMAM results of POM in Table 3.

Table 3: POM Results of 4-(Octyloxy) benzoic acid-PAMAM, 4-(4-Octyloxyphenyl) benzoic acid-PAMAM and 4-(4-Dodecyloxyphenyl) benzoic acid-PAMAM.

Name	Phase Transitions by POM
4-(Octyloxy) benzoic acid **(C8)**	Iso 145^{0}C N 105^{0}C SmX 100^{0}C Cr

C8-G0.0 PAMAM	Cr 119^{0}C SmX (SmA) 163-183^{0}C Iso Iso 178^{0}C SmX (SmA) 113^{0}C Cr
C8-G1.0 PAMAM	Not Liquid Crystal. Becoming isotropic at 224^{0}C, decomposition is observed.
C8-G2.0 PAMAM	Not Liquid Crystal. Becoming isotropic at 220^{0}C, decomposition is observed.
C8-G3.0 PAMAM	Not Liquid Crystal.
4-(4-Octyloxyphenyl)benzoic acid **(C8BP)**	Cr 183^{0}C SmX 255^{0}C N 264.5^{0}C Iso
C8BP-G0.0PAMAM	Not Liquid Crystal. Heated up to 245^{0}C, decomposition starts.
C8BP-G1.0PAMAM	Not Liquid Crystal. Melting point higher than 270^{0}C
C8BP-G2.0PAMAM	Not Liquid Crystal. Heated up to 257^{0}C, decomposition starts.
C8BP-G3.0PAMAM	Not Liquid Crystal. Melting point higher than 270^{0}C
4-(4-Dodecyloxyphenyl) benzoic acid **(C12BP)**	Cr 165^{0}C SmX 252^{0}C Iso
C12BP-G0.0 PAMAM	Iso 214^{0}C SmC 126^{0}C Cr
C12BP-G1.0 PAMAM	Liquid Crystal, Not observable due to reaching around 230^{0}C, decomposition starts
C12BP-G2.0 PAMAM	Cr 134^{0}C SmC 217-228^{0}C Iso, due to decomposition not perfectly clear.
C12BP-G3.0 PAMAM	Cr 170^{0}C SmC 226-236 Iso, due to decomposition not perfectly clear.

Generally, we did not observe mesomeric properties form salts, synthesized from the octyl chains, single phenyl groups (C8) and biphenyl groups (C8-BP). The exception is C8-G0.0 PAMAM that shows smectic X phase from around 110-120^{0}C to 170-180^{0}C (see Figure 33). The phase transition range is clearly higher than its building block (C8) benzoic acid. For the rest three generations (C8-G1.0 PAMAM, C8-G2.0 PAMAM), C8-G3.0 PAMAM), we could not observe liquid crystal. The reason for this situation can be decomposition of materials at higher temperature or difficulties to obtain very clear solution. In addition, main reason for non-mesomeric phase for both single phenyl groups (C8) and biphenyl groups (C8-BP) is relatively short chain to make liquid crystal.

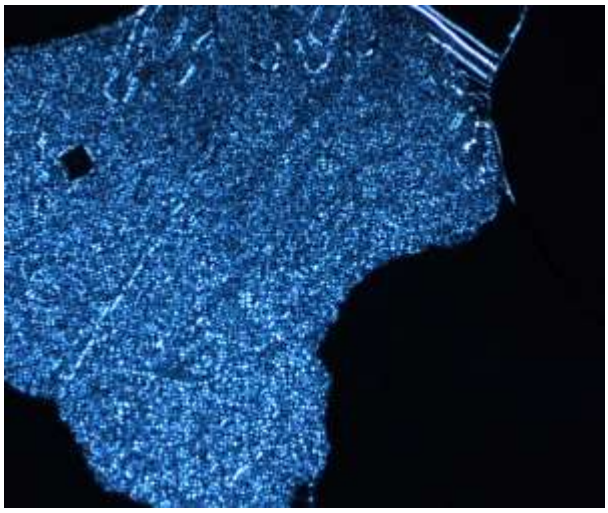

Figure 33: C8-G0.0 PAMAM at 163^{0}C SmX (SmA)

For the 4-(4-Dodecyloxyphenyl) benzoic acid (C12BP)-PAMAM salts, liquid crystal is observed. Some of their mesomeric properties cannot be fully comprehended due to decomposition of materials reaching high temperatures around 250 ^{o}C. The building block has mesomeric range from 165^{0}C to 252^{0}C. Under polar microscopy, it is much higher than 252^{0}C. For this reason, oil type PAMAM dendrimers cannot be perfectly thermal stable at such temperatures. Although this heavy conditions, for C12BP-G0.0 PAMAM, C12BP-G2.0 PAMAM, C12BP-G3.0 PAMAM, as shown in Figure 34-37, we observed Smectic C mesophase, starting temperature lower than crystallization temperature of C12BP. A clear enhancement of mesomeric range was observed. This enhancement can be attributed to flexible and oil type properties of core and branch of dendrimers. It means that total system (mesomeric unit +dendrimer) approaches to liquid side. On the other hand, by increasing generation, we observed that the starting

temperature of mesophase is clearly increased. However, there is no change for isotropization temperature. It means that by increasing generation, mesophase range shrinks. Its reason can be explained by overcrowding of surface amino groups at such high numbers like 16 or 32.

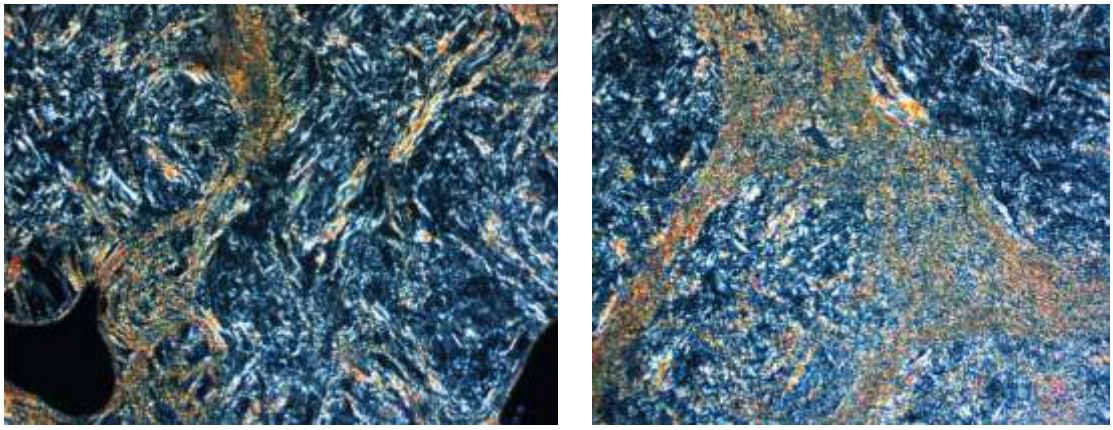

Figure 34: SmC Phase of C12BP-G0.0 PAMAM at 129^0C (left) and 172^0C (right)

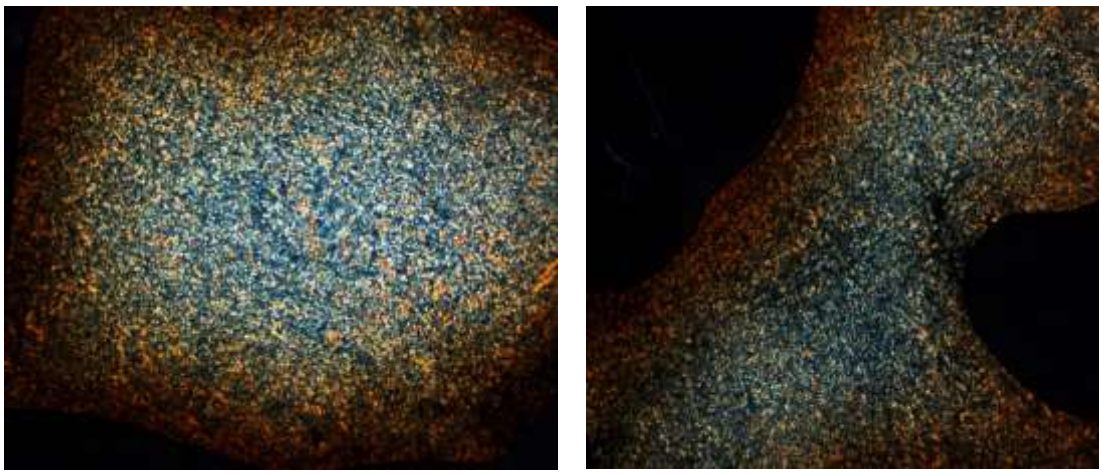

Figure 35: SmC Phase of C12BP-G1.0 PAMAM at 204^0C (left) and 224^0C (right)

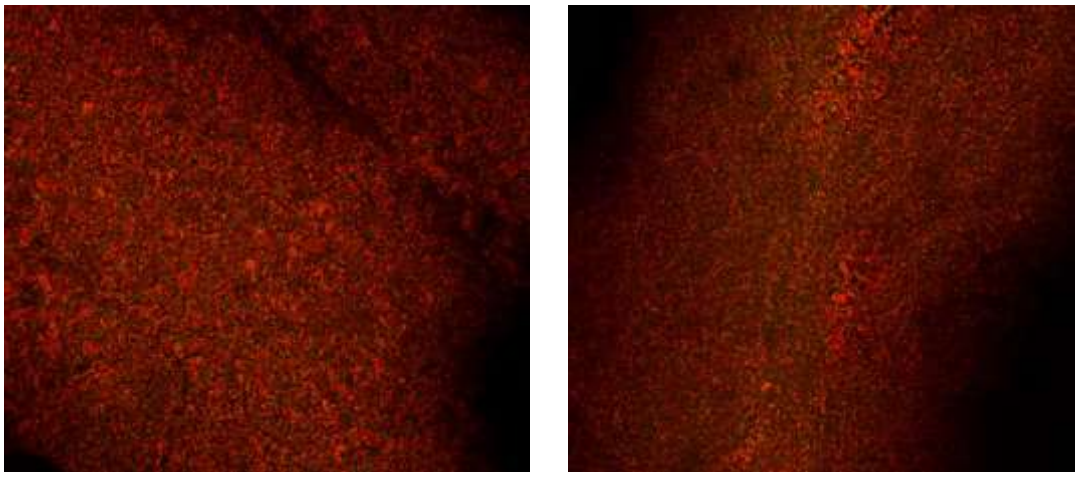

Figure 36: SmC Phase of C12BP-G2.0 PAMAM at 150^0C (left) and 187^0C (right)

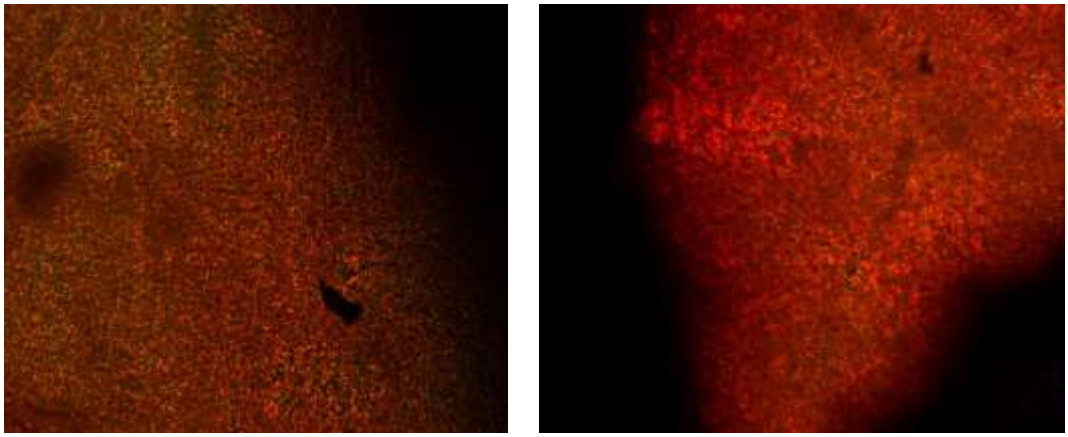

Figure 37: SmC Phase of C12BP-G3.0 PAMAM at 163^0C (left) and 201^0C (right)

4.1.8 C12-PAMAM and C10*BP-PAMAM Ionic Liquids

Two mesomeric molecules (C12 and C10*BP), shown in Figure 28, were reacted with PAMAM dendrimers as described in Figure 29. Structural characterization is firstly performed by FT-IR.

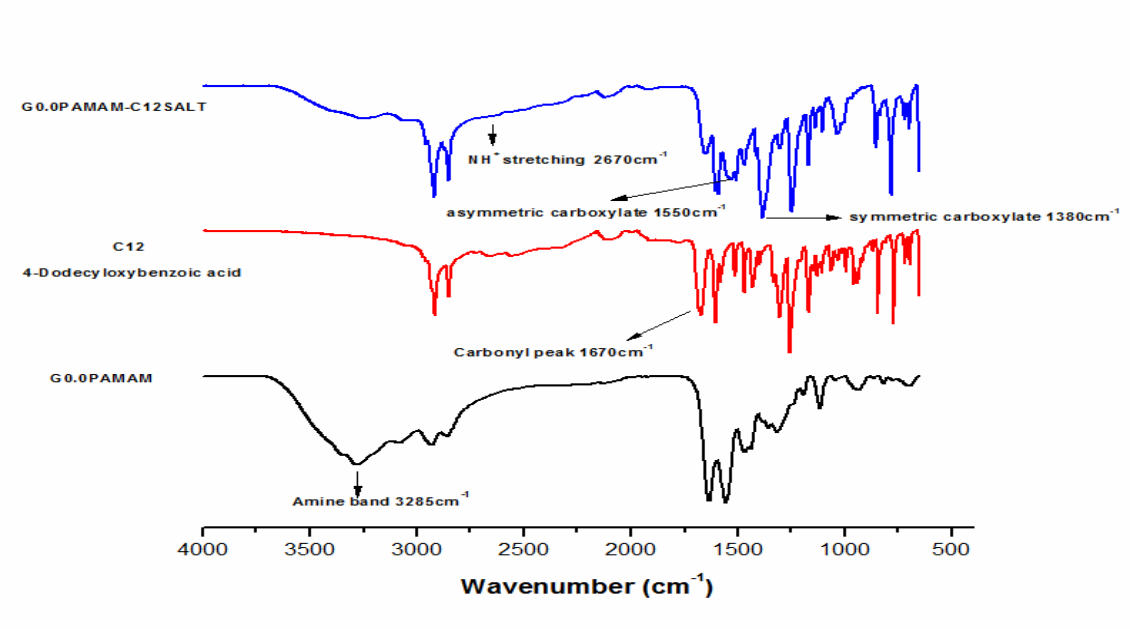

Figure 38: FT-IR Spectra of G0.0 PAMAM, C12, G0.0 PAMAM-C12 Salt

As shown in Figure 38 for G0.0 PAMAM-C12 salt, in addition to disappearing of carbonyl group and amine group, symmetric carboxylate peak was distinctively detected at 1380cm^{-1}. 1550 cm^{-1} band has stronger intensity due to the combination of amide II and asymmetric carboxylate.

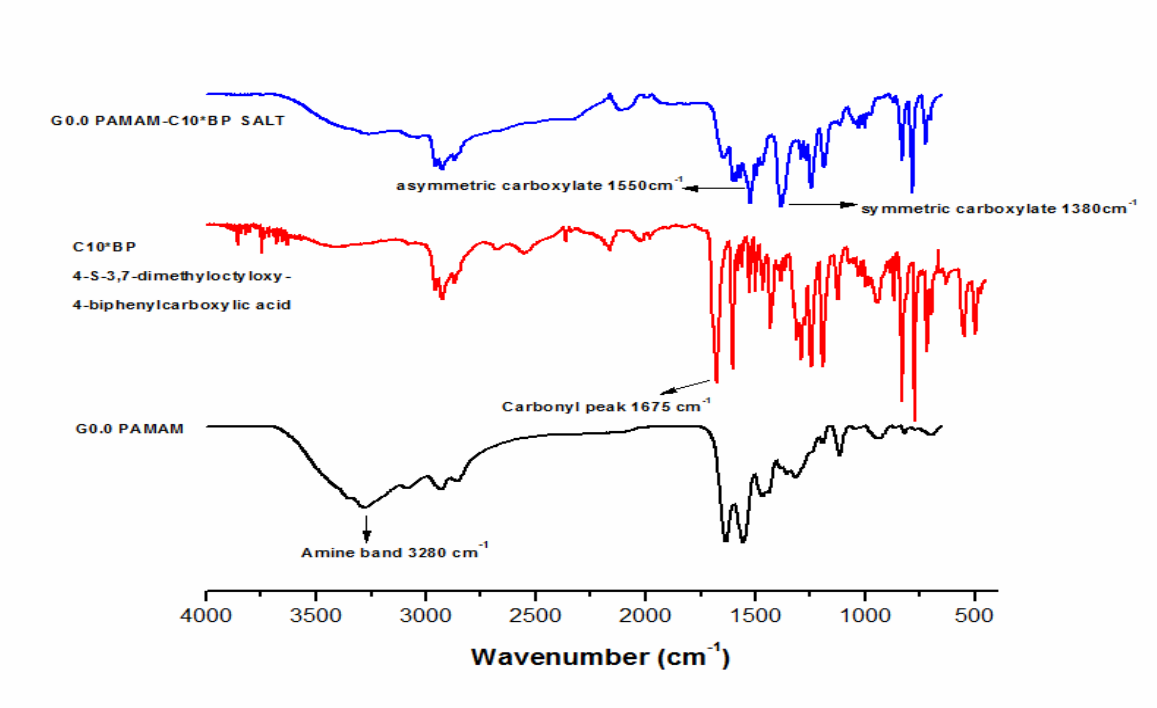

Figure 39: FT-IR Spectra of G0.0 PAMAM, C10*BP, G0.0 PAMAM-C10*BP Salt

FT-IR spectra G0.0PAMAM-C10*BP salt, shown in Figure 39, is similar to G0.0PAMAM-C12. Another confirmation of ionic reaction is proton and carbon NMR spectra.

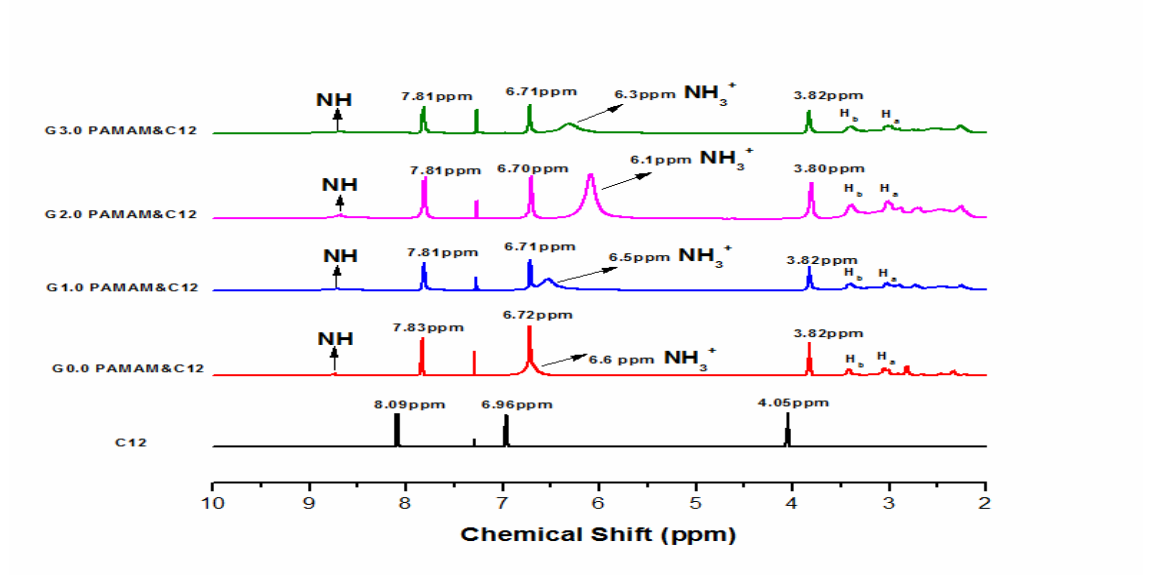

Figure 40: ^{1}H NMR Spectra of G0.0-G3PAMAM C12 Salts and C12 acid ($CDCl_3$)

As shown in Figure 40, N***H***$_3^+$ broad band started to be appeared around 6.1ppm to 6.6 ppm compared to C12 alkoxy benzoic acid. In addition, very small N-***H*** peak is observed around 8.7ppm for all four salts. Aromatic peaks (8.09ppm and 6.96ppm) of C12 acid are shifted to upper field (ca 7.81ppm and ca 6.71ppm) respectively in ionic form for four samples. Similarly, oxymethylene peak located at 4.05ppm is shifted to ca 3.82ppm for salts. Another indication of protonation of primary amines is proved by observing H^b at 3.41 ppm and observing H^a at 3.01ppm for CH_2^b-CH_2^a-NH_3^+ in all four ionic states.

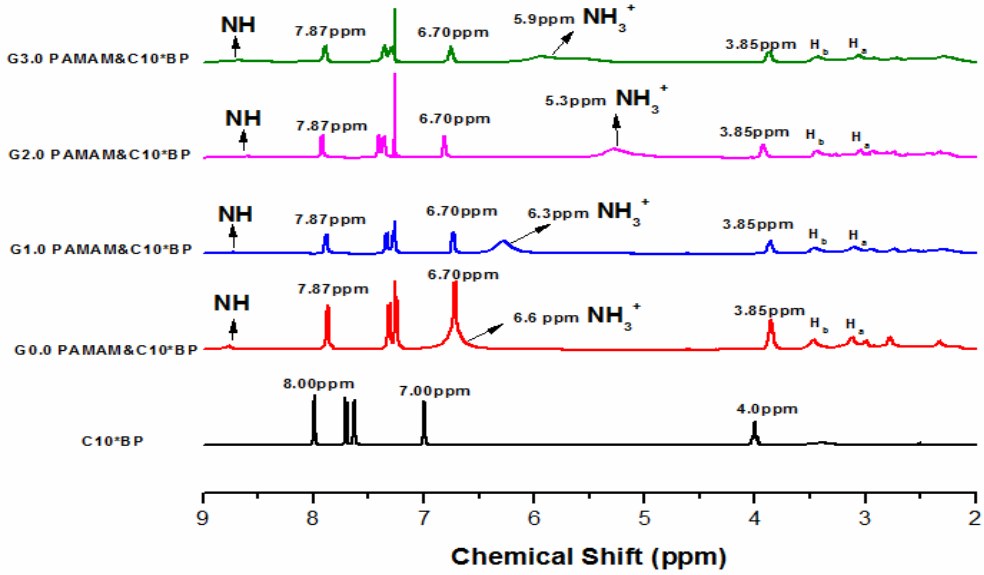

Figure 41: ^{1}H NMR Spectra of G0.0-G3PAMAM-C10*BP Salts and C10*BP acid ($CDCl_3$)

As described in Figure 41, for C10*BP based PAMAM salts, aromatic peaks (8.0ppm, 7.7ppm, 7.63ppm and 7.0ppm) of C10*BP shift to upper field to 7.87ppm, 7.35ppm,7.26ppm and 7.0ppm respectively in ionic form. Similarly, oxymethylene peak of C10*BP shifts from 4.0ppm to 3.85ppm. Also, in ionic state, the small and characteristic peak of (N***H***-C=O) is observed at 8.03ppm. Similarly, the peak of N***H***$_3^+$ is appeared as a broad peak at 6.6ppm, 6.3 ppm, 5.3ppm and 5.9ppm for four salts. Another indication of protonation of primary amines is demonstrated by detecting H^b at 3.45 ppm and H^a at 3.10ppm for CH_2^b-CH_2^a-NH_3^+.

The location of carbonyl peak (171.69ppm) peak of C12 acid, as shown in Figure 42 (^{13}C NMR Spectra and demonstration on the right side), shifts to lower field 173.71ppm (around +2.02ppm). On the other side, aromatic carbon (next to oxygen) of C12 acid has moved from 163.72ppm to 161.36ppm (around -2.36ppm) in the direction of upper field. It means that chemical shift difference of two lower field peaks is increased from 7.97ppm (171.69ppm; 163.72ppm) to 12.35ppm (173.71ppm; 161.36ppm).

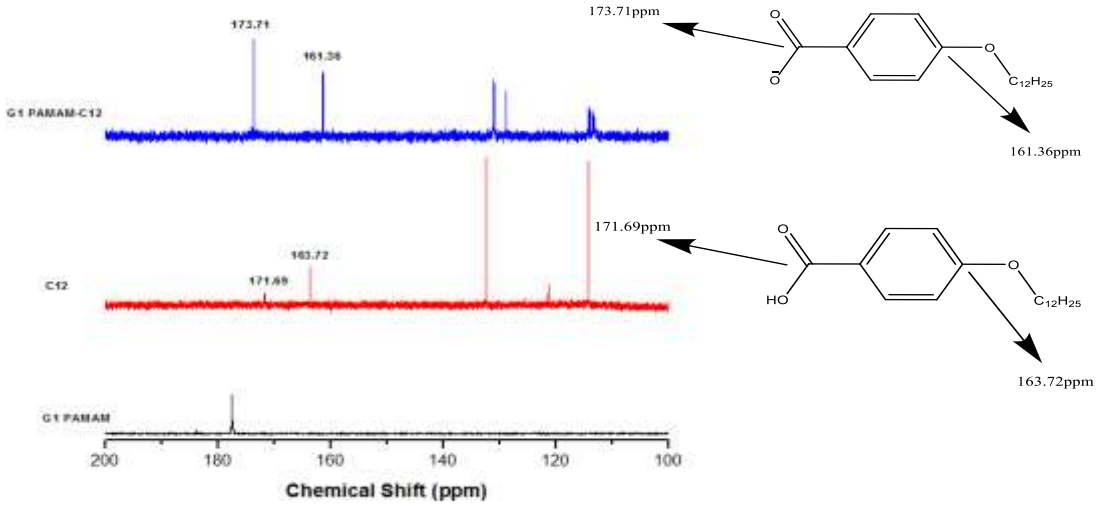

Figure 42: ^{13}C NMR Spectra of G1.0 PAMAM (D2O), C12 acid ($CDCl_3$) and G1.0PAMAM&C12 Salt ($CDCl_3$).

As ^{13}C NMR Spectra demonstrated in Figure 42, like C12&PAMAM salts, the similar observation is coincided with C10*BP&PAMAM salts (see Figure 43). The location of carbonyl peak of C10*BP acid dramatically shifts to lower field 167.65ppm to 173.76ppm (around +6.11ppm). In addition, aromatic carbon (next to oxygen) of C10*BP acid has moved from 159.42ppm to 158.96ppm (around -0.46ppm) in the direction of upper field. It means that chemical shift difference of two lower field peaks is increased drastically from 8.23 ppm (167.65ppm; 159.42ppm) to 14.80ppm (173.76ppm; 158.96ppm).

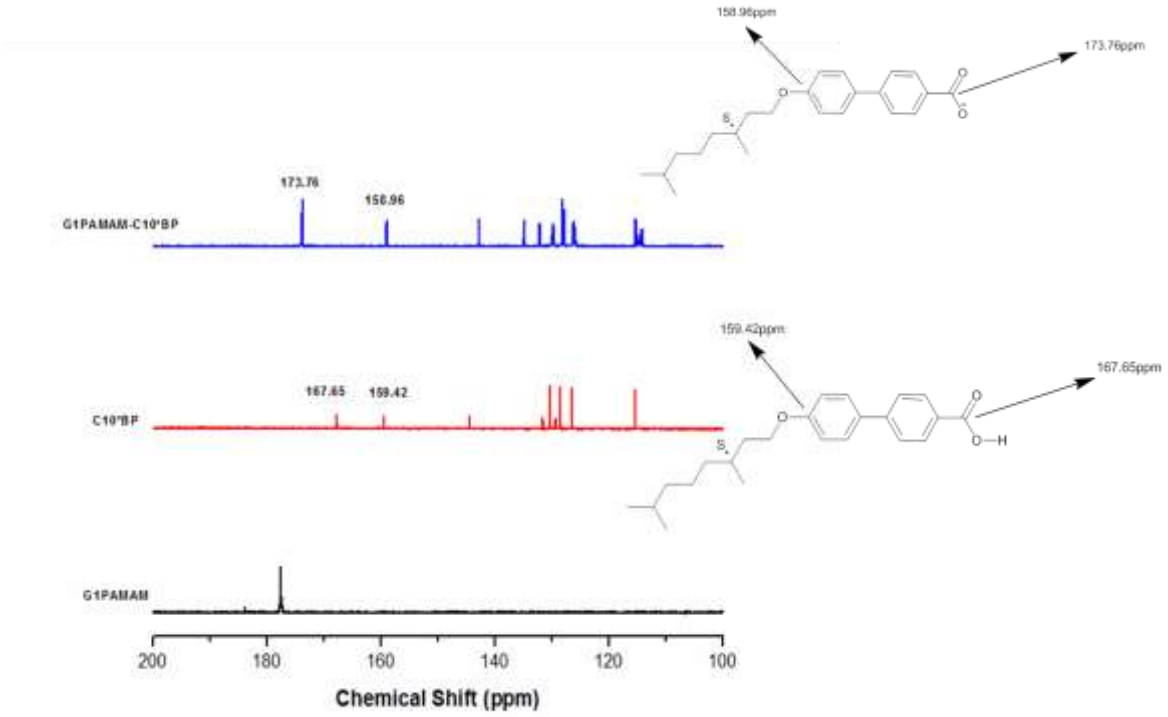

Figure 43: 13C NMR Spectra of G1.0 PAMAM (D_2O), C10*BP acid ($CDCl_3$) and G1.0PAMAM& C10*BP Salt ($CDCl_3$).

Liquid crystal properties of 4-(Dodecyloxy) benzoic acid (**C12**)-PAMAM salts, 4'-(3S)-3,7-dimethyloctyloxy-4-biphenylcarboxylic acid (**C10*BP**)-PAMAM salts were investigated by POM and DSC. Results are shown below Table 4.

Table 4: POM Results of 4-(Dodecyloxy) benzoic acid-PAMAM

Name	**Phase transitions by Polar Microscope**	**Phase transitions and enthalpy values (J/gr) by DSC**
4-(Dodecyloxy) benzoicacid **(C12)**	Cr 88ºC SmC 119 ºC N 134 ºC Iso Iso 130 ºC N 119 ºC SmC 81 ºC Cr	
C12-G0.0 PAMAM	Iso 171 ºC SmA101-91 ºC Cr	Cr 90 ºC SmA 185 ºC I
C12-G1.0 PAMAM	Iso 179 ºC SmA 108-97 ºC Cr	Cr 120 ºC (7.73 J/gr) SmA 190 ºC I
C12-G2.0 PAMAM	Iso 168 ºC SmA89-82 ºC Cr	Cr 115 ºC (25.4 J/gr) SmA 186 ºC I
C12-G3.0 PAMAM	Iso 173 ºC SmA104-93 ºC Cr	Cr 116 ºC (16.83 J/gr) SmA 185 ºC I

According to results shown at Table 4, both ionic groups 4-(Dodecyloxy) benzoic acid-PAMAM and 4'-(3S)-3,7-dimethyloctyloxy-4-biphenylcarboxylic acid-PAMAM have mesomeric properties. Figure 44-47 show smectic A phase of four generation salts. Mesomeric range of C12- PAMAM is clearly increased compared to its building block promesogenic unit (C12). 4-(Dodecyloxy) benzoic acid has smectic C and nematic phases starting from about 80-90 ^{o}C to 130 ^{o}C. C12-PAMAM salts have smectic A mesophase from 90-110 ^{o}C to 170-190 ^{o}C. There is a mesophase enlargement about 40-60 ^{o}C. Moreover, according to POM results, we cannot say meaning change by changing generation of dendrimers. However, according to DSC results there is a slight shrinkage of mesomeric range by increasing generation. It can be again attributed to overcrowding of amino groups at surface of dendrimer.

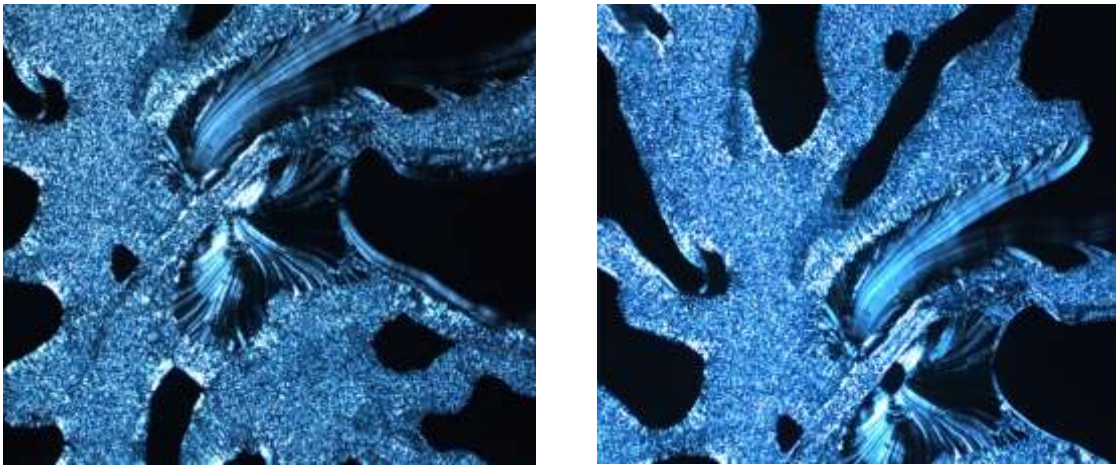

Figure 44: SmA Phase of C12-G0.0 PAMAM at 98^{0}C (left) and 150^{0}C (right)

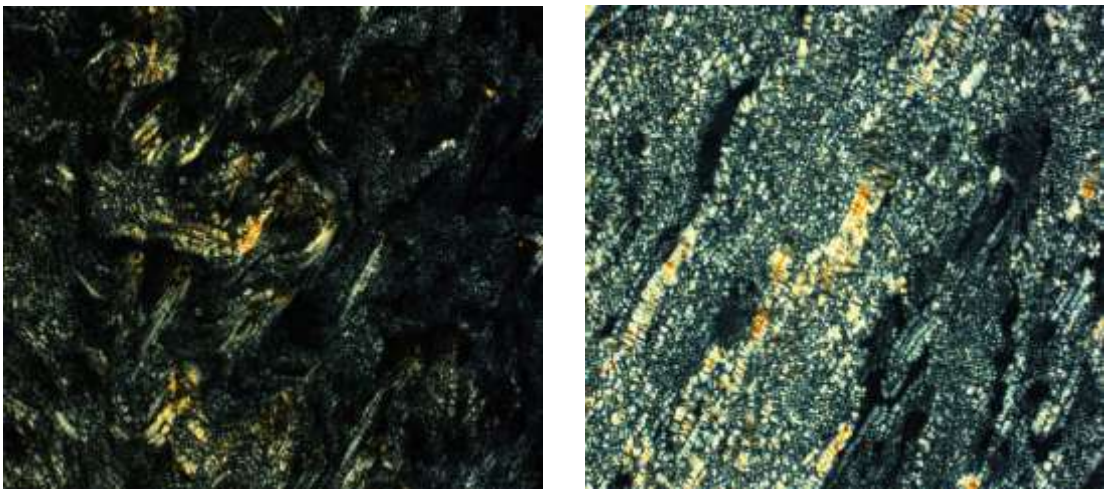

Figure 45: SmA Phase of C12-G1.0 PAMAM at 96^{0}C (left) and 130^{0}C (right)

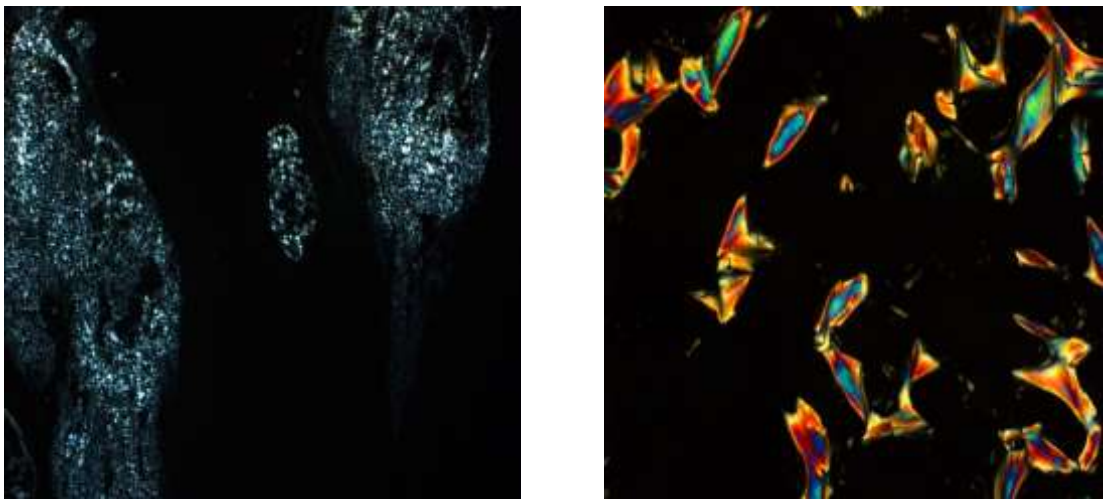

Figure 46: SmA Phase of C12-G2.0 PAMAM at 113^0C (left) and 159^0C (right)

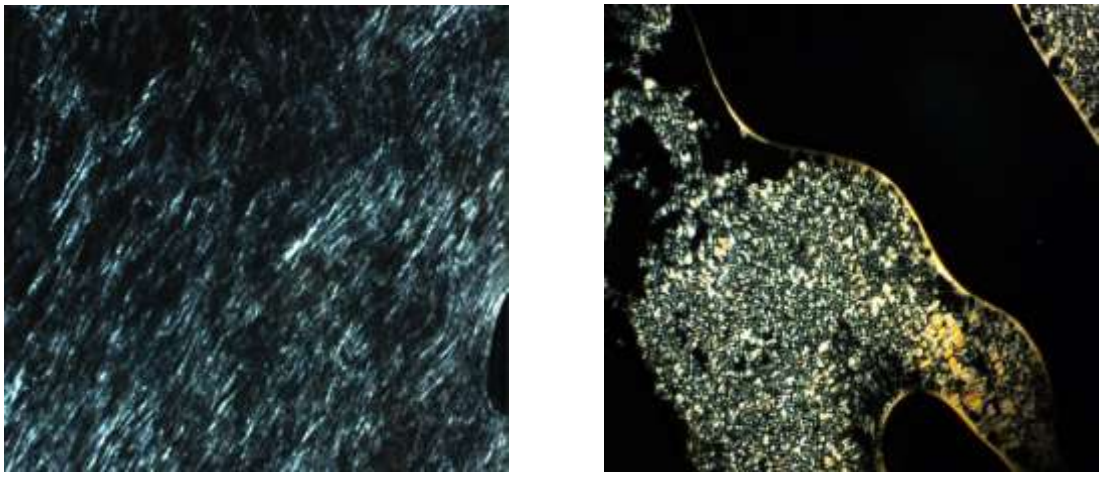

Figure 47: SmA Phase of C12-G3.0 PAMAM at 93^0C (left) and 160^0C (right)

Similarly, there is distinctive increase for mesomeric range for C10*BP- PAMAM compared to 4'-(3S)-3,7-dimethyloctyloxy-4-biphenylcarboxylic acid (C10*BP) having two mesophases (SmI and nematic). As shown in Table 5, mesomeric range of C10*BP starts at 163 ºC and diminishes at 226 ºC. Mesomeric range of PAMAM- C10*BP salts starts around 110-130 ºC and vanishes around 230 ºC. DSC results are generally coherent with POM results. According to both results, we can say that there is an enlargement around 30-50 ºC for SmX phase. Figure 48-51 demonstrate Smectic X phase of all generation salts for different temperature points. By increasing generation, there is no meaningful change. It means that mesomeric properties of total system are independent of dendrimer generation.

Table 5: POM Results of 4'-(3S)-3,7-dimethyloctyloxy-4-biphenylcarboxylic acid-PAMAM

Name	**Phase transitions by Polar Microscope**	**Phase transitions and enthalpy values (J/gr) by DSC**
4'-(3S)-3,7-dimethyloctyloxy-4-biphenylcarboxylicacid **(C10*BP)**	Cr 163 ºC SmI* 224 N* 226 ºC Iso	
C10*BP-G0.0 PAMAM	Cr 135 ºC SmX* 232 ºC Iso	Cr 113 ºC (8.67 J/gr) SmX* 246 ºC (6.49) I
C10*BP-G1.0 PAMAM	Cr 122 ºC SmX* 225 ºC Iso	Cr 101 ºC (14.69 J/gr) SmX*242 ºC I
C10*BP-G2.0 PAMAM	Cr 113 ºC SmX* 224 ºC Iso Iso 227 ºC SmX* 124 ºC Cr	Cr 130 ºC (4.80 J/gr) SmX*246 ºC I
C10*BP-G3.0 PAMAM	Cr 137 ºC SmX* 198-213 ºC Iso	Cr 109 ºC (28.2 J/gr) SmX* 236 ºC I

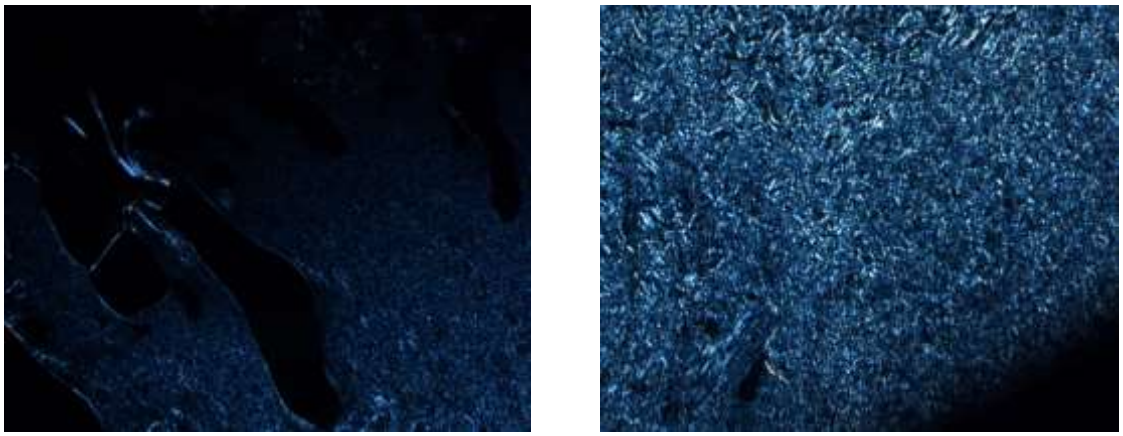

Figure 48: SmX Phase of C10*BP-G0.0 PAMAM 149ºC (left) and 185ºC (right)

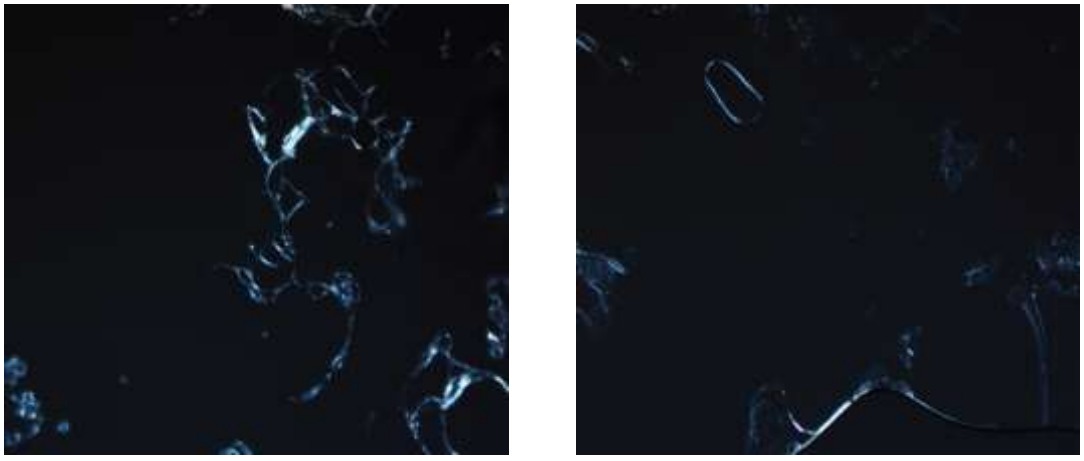

Figure 49: SmX Phase of C10*BP-G1.0 PAMAM 167^{o}C (left) and 189^{o}C (right)

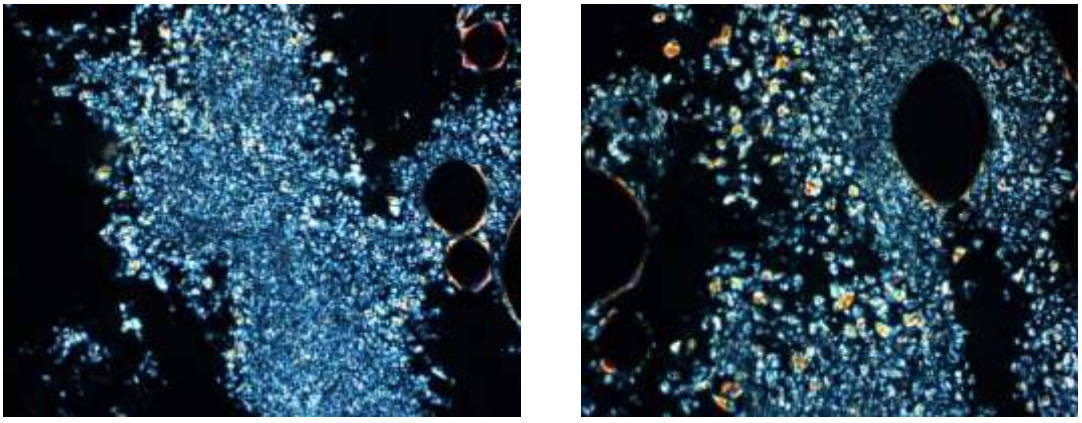

Figure 50: SmX Phase of C10*BP-G2.0 PAMAM 163^{o}C (left) and 212^{o}C (right)

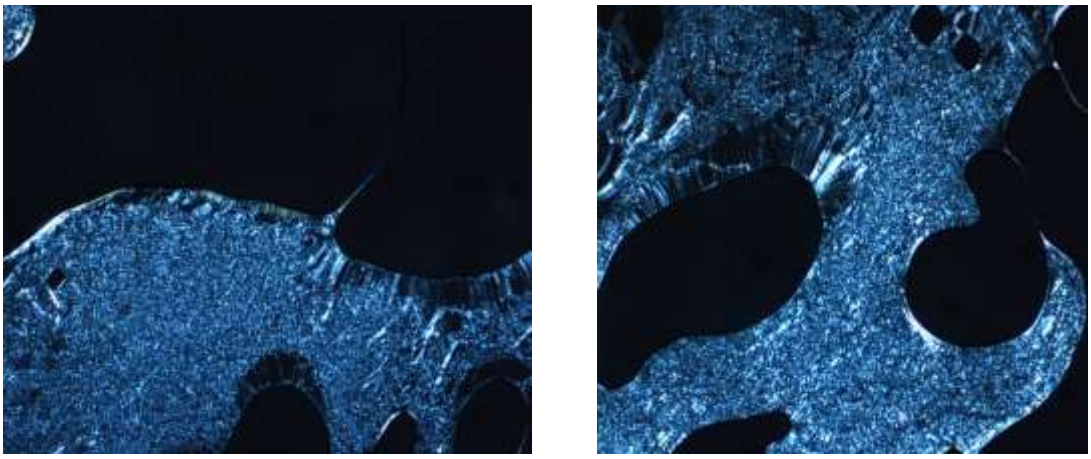

Figure 51: SmX Phase of C10*BP-G3.0 PAMAM 137^{o}C (left) and 171^{o}C (right)

4.1.9 S-CBA (S-4-Citronellyoxy benzoic acid) -PAMAM Ionic Liquids

For studies all five mesomeric units (4-(4-Octyloxyphenyl)benzoic acid (**C8BP**), 4-(4-Dodecyloxyphenyl) benzoic acid (**C12BP**), 4-(Octyloxy) benzoic acid (**C8**), 4-(Dodecyloxy) benzoicacid (**C12**), 4'-(3S)-3,7-dimethyloctyloxy-4-biphenylcarboxylic acid (**C10*BP**), we faced seriously or partially thermal degradation problems due to mesomeric range of mesomeric units at high temperatures (isotropization temperature higher than 150 ^{o}C). For this reason, we also would like to choose a mesomeric unit having lower isotropization temperature. This mesomeric unit (S-4-Citronellyoxy benzoic acid) shown in Figure 52 has very narrow mesomeric range and lower isotropization temperature. S-CBA is a new molecule synthesized by Eran group according to literature [106].

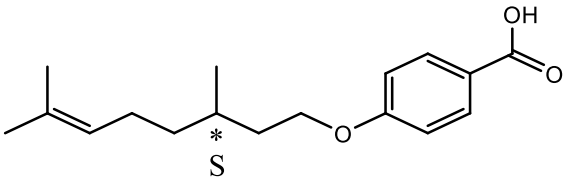

Figure 52: S-4-Citronellyoxy benzoic acid (S-CBA)

By using this molecule and PAMAM dendrimers, series of ionic dendrimers were synthesized by ultrasonication in tetrahydrofuran solvent as described in Figure 29. Structural characterization is performed by firstly FT-IR and later ^{1}H NMR and ^{13}C NMR spectroscopy. FT-IR spectroscopy, in Figure 53, shows disappearing of carbonyl group at 1670cm^{-1} of S-CBA acid and primary amine groups around 3300cm^{-1} of PAMAM Symmetric carboxylate peak of ionic form was clearly detected at 1380cm^{-1} without significant interference. 1550 cm^{-1} band in the ionic form has stronger intensity than pure amide II peak of PAMAM dendrimer due to the combination of amide II and asymmetric carboxylate.

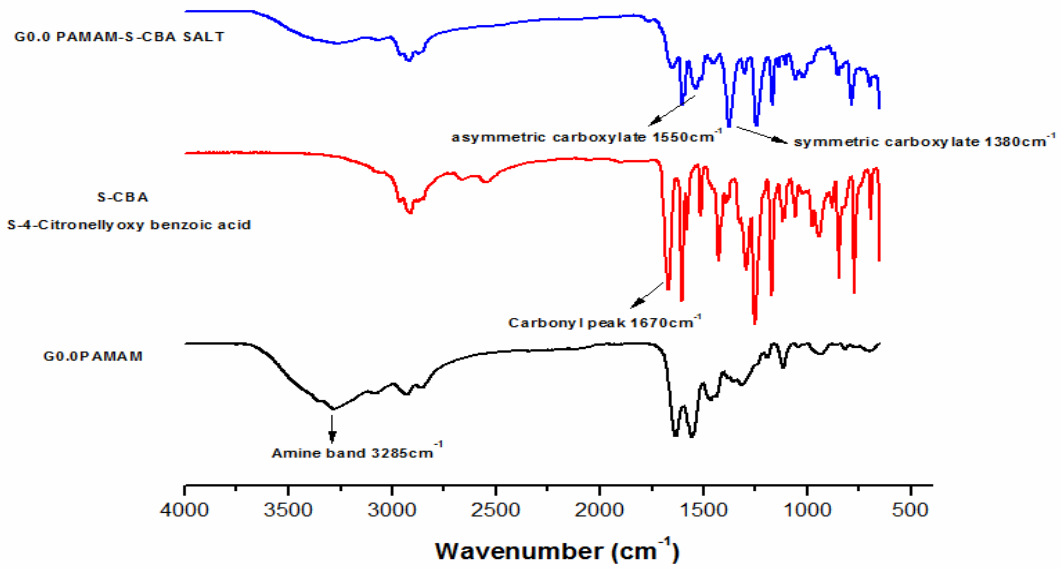

Figure 53: FT-IR Spectra of G0.0 PAMAM, S-CBA, G0.0 PAMAM-S-CBA Salt

A shown in Figure 54, the proton of olefin keeps its position at 5.08ppm for ionic form and S-CBA acid molecule due to non-significant change of its electronic environment. It also means that this peak can be accepted as reference for this study. New peaks in electrostatic form compared to S-CBA acid are characteristic peak of (N***H***-C=O) is observed at 8.70ppm and the broad and significant ammonia ($N\boldsymbol{H}_3^+$) peak at 6.1ppm. On the cationic side, when CH_2^b-CH_2^a-NH_2 state moves to CH_2^b-CH_2^a-NH_3^+, H^b moves from 3.15 ppm to 3.37ppm and H^a from 2.65ppm to 3.00ppm. Aromatic peaks of S-CBA shifts from 8.05ppm and 6.92ppm to 7.80ppm and 6.68ppm respectively.

As demonstrated in Figure 55, like dendritic ionic liquids, the location of carbonyl peak of S-CBA acid shifts from 172.37ppm to 173.67ppm (around +1.34ppm). On the other hand, aromatic carbon (next to oxygen) of S-CBA acid has moved from 163.70ppm to 161.33ppm (around -2.37ppm). It means that chemical shift difference of two lower field peaks is increased from 8.67 ppm (172.37ppm; 163.70ppm) to 12.38ppm (173.67ppm; 161.33ppm).

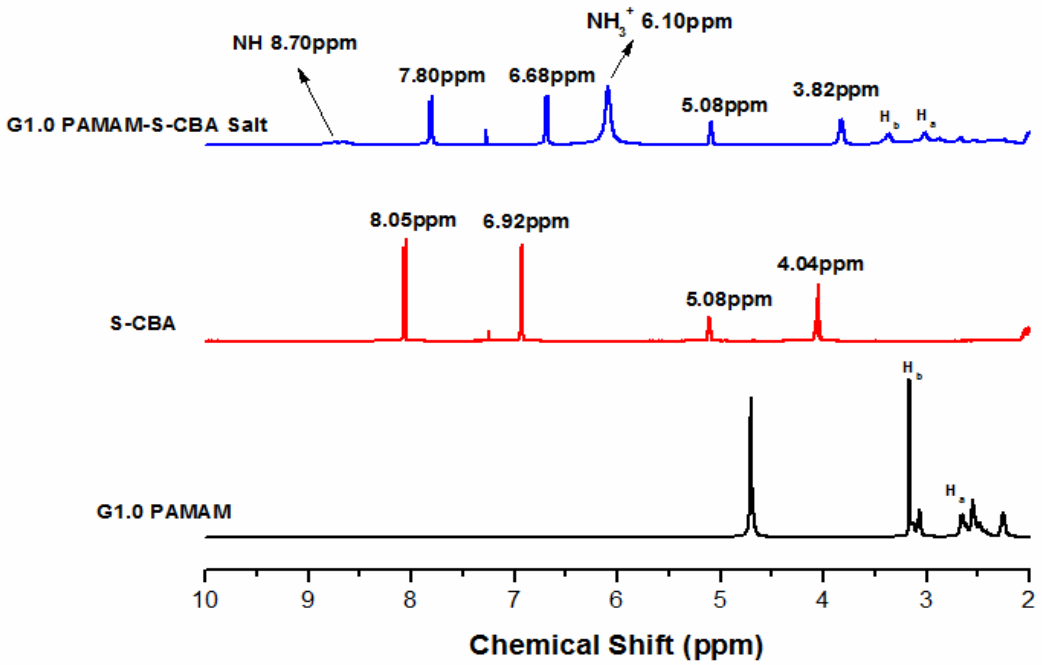

Figure 54: ^{1}H NMR Spectra of G1.0 PAMAM (D_2O), S-CBA acid ($CDCl_3$) and G1.0PAMAM&S-CBA Salt ($CDCl_3$).

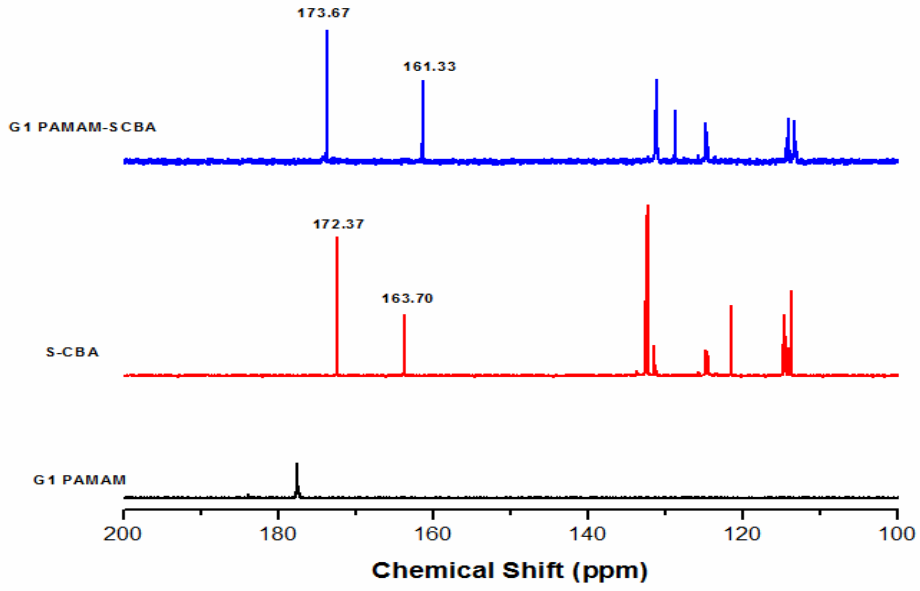

Figure 55: ^{13}C NMR Spectra of G1.0 PAMAM (D_2O), S-CBA acid ($CDCl_3$) and G1.0PAMAM&S-CBA Salt ($CDCl_3$).

All ionic dendrimers show liquid crystal property. Polarized Optical Microscopy and Differantial scanning calorimetry shown below Table 6 were used for characterization.

Table 6: S-4-Citronellyoxy benzoic acid (S-CBA)-PAMAM Salts

Name	**Phase transitions by Polar Microscope**	**DSC**
S-4-Citronellyoxy benzoic acid **(S-CBA)**	**Heating:** Cr 73 SmC* 80 Iso **Cooling:** SmC* 66.5 °C Cr	
S-CBA-G0.0 PAMAM	**Heating:** Cr 78°C SmA 118-120°C Iso **Cooling:** Iso 92-93°C SmA 30°C Cr	Cr 26°C SmA Not Clear Iso
S-CBA & G1.0 PAMAM	**Heating:** $Cr_1$88°C (softening) Cr_2 127 °C SmA 151°C Iso **Cooling:** Iso 141°C SmA 90°C (viscous) 71°C Cr	Cr 40,23°C SmA 120°C Iso
S-CBA & G2.0 PAMAM	**Heating:** Cr 70°C (softening and SmA) 139°C Iso **Cooling:** Iso 109°C SmA 55°C (viscous)38°C Cr	Cr 45°C SmA Not Clear Iso
S-CBA & G3.0 PAMAM	**Heating:** SmA 145-150°C Iso **Cooling:** Iso 127°C SmA 65°C (viscous) 60°C Cr	Cr 46°C SmA 90-120°C (very broad&ambigous) Iso

According to results in Table 6, mesomeric range of S-CBA is 7°C, it was increased to at least 40°C and at maximum 70°C. This increase is again related to oil property or inherit flexible property of dendrimer. Figure 56-59 depict smectic A phases at different temperatures for salts of all generations. It was seriously difficult to determine isotropization point by DSC. Even by POM, transition to isotropization or transition to crystallization were observed as step by step. This situation can be peculiar to macromolecular-polymeric system or ionic state.

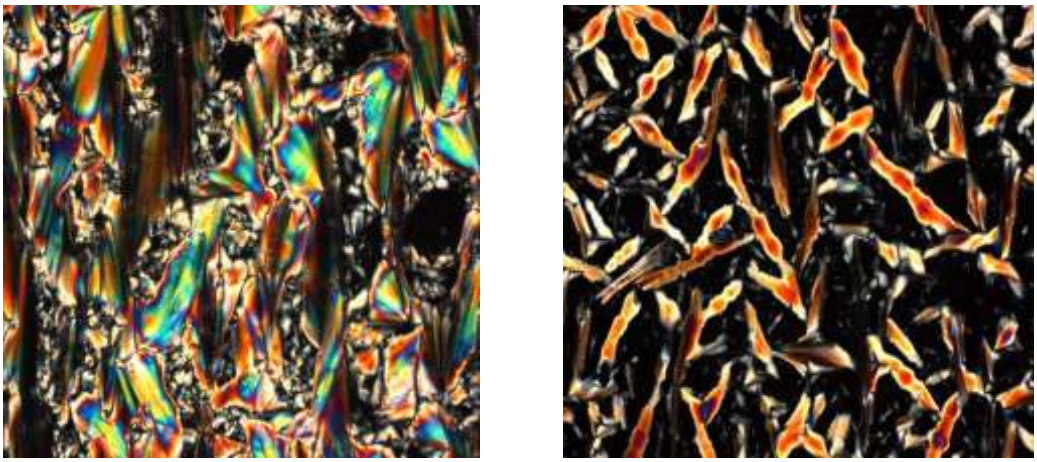

Figure 56: SmA Phase of S-CBA-G0.0 PAMAM 35^{o}C (left) and 85^{o}C (right)

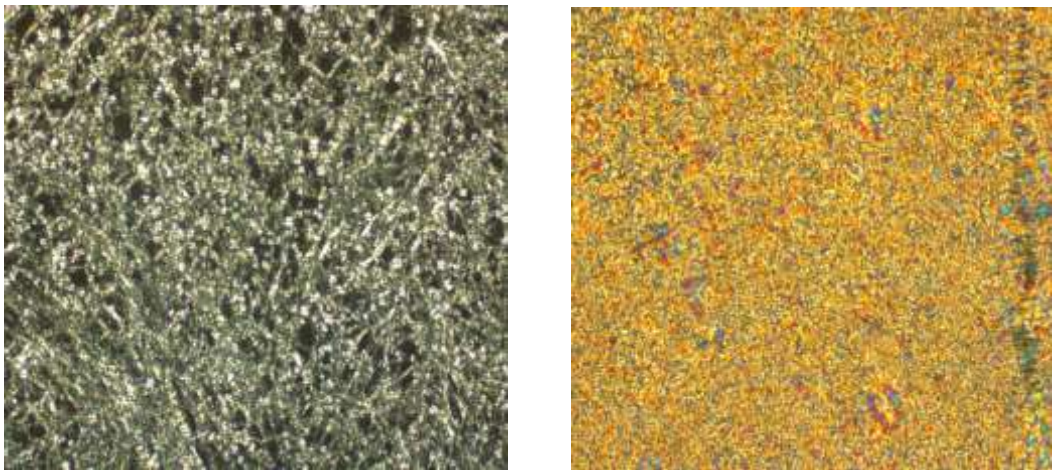

Figure 57: SmA Phase of S-CBA-G1.0 PAMAM 94^{o}C (left) and 139^{o}C (right)

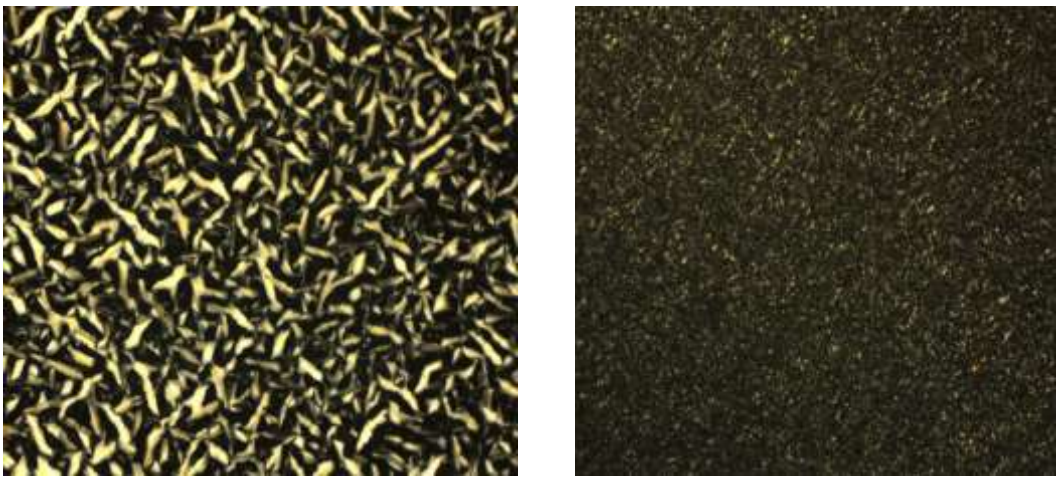

Figure 58: SmA Phase of S-CBA-G2.0 PAMAM 100^{o}C (left) and 103^{o}C (right)

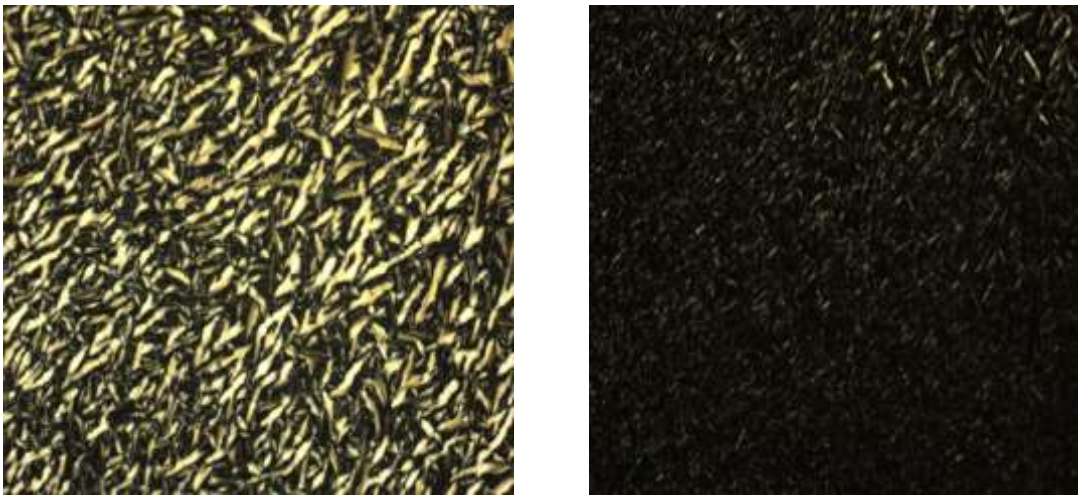

Figure 59: SmA Phase of S-CBA-G3.0 PAMAM 103ºC (left) and 126ºC (right)

4.2 Trimesic Acis Rooted Amidoamine ($Tr\text{-}(NH_2)_n$) Dendritic Ionic Liquids

As cationic part, trimesic acid rooted polyamidoamine dendrimers are chosen. After the synthesis of them, various types of dendritic liquid crystal salts are studied.

4.2.1 $Tr\text{-}(NH_2)_n$ Dendrimers

These amidoamine dendrimers have trimesic acid core, later in second step trimesic acid ester. This is different from PAMAM dendrimers having ethylene diaminde core. In literature, trimesic acid based dendrimers are studied until first two generations. In our studies, two more generations have been built on them. Next sections, synthesis and characterization of them were described.

4.2.2 Synthesizing $Tr\text{-}(NH_2)_n$ Dendrimers

To study another form of ionic liquid crystal macromolecules, we synthesized trimesic acid ester from trimesic acid using concentrated sulfuric acid and excess amount of methanol. Next step, we added excess amount of ethylene diamine into trimesic acid ester at around 10^0C utilizing the reference [107-108]. We named this amine terminated molecule $Tr\text{-}(NH_2)_3$. Consecutively, as shown in Figure 60-61, we synthesized $Tr\text{-}(NH_2)_6$, $Tr\text{-}(NH_2)_{12}$ and $Tr\text{-}(NH_2)_{24}$ macromolecules by cycling of methyl acrylate and ethylenediamine. For purification, we used dialysis mechanism with 500, 1000 and 3000 Dalton poresize.

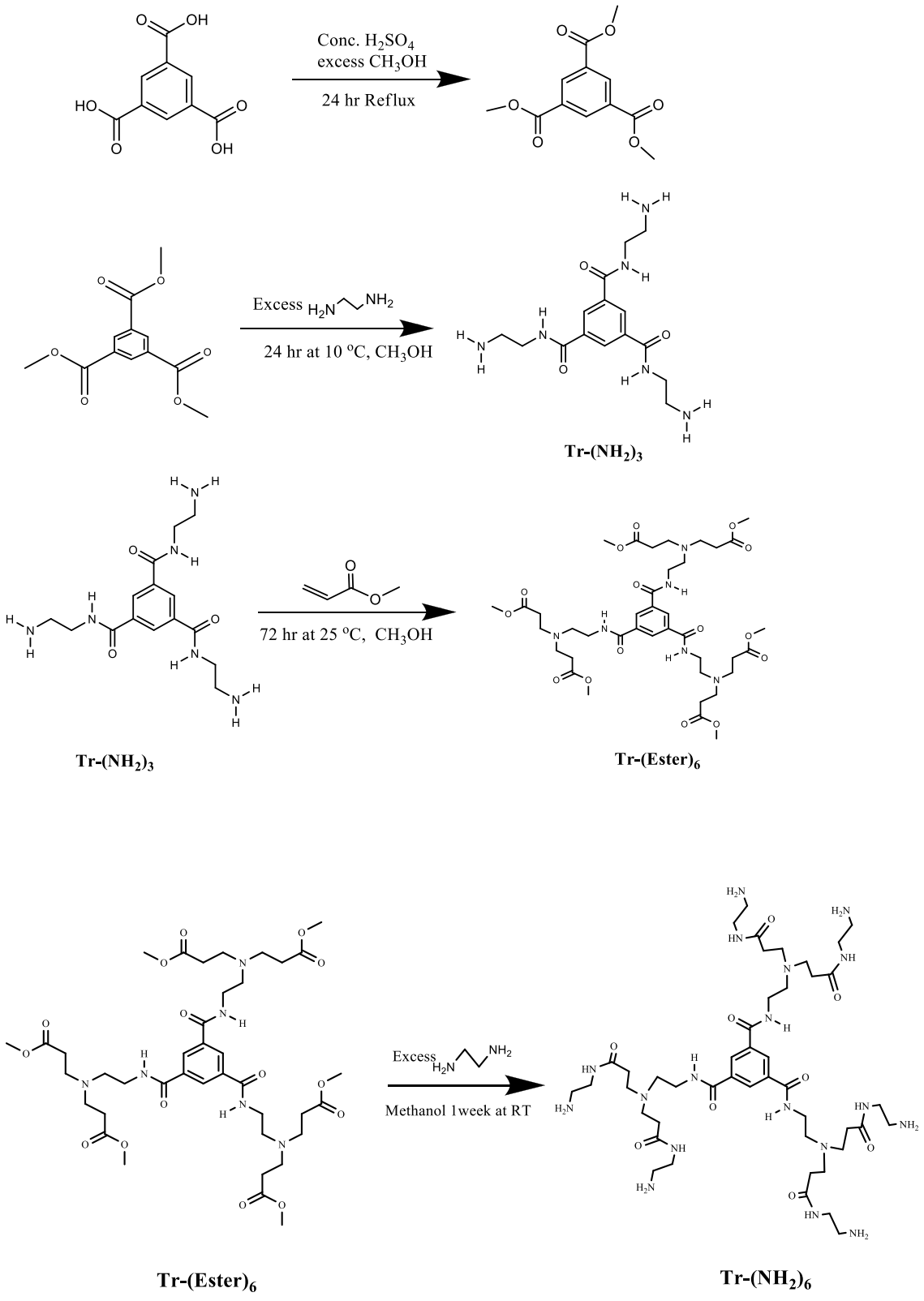

Figure 60: Reaction representation of Tr-$(NH_2)_6$ starting from trimesic acid.

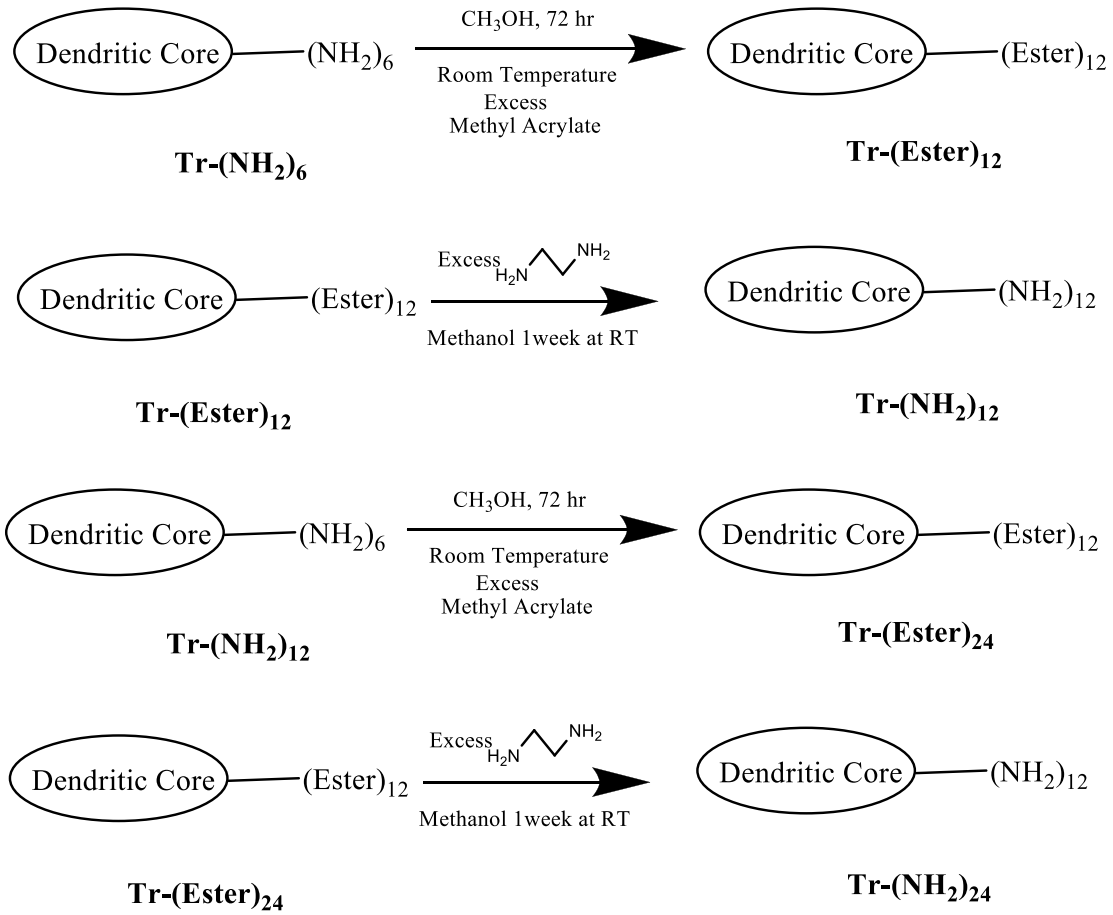

Figure 61: Iterative reaction representation of trimesic acid rooted amidoamine dendrimer (from Tr-$(NH_2)_6$ to Tr-$(NH_2)_{24}$)

4.2.3 Characterization of Tr-$(NH_2)_n$ Dendrimers

The amidation reaction has been followed by IR inspecting primary amine peaks around 3300 cm^{-1} and ester peaks around 1730 cm^{-1} (see Figure 62). Half generations have ester peaks due to carbonyl group. Full generations have lost ester peaks and gained amine peaks.

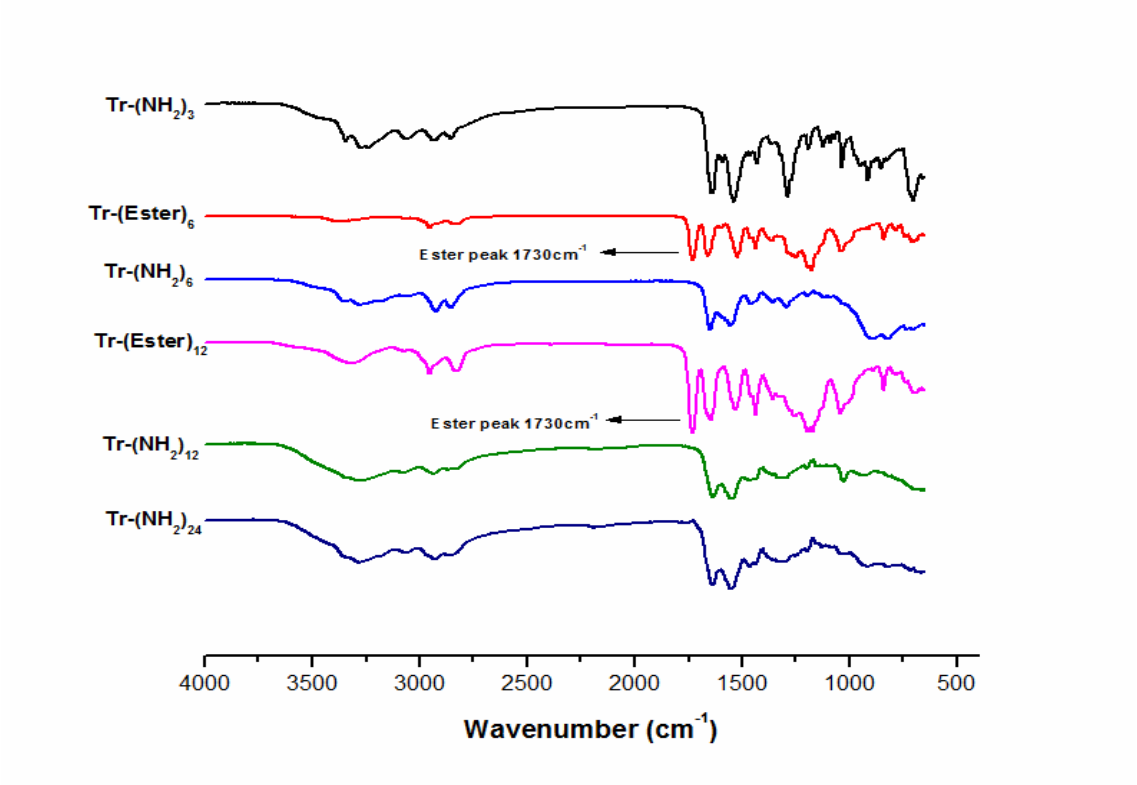

Figure 62: FT-IR Spectra of half and full generations of trimesic acid rooted amidoamine dendrimer

^{13}C NMR spectra of Tr-$(NH_2)_6$ and Tr-$(NH_2)_{12}$ clearly confirm the synthesis has been performed. As shown in Figure 63, 171.55ppm of Tr-$(NH_2)_6$ and 172.20ppm of Tr-$(NH_2)_{12}$ belongs to outer amide peak which is clear indication of reaction occurring. 165.57ppm of Tr-$(NH_2)_6$ and 165.86ppm of Tr-$(NH_2)_{12}$ belong to inner core amide (close to benzene ring). Since inner core (close to benzene ring) has just three amide groups, the intensity of inner core amide peak is relatively lower than that of outer core amide peak. However, the number of outer amide group is 24 for Tr-$(NH_2)_{12}$ and is 6 for Tr-$(NH_2)_6$. For this reason, the intensity of 172.20ppm is more powerful that of 165.86ppm for Tr-$(NH_2)_{12}$ compared to Tr-$(NH_2)_6$. In addition, the observation of aromatic peaks (around 135ppm and 128ppm) is more difficult for Tr-$(NH_2)_{12}$ (higher generation) due to excessive number of carbons other than benzene carbons.

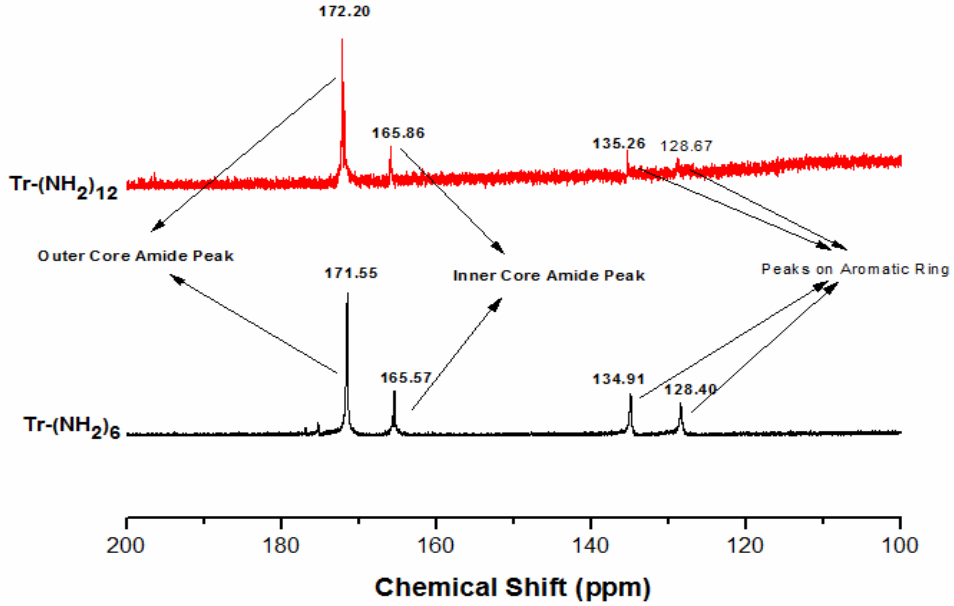

Figure 63: ^{13}C NMR Spectra of Tr-$(NH_2)_6$ and Tr-$(NH_2)_{12}$ Dendrimer (D_2O Solvent)

^{13}C NMR spectra of Tr-$(NH_2)_{24}$ is shown in Figure 64. Inner core amide peak and aromatic cannot be observed due to extremely fewer number of inner core amide and aromatic groups than the number of outer core amide groups and rest of carbon chains. Outer core amide peak cleary was detected at 171.90 ppm.

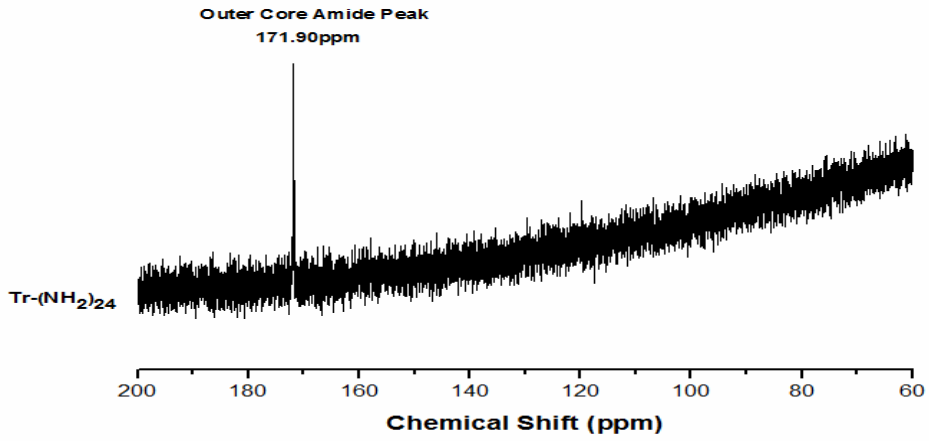

Figure 64: ^{13}C NMR Spectra of Tr-$(NH_2)_{24}$ Dendrimer (D_2O Solvent)

4.2.4 Synthesizing Trimesic Acid Rooted Dendritic Ionic Liquids

As described ahead in Figure 29, 4'-(3S)-3,7-dimethyloctyloxy-4-biphenylcarboxylic acid (C10*BP) and S-4-Citronellyoxy benzoic acid (S-CBA) were reacted with (Tr-$(NH_2)_3$, Tr-$(NH_2)_6$, Tr-$(NH_2)_{12}$, Tr-$(NH_2)_{24}$) dendrimers to obtain ionic dendrimers.

As shown in Figure 65, when ionic structure forms, the peak for carbonyl group of S-CBA and the peak for primary amine group of Tr-$(NH_2)_3$ disappear. The symmetric peak (1380cm^{-1}), the characteristic peak peaks of the salt, is appeared. Another characteristic peak of salt, asymmetric carboxylate (1550cm^{-1}), cannot be clearly observed. The reason for that is amide II peak of amidoamine dendrimer at 1550cm^{-1} band.

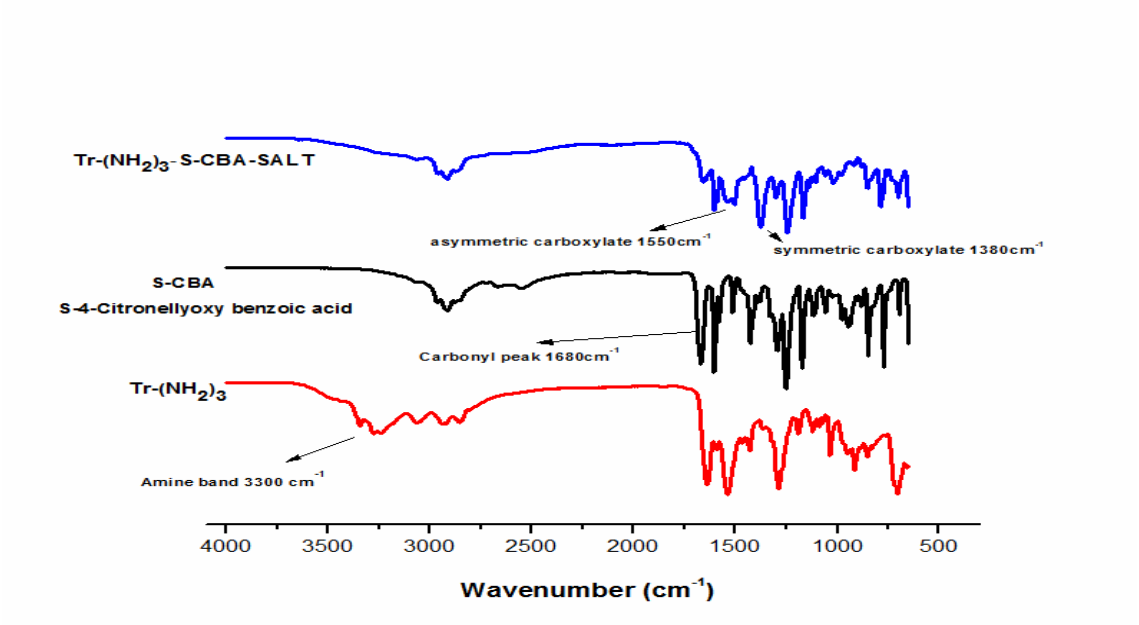

Figure 65: FT-IR Spectra of Tr-$(NH_2)_3$, S-CBA and Tr-$(NH_2)_3$-S-CBA Salt

Figure 66 shows ^{13}C NMR spectra of Tr-$(NH_2)_6$, S-CBA and Tr-$(NH_2)_6$-S-CBA salt. When carboxylic acid peak shifts from 172.37 ppm to lower field 173.34ppm (+0.97ppm), aromatic peak of S-CBA shifts from 163.70ppm to 161.54ppm (-2.16ppm).

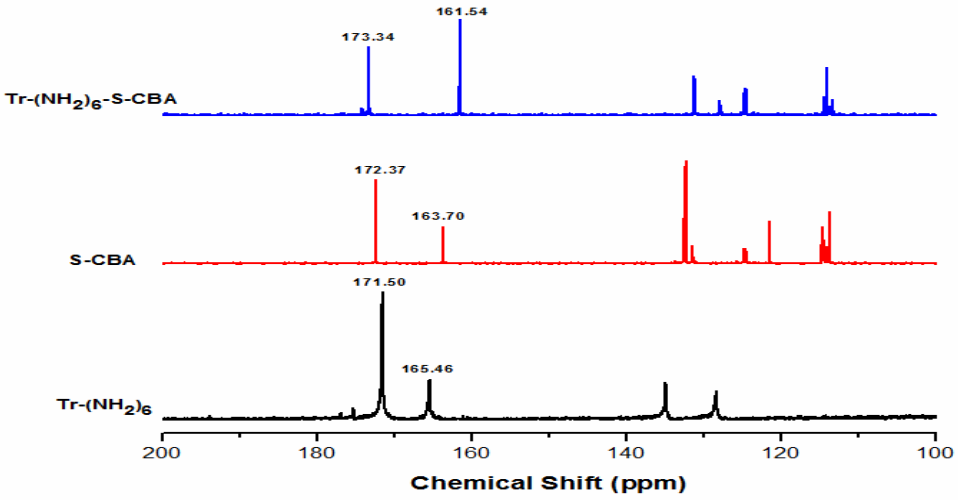

Figure 66: ^{13}C NMR Spectra of Tr-$(NH_2)_6$ (D_2O), S-CBA ($CDCl_3$) and Tr-$(NH_2)_6$ S-CBA Salt ($CDCl_3$)

4.2.5 Mesomeric Characterization of Tr-$(NH_2)_n$ Based Dendritic Ionic Liquids

POM analysis of these salts was completed for all. For some of them, DSC characterization was also performed. Table 7 shows the POM and DSC results of S-CBA- Tr-$(NH_2)_n$ and C10*BP- Tr-$(NH_2)_n$ salts.

Table 7: POM Results of Salts from 4'-(3S)-3,7-dimethyloctyloxy-4-biphenylcarboxylic acid (C10*BP) and S-4-Citronellyoxy benzoic acid (S-CBA) with (Tr-$(NH_2)_3$, Tr-$(NH_2)_6$, Tr-$(NH_2)_{12}$, Tr-$(NH_2)_{24}$) dendrimers

Name	POM Results	DSC Results
S-4-Citronellyoxy benzoic acid **(S-CBA)**	**Heating:** Cr 73^{0}C SmC* 80^{0}C Iso **Cooling:** SmC* 66.5 °C Cr	
Tr-$(NH_2)_3$-S-CBA	**Heating:** Cr 89^{0}C Smectic 152^{0}C Iso **Cooling:** Iso 142^{0}C Smectic 67^{0}C Cr	

Tr-$(NH_2)_6$ -S-CBA	**Heating:** Cr 77^0C SmA 159-162^0C Iso **Cooling:** Iso 146^0C SmA 81^0C Cr	Cr 51^0C SmA 123^0C Iso
Tr-$(NH_2)_{12}$-S-CBA	**Heating:** Cr 75-80 ^{o}C SmA 150 ^{o}C Iso **Cooling:** Iso 145 ^{o}C SmA 70 ^{o}C Cr	
Tr-$(NH_2)_{24}$ -S-CBA	**Heating:** Cr 68 ^{o}C SmA 145-150 ^{o}C Iso **Cooling:** Iso 150 ^{o}C SmA 58 ^{o}C Cr	
4'-(3S)-3,7-dimethyloctyloxy-4-biphenylcarboxylic acid **(C10*BP)**	**Heating:** Cr 163 ^{o}C SmI* 224 N* 226 ^{o}C Iso	
Tr-$(NH_2)_3$-C10*BP	**Heating:** Cr 85 ^{o}C SmX (SmA) 198-230 ^{o}C Iso **Cooling:** Iso 217 ^{o}C SmX (SmA) 80 ^{o}C Cr	Iso 165 ^{o}C Smectic
Tr-$(NH_2)_6$ -C10*BP	**Cooling:** Iso 160 ^{o}C Smectic	Iso 148 ^{o}C Smectic
Tr-$(NH_2)_{12}$-C10*BP	Material is LC, However due to heating at higher temperatures, characterization is not possible	

Similarly, by using of trimesic acid base amidoamine dendrimers makes the effect of enlargement of mesomeric range of S-4-Citronellyoxy benzoic acid (S-CBA) and 4'-(3S)-3,7-dimethyloctyloxy-4-biphenylcarboxylic acid (C10*BP). There is a considerable range (70^0C) for Tr-$(NH_2)_n$-S-CBA system. By increasing of generation, we did not observe any significant difference for both transition and type of mesomeric range. Figure 67-69 shows SmA phases of Tr-$(NH_2)_n$-S-CBA salts.Again, there is a significant range (140 ^{o}C) for Tr-$(NH_2)_3$-C10*BP system. However, for Tr-$(NH_2)_6$ -C10*BP and Tr-$(NH_2)_{12}$-C10*BP systems, due to heating at high temperatures, characterization was not able to be determined perfectly. Overheating like 180^{o}C makes disintegration of dendrimer. Although characterization is incomplete, texture type of

these two salts is definitely liquid crystal. Figure 70-71 shows mesomeric phase photographs of C10*BP –Tr-$(NH_2)_n$ system.

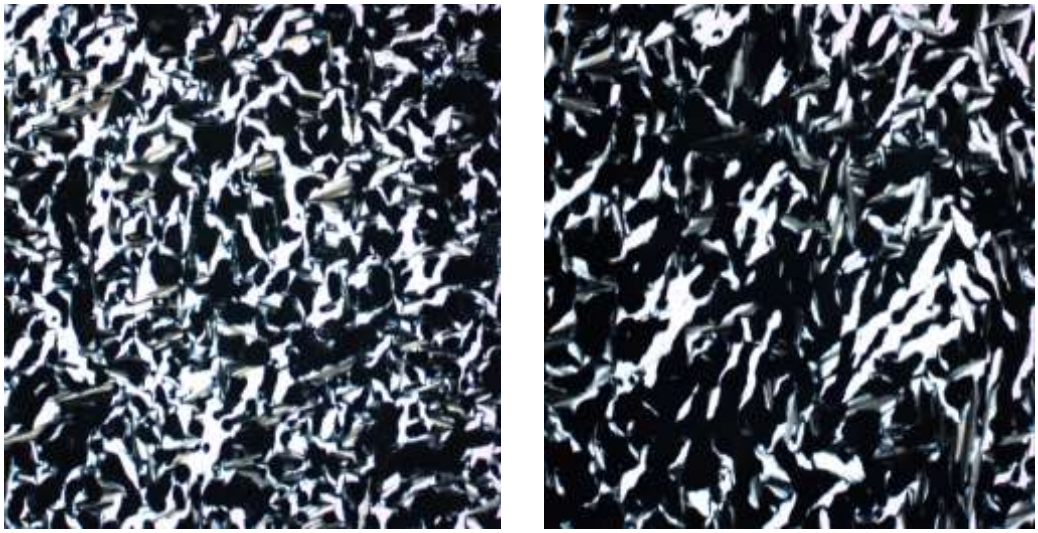

Figure 67: SmA Phase of S-CBA- Tr-$(NH_2)_3$ at 97^oC (left) and 125^oC (right)

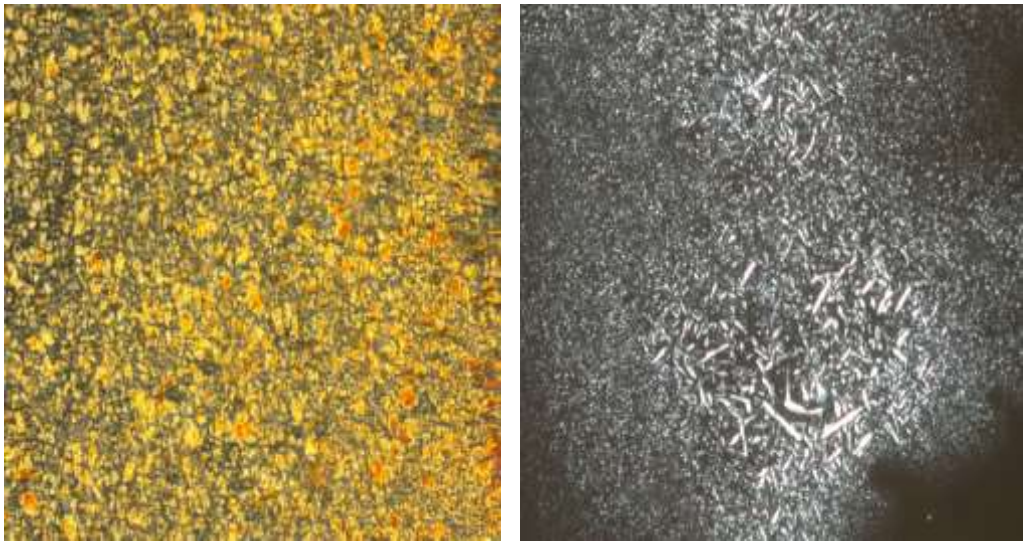

Figure 68: SmA Phase of S-CBA-Tr-$(NH_2)_6$ at 45^oC (left) and S-CBA-Tr-$(NH_2)_{12}$ at 134^oC (right)

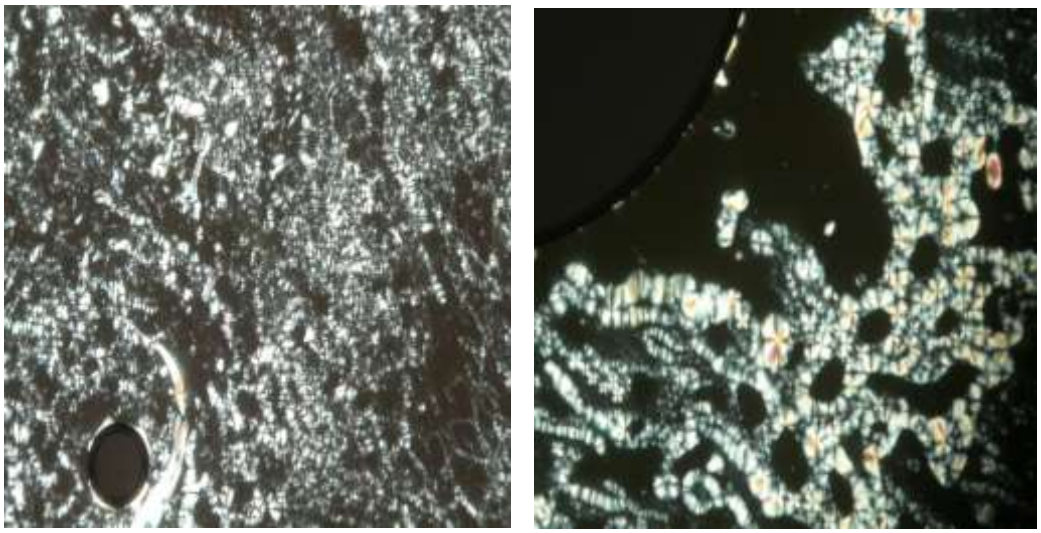

Figure 69: SmA Phase of S-CBA-Tr-$(NH_2)_{24}$ 89ºC (left) and 108ºC (right)

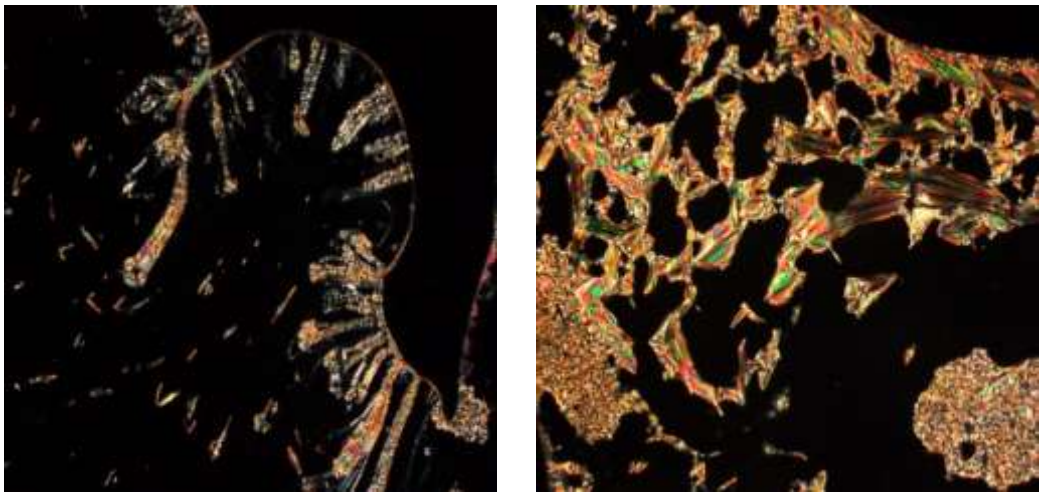

Figure 70: SmX (SmA) Phase of C10*BP - Tr-$(NH_2)_3$ 131ºC (left) and 186ºC (right)

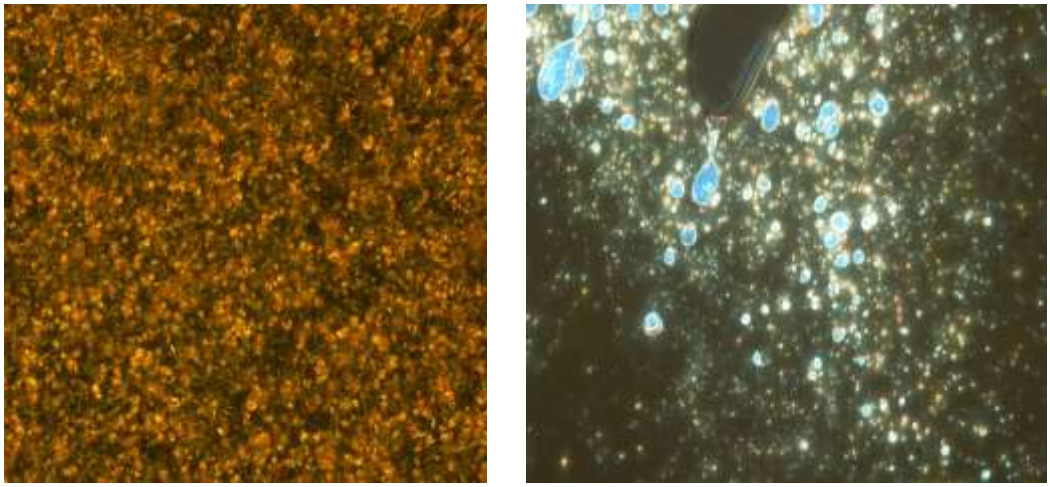

Figure 71: C10*BP –Tr-$(NH_2)_6$ at 160ºC (left) and C10*BP –Tr-$(NH_2)_{12}$ 159ºC (right)

4.3 PPI Based Dendritic Ionic Liquids

4.3.1 PPI Dendrimers

We planned to study with another type of dendrimer called polypropylene imine (PPI). In literature, there are substantial amount of successful works with PPI dendrimers for dendritic ionic liquid crystals. We purchased diamibobutane (DAB) core PPI dendrimer shown in Figure 72 from SyMO-Chem, Netherland. Four generations, (DAB-4, DAB-8, DAB-16, DAB32) were studied without further purification.

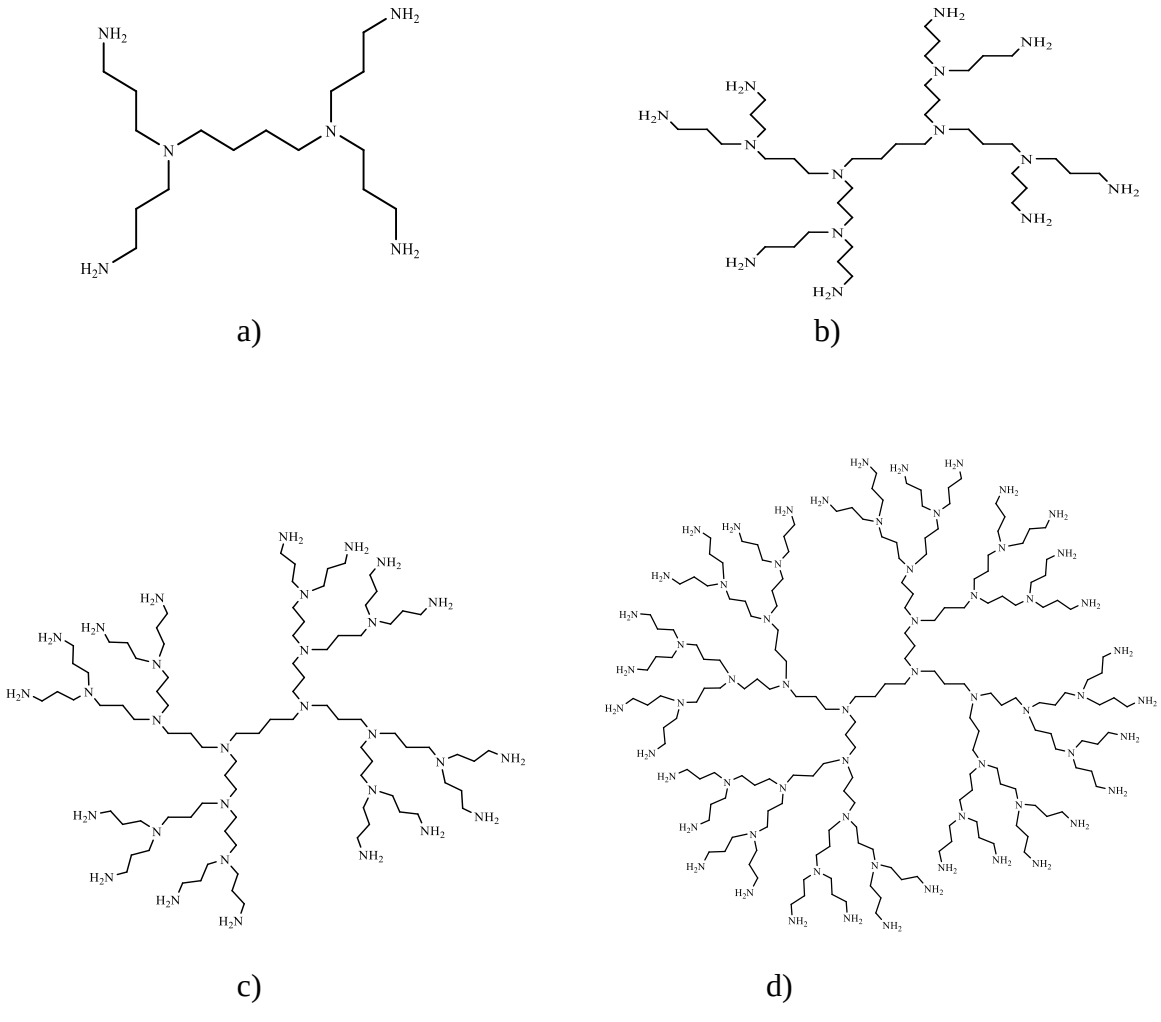

Figure 72: Chemical structures of a) DAB-4, b) DAB-8, c) DAB-16 and d) DAB-32 PPI dendrimers

4.3.2 Synthesizing PPI based Dendritic Ionic Liquids

Those PPI dendrimers are 4, 8, 16, 32 amine end groups respectively. As described in Figure 73, four dendrimers were reacted with S-4-Citronellyoxy benzoic acid (S-CBA)

in dry THF using ultrasonication bath for 15 minutes. Then, solvent was removed by rotary evaporator, and salts were waited for 1 day at 50^0C in vacuum oven.

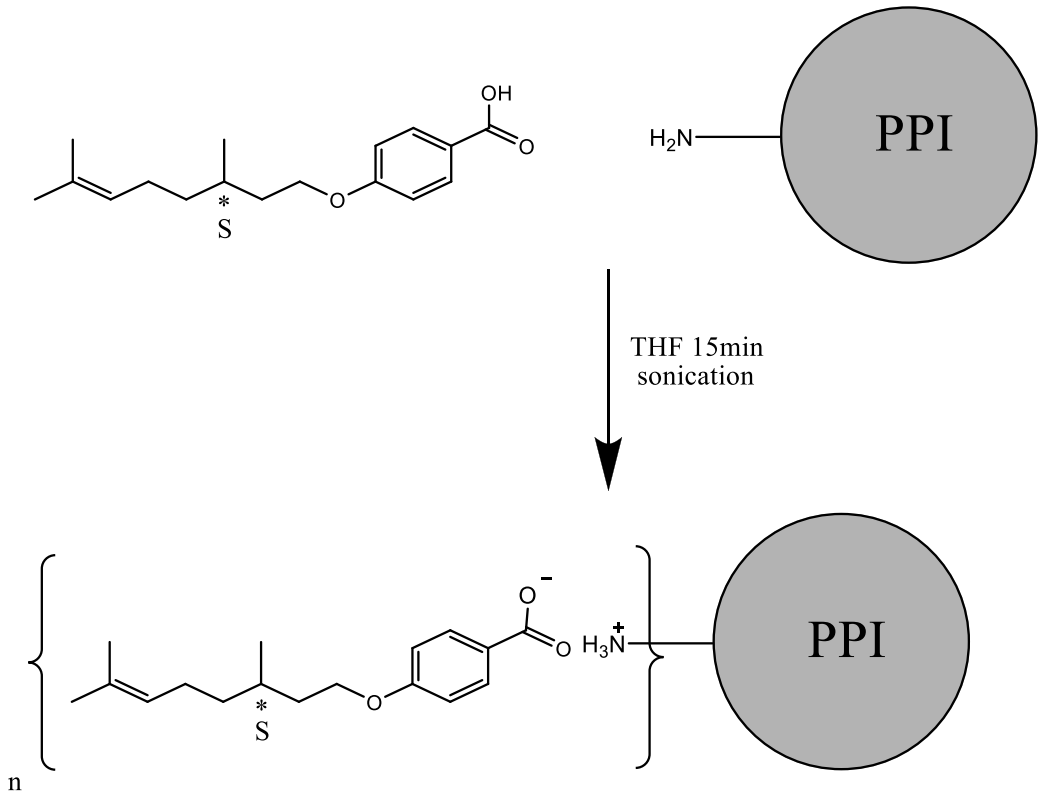

Figure 73: Ionic reaction between S-4-Citronellyoxy benzoic acid (S-CBA) and (DAB-4, DAB-8, DAB16, DAB-32) PPI dendrimers

Structural characterization of DAB based PPI-SCBA salts is firstly investigated by FT-IR spectra. When salt forms, primary amine peaks of DAB-4 and carbonyl peak of S-CBA disappears. In ionic form, symmetric carboxylate (1380cm^{-1}) and asymmetric carboxylate (1550cm^{-1}) are observed. Asymmetric carboxylate peak is clearly observed compared to asymmetric carboxylate peak belonging to amidomine based salts due to the fact that DAB-4 does not have amide II peak at 1550 cm^{-1} (see Figure 74).

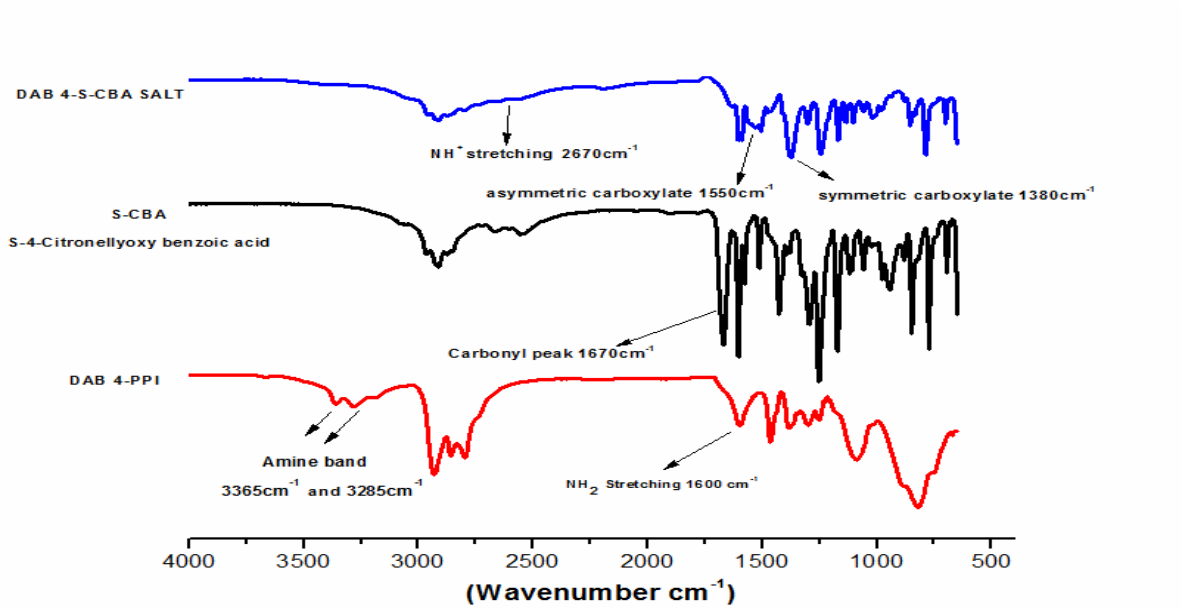

Figure 74: FT-IR Spectra of DAB-4, S-CBA and DAB-4-S-CBA Salt

The ^{13}C NMR spectrum in Figure 75 illustrates shifts of carbonyl peak and aromatic carbon peak from acid form to carboxylate form. In acidic form, carbonyl peak at 172.37ppm shifts from to 173.26ppm (+0.89ppm). Aromatic peak at 163.70ppm shifts in reverse direction to 161.17ppm (2.56ppm). The difference between two peaks (carbonyl and aromatic) increases from 8.67ppm to 12.09ppm.

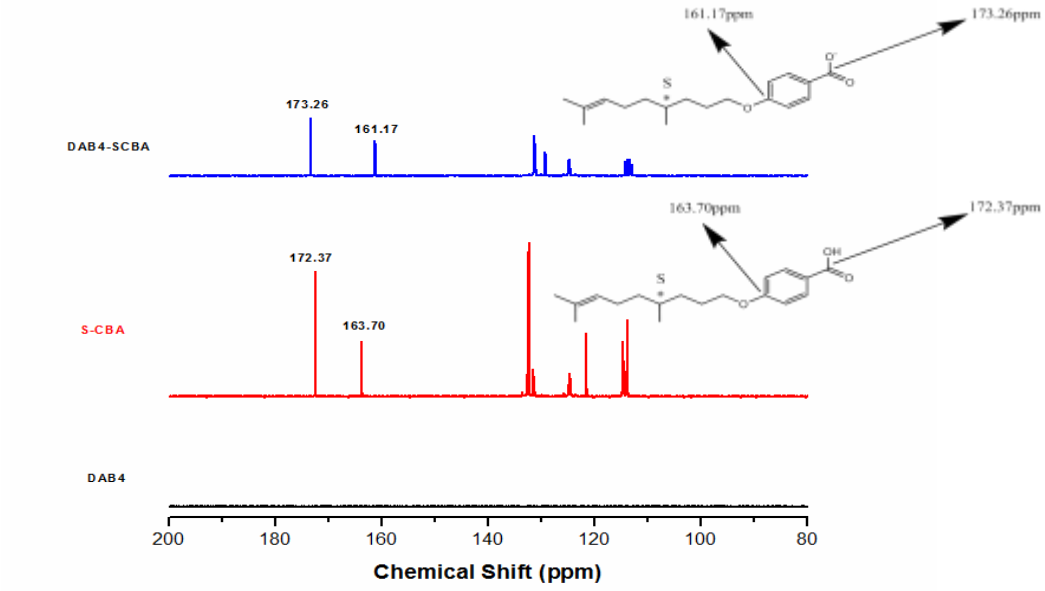

Figure 75: ^{13}C NMR Spectra of DAB-4, S-CBA and DAB-4- S-CBA Salt ($CDCl_3$)

Figure 76 illustrates proton NMR spectrum of DAB-4, S-CBA, DAB-4-S-CBA Salt.NH_3^+ broad peak at 7.6ppm and shifting of α-proton from $C\underline{\boldsymbol{H}}_2NH_2$ at 2.63ppm to $C\underline{\boldsymbol{H}}_2NH_3^+$ at 2.88ppm. Moreover, the oxymethylene peak of S-CBA moves from 4.04ppm to 3.85 ppm. Aromatic proton peaks (8.06ppm and 6.93ppm) moves to upper field direction (7.89ppm and 6.70ppm). Olefin proton keeps its position at 5.09ppm as reference peak for acidic and ionic form.

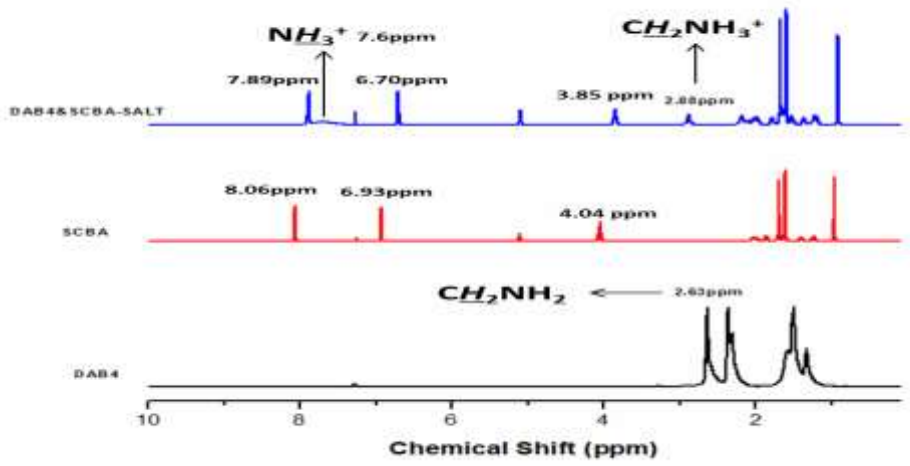

Figure 76: ^{1}H NMR Spectra of DAB-4, S-CBA and DAB-4-S-CBA Salt ($CDCl_3$)

As shown in Figure 77, ^{1}H NMR spectrum of all four generation of PPI dendritic ionic salts have similar characteristic properties and shifts. DAB-8&S-CBA, DAB-16&S-CBA, DAB-32&S-CBA have very small additional peak at 2.55ppm compared to DAB-4&S-CBA. Its reason can be explained by protonation of tertiary amine at higher generations due to increasing number of tertiary amine parts.

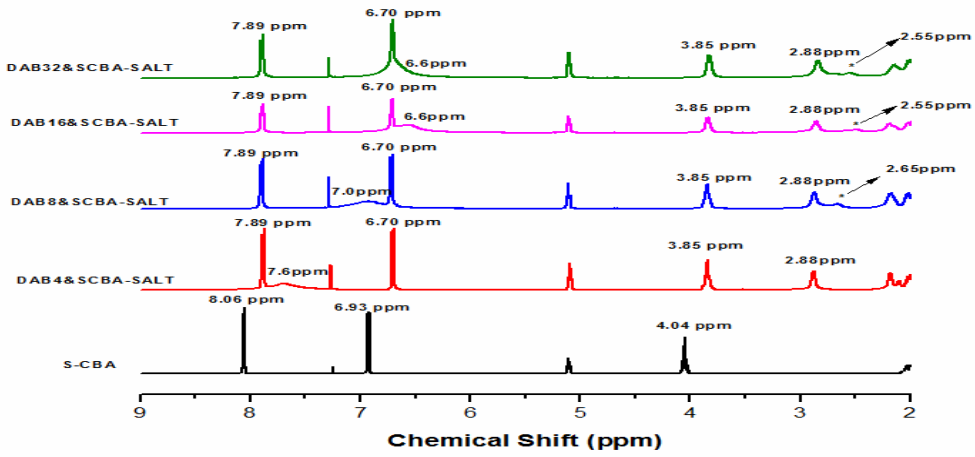

Figure 77: ^{1}H NMR Spectra of S-CBA and four generation PPI-S-CBA Salts ($CDCl_3$)

According to results represented in Table 8, all of dendritic ionic molecules have shown liquid crystalline property. In addition, all of them have seriously expanded mesomeric range compared to building unit (S-CBA). These results are similar to PAMAM based mesomeric molecules. For PPI based molecules, we have observed SmA phase. According to POM results, we observed similar phase transition for first three generations (S-CBA-DAB4, S-CBA-DAB8, S-CBA-DAB16). Last generation (S-CBA-DAB32) phase transition and phase type are quite different.

Table 8: POM Results of Salts from S-4-Citronellyoxy benzoic acid (S-CBA) with (DAB-4, DAB-8, DAB16, DAB-32) PPI dendrimers

Name	**POM Results**	**DSC Results, Enthalpy values (J/g)**
S-4-Citronellyoxy benzoic acid **(S-CBA)**	**Heating:** Cr 73^0C SmC* 80^0C Iso **Cooling:** SmC* 66.5 °C Cr	
DAB4-S-CBA	**Cooling:** Iso 165°C SmA NC*Cr	Cr 29,3°C (3,30) SmA 164,3°C (4,75) Iso
DAB8-S-CBA	**Cooling:** Iso 166-164°C SmA NC*Cr	Cr 31,6°C (3,05) SmA 163,2°C (3,17)Iso
DAB16-S-CBA	**Cooling:** Iso 166°C SmA NC*Cr	Cr 35,6°C (1,94) SmA 160,6°C (3,05) Iso
DAB32-S-CBA	**Cooling:** Iso 155°C SmX 100°C Cr	Cr 35,9°C (1,86) SmX 142,5°C (1,05) Iso

NC*=Not clear

This situation can be explained by overcrowding of upcoming extra 16 surface amine end groups. According to DSC results, there is a gradual decreasing of isotropization point from 164,3°C (S-CBA-DAB4) to 142,5°C (S-CBA-DAB32). Overcrowding of surface amino groups prevents keeping the system liquid crystalline, and the system favors more readily thermodynamically more comfortable isotropic side (lowering isotropization point).

One more advantage of the system is choosing lower isotropization temperature. This makes system is much more thermally stable. We investigated the thermal stability of the system by using Thermal Gravimetric Analysis (TGA) under nitrogen ambient by the speed of 5°C/min in Table 9. Analysis results demonstrate that dendritic ionic system survives well up to 170 °C which is above isotropization point. Between 170-200 °C, there is a small amount of degradation caused by oxidation or chemical disintegration. After 200 °C, system loses the stability extreme sharply.

Table 9: TGA results of the dendritic ionic systems

Sample	**(%) Loss at 170 °C**	**(%) Loss at 200 °C**	**(%) Loss at 300 °C**
DAB4& S-CBA	4,5	6,3	74,5
DAB8& S-CBA	7,4	9,0	74,5
DAB16& S-CBA	8,3	10,4	73,2
DAB32& S-CBA	4,5	6,0	77,7

Figure 78-81 depict polar microscope photographs of all series of DAB-S-CBA dendritic ionic liquids at different temperature points. All samples have clean and pure texture and smectic A mesopahe.

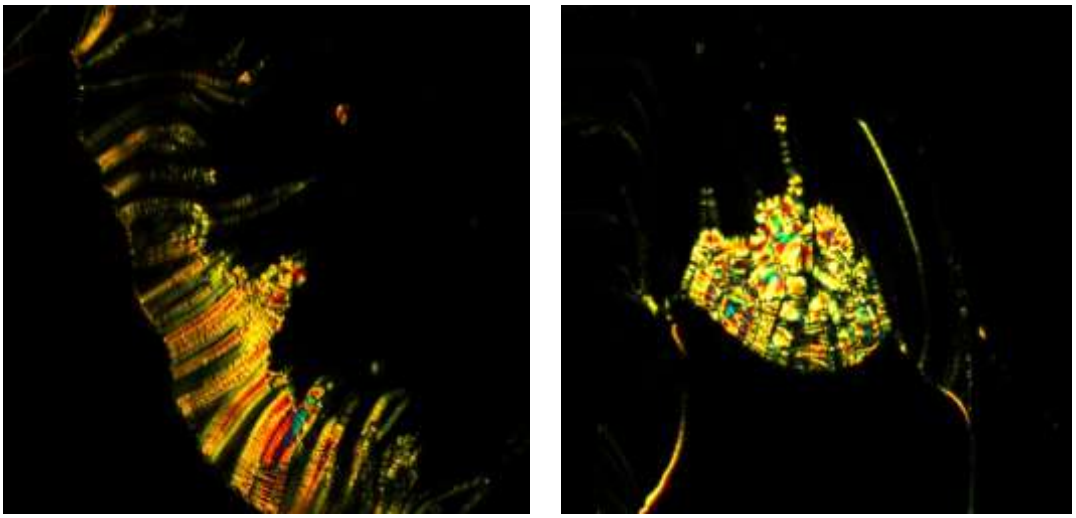

Figure 78: SmA Phase of S-CBA-DAB4 at 65°C (left) and 136°C (right)

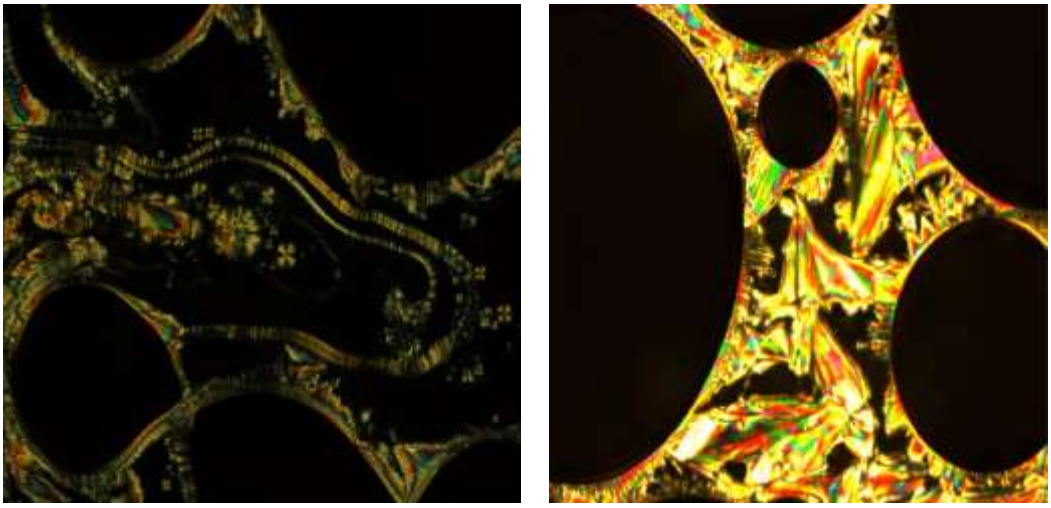

Figure 79: SmA Phase of S-CBA-DAB8 at 55^{o}C (left) and 160^{o}C (right)

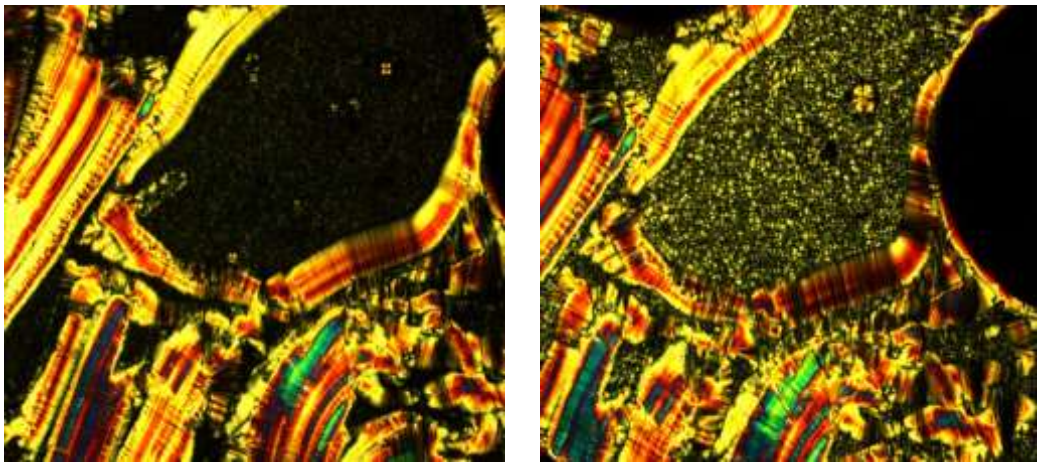

Figure 80: SmA Phase of S-CBA-DAB16 at 110^{o}C (left) and 140^{o}C (right)

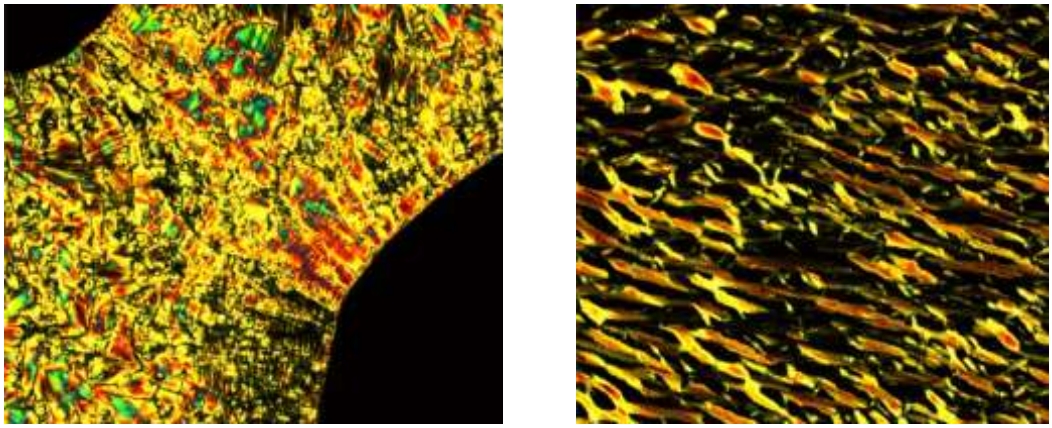

Figure 81: SmA Phase of S-CBA-DAB32 at 90^{o}C (left) and 150^{o}C (right)

4.4 PPI Based Covalent Compounds

4.4.1 Addition of S-CBA onto Periphery of PPI

Until now, we studied with ionic liquid crystalline macromolecules. By using DCC Coupling reaction, we would like to add mesogenic units onto periphery of PPI dendrimers by covalent way. Firstly, we added N,N'-dicyclohexycarbodiimide (DCC), 1-hydroxybenzatriazole (1-HOBt) into S-CBA in dry tetrahydrofuran under nitrogen environment. Later, we added corresponding diamino based dendrimers gradually into this mixture. Reaction was proceeded for two days at room temperature. Figure 82 illustrates main reaction body and structures of synthesized macromolecules.

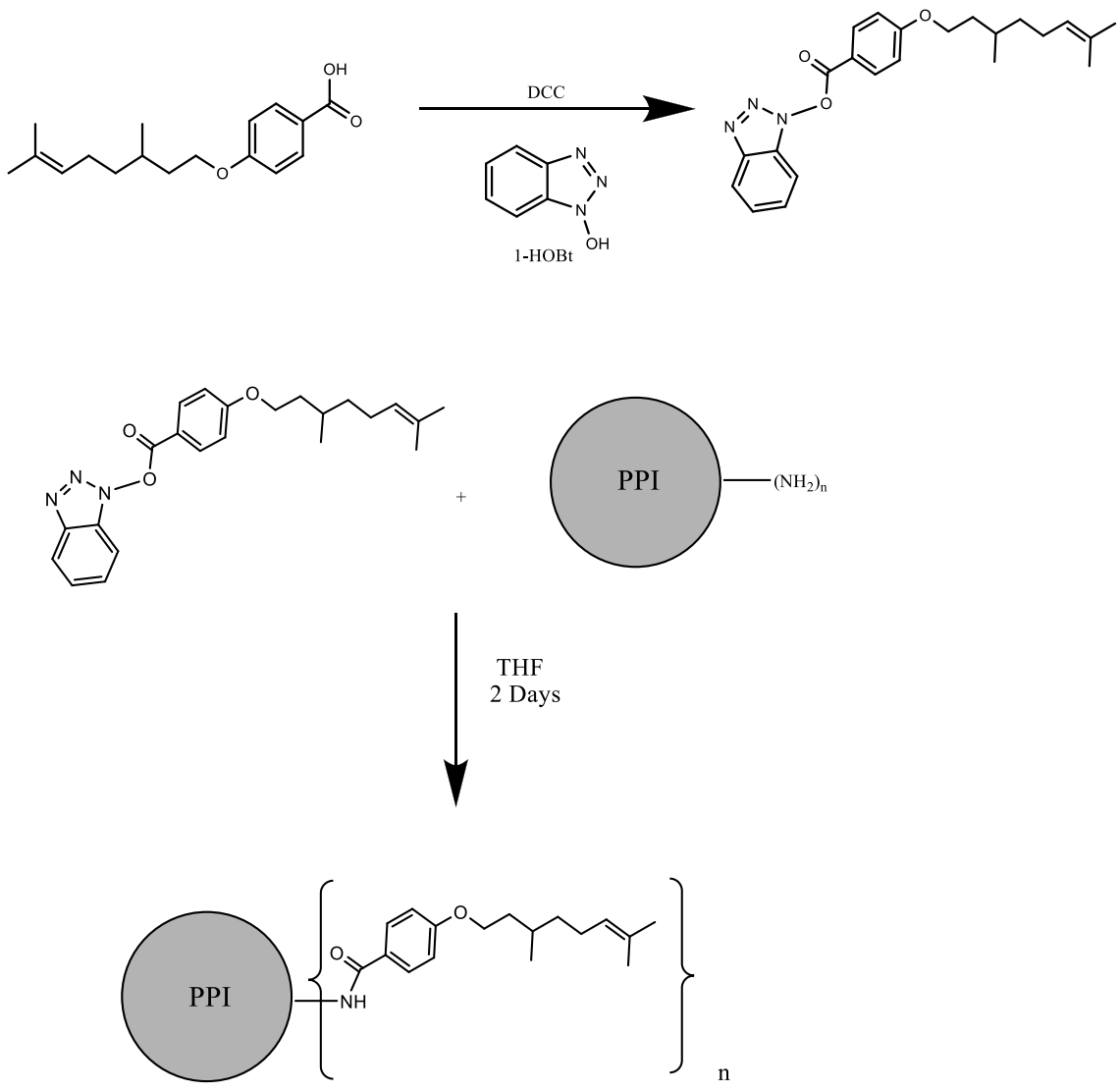

Figure 82: Representation of amidation reaction at periphery of DAB-4 by S-CBA

After synthesis is complete, the mixture was filtered. Then, THF was evaporated. Later, chloroform-water extraction was performed. After water side removed, chloroform part is evaporated. Then, according to molecular weight, it was purified by dialysis having 500, 1000 and 3000 Dalton pore-size in methanol-ethanol solvent mixture. Then, the alcohol mixture was evaporated. The color of substance for all of them is dark orange.

4.4.2 Characterization of PPI-(S-CBA)$_n$

According to Figure 83, ^{13}C NMR Spectra of the DAB-32&S-CBA has amidation peak at 167.78ppm which is the indication of finishing reaction. The peak at 161.59ppm belonging to aromatic carbon next to oxygen of alkoxy part of S-CBA retains its position in amidation product by non-significant change. In addition, the carbonyl at 172.37ppm of S-CBA was disappeared. In addition, at ^{1}H NMR spectra (O=CN-***H***) has a peak at 8.10ppm.

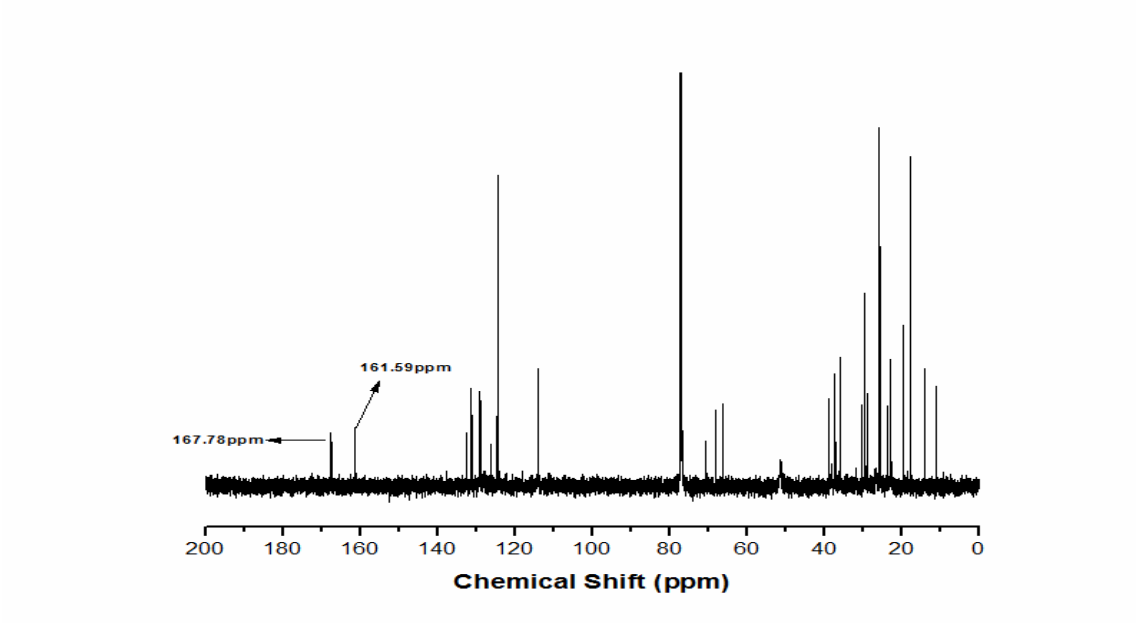

Figure 83: ^{13}C NMR Spectra of DAB-32&S-CBA ($CDCl_3$)

POM results of DAB-16&S-CBA and DAB-32&S-CBA covalent based macromolecules shows that they are not liquid crystalline.

4.5 Conclusion

This study is a collection of various dendritic ionic liquid crystals and additional study of covalent based dendritic molecules. The dendritic liquid crystals are composed of promesogenic units and various amine ended dendrimers. The promesogenic units are aromatic carboxylic acids linked by alkoxy chains in the para position. Those mesogenic building blocks, anionic part, span from relatively short alkoxy chain (C8-8 carbon) to relatively longer ones (C12-12 carbon). Some of them have chiral carbons. Amine ended dendrimers, cationic part, are all generations of PAMAM, PPI and trimesic acid core. In addition, four generations of PPI are covalently linked to S-CBA, promesogenic building block to compare covalent and ionic based molecules built from same constituents.

Using shorter mesogenic building blocks like 4-(Octyloxy) benzoic acid **(C8)** and 4-(4-Octyloxyphenyl) benzoic acid (**C8BP**) connected to PAMAM could not lead to form liquid crystals. There are various examples in the literature for short terminal chains like [51]. Exception to these results is G0.0 PAMAM-C8 salt showing SmX phase sort of a SmA phase. 4-(4-Dodecyloxyphenyl) benzoic acid **(C12BP)** connected to PAMAM ionic complexes show SmC phase. There is no dramatic change about mesophase transitions by addition of PAMAM for **C12BP**. SmX phase of **C12BP** turns to SmC in the form of PAMAM-**C12BP** ionic complexes. Both **C8BP** and **C12BP** have higher clearing point which contributes to high isotropization point for ionic complex. Due to the fact that PAMAM molecules have lots of amide bond, ionic complexes suffer from this high isotropization. In addition, sustainability cannot be performed for addition heating and cooling cycles. 4-(Dodecyloxy) benzoic acid **(C12)** based all PAMAM salts have SmA phase with wide mesomeric range compared to its mesomeric building part. Polymorphism (nematic and smectic C) of **C12** converts itself in one straight and wide range smectic A mesophase in ionic complexes. One advantage of **C12** molecule is relatively lower isotropization point which contributes PAMAM ionic complexes repeatable thermogram and healthy observation of full-range of mesomorphism. All PAMAM based 4'-(3S)-3,7-dimethyloctyloxy-4-biphenylcarboxylicacid **(C10*BP)** salts, having interesting SmI mesophase and nematic phases for its own mesogenic unit **C10*BP**, show SmX phase with wide range compared to its mesomeric building part. The disadvantage of **C10*BP** mesophase is relatively higher clearing point. Actually, mesomeric properties of PAMAM-**C10*BP** are fully characterized. However, high

clearing point of PAMAM-**C10*BP** is an obstacle for sustainability of the system. Especially, the there is no effect of generation of dendrimer for PAMAM-**C12** and PAMAM-**C10*BP** complexes. These results are consistent with results from literature. **S-CBA** molecule with very narrow mesomeric range and considerably lower isotropization point enable considerable wide mesomeric range of PAMAM ionic molecules. Mesophase changes form tilted smectic phase to smectic A mesophase. In addition, just 7^0C mesomeric range increases up to 70^0C and relatively lower clearing point like 120-140^0C is another significant advantage. In addition, there is no meaningful change of mesomeric properties depending on the generation of dendrimer. In addition, by POM and DSC observations, crystallization point cannot be determined ideally due to the fact that there is still continuation of liquid crystallinity. Similar study for trimesic based amidoamine dendrimers Tr-(NH_2)n with **S-CBA** is performed. Similar results are obtained such as wide range lamellar mesophormism. Due to the relatively low clearing point is another advantage of Tr-(NH_2)n- **S-CBA.** However, Tr-(NH_2)n-**C10*BP** system showing smectic mesophase suffers from high isotropization points especially for higher generations due to higher number of amide groups. PPI- **S-CBA** salts have considerably wide mesomeric range like 70^0C. Similarly, smectic character still continues at room temperature on cooling regime like PAMAM-S-CBA series. PPI- **S-CBA** complexes have smectic A character except to lasr generation $(DAB)_{32}$-**S-CBA** has smectic X mesophase. Isotropization point becomes slightly lowered by increasing generation. Literature explains the situation by surface congestion at periphery of higher generation of dendrimer. Covalent analogues of PPI-**S-CBA** do not show mesomorphism. This shows the strong side of ionic complexes. In the literature [86] and [87], while ionic complexes have mesomorphism, covalent analogues from same constituents do not have. Although explanation is not brought [86] about this case, it can be tried to be explained by rigidity of covalent bondage fixing the system more crystalline side.

To sum up, this study show that dendritic ionic liquids by choosing appropriate promesogenic units can have wide mesomorphic range and significantly sustainable sustainability (repeatable thermograms).

REFERENCES

[1] Donnio, B., Guillon, D., (2006). “Liquid Crystalline Dendrimers and Polypedes”, “Adv. Polym. Sci.”, 201: 45-155.

[2] Gingras, M., Raimundo, J. M., Chabre, Y. M., (2007). “Cleavable Dendrimers”, Angew. Chem., Int. Ed., 46: 1010-1017.

[3] Shcharbin, D., Klajnert, B., Bryszewska, M., (2010). “Practical Guide to Studying Dendrimers”, 1-8.

[4] Kato, T., Mizoshita, N., Kishimoto, K., (2006). “Functional Liquid-Crystalline Assemblies: Self-Organized Soft Materials”, Angew. Chem., Int. Ed., 45: 38-68.

[5] Tschierske, C., (2001). “Micro-segregation, molecular shape and molecular topology – partners for the design of liquid crystalline materials with complex mesophase morphologies”, J. Mater. Chem., 11: 2647-2671.

[6] Ponomarenko, S. A., Agina, E. V., Boiko, N. I., Rebrov, E. A., Muzafarov, A. M. , Richardson, R. M., Shibaev, V. P., (2001). “Liquid Crystalline Carbosilane Dendrimers with Terminal Phenyl Benzoate Mesogenic Groups: Influence of Generation Number on Phase Behaviour”, Mol.Cryst. Liq. Cryst., 364: 93-100.

[7] Richardson, R. M., Ponomarenko, S. A., Boiko, N. I., Shibaev, V. P., (1999). “Liquid crystalline dendrimer of the fifth generation: From lamellar to columnar structure in thermotropic mesophases”, Liq. Cryst., 26: 101-108.

[8] Barbera, J., Donnio, B., Gehringer, L., Guillon, D., Marcos, M., Omenat, A., Serrano, J. L., (2005). “Self-organization of nanostructured functional dendrimers”, J. Mater. Chem., 15: 4093-4105.

[9] Hernandez-Ainsa, S., Barbera, J., Marcos, M., Serrano, J. L., (2011). “Nanoobjects coming from mesomorphic ionic PAMAM dendrimers”, Soft Matter, 7: 2560-2568.

[10] Tsiourvas, D., Stathopoulou, K., Sideratou, Z., Paleos, C. M., (2002). “Body-Centered-Cubic Phases Derived from n-Dodecylurea Functionalized Poly(propylene imine) Dendrimers”, 35: 1746-1750.

[11] Tsiourvas, D., Felekis, T., Sideratou, Z., Paleos, C. M., (2002). “Liquid Crystals Derived from Cholesterol Functionalized Poly(propylene imine) Dendrimers”, Macromolecules, 35: 6466-6469.

[12] Pastor, L., Barbera, J., McKenna, M., Marcos, M. , Martin-Rapun, R., Serrano, J.L., Luckhurst, G.R., Mainal, A., (2004). “End-on and Side-on Nematic Liquid Crystal Dendrimers”, Macromolecules, 37: 9386-9394.

[13] Martin-Rapun, R., Marcos, M. , Omenat, A., Serrano, J. L., Luckhurst, G. R., Mainal, A., (2004).“Poly(propyleneimine) Liquid Crystal Codendrimers Bearing Laterally and Terminally Attached Promesogenic Groups”, Chem. Mater., 16: 4969-4979.

[14] Felekis, T., Tsiourvas, D., Tziveleka, L., Paleos, C. M., (2005). “Hydrogen-bonded liquid crystals derived from supramolecular complexes of pyridylated poly(propyleneimine) dendrimers and a cholesterol-based carboxylic acid”, Liq.Cryst., 32: 39-43.

[15] Cho, B. K., Jain, A., Mahajan, S., Ow, H. , Gruner, S. M., Wiesner, U., (2004). “Nanohybrids from Liquid Crystalline Extended Amphiphilic Dendrimers”, J. Am. Chem. Soc., 126: 4070-4071.

[16] Percec, V., Kawasumi, M., (1992). “Synthesis and Characterization of a Thermotropic Nematic Liquid Crystalline Dendrimeric Polymer”, Macromolecules, 25: 3843-3850.

[17] Busson, P., Ortegren, J., Ihre, H., Gedde, U.W., Hult, A., Andersson, G., (2001) Ferroelectric Liquid Crystalline Dendrimers: Synthesis, Thermal Behavior, and Electrooptical Characterization Macromolecules 34: 1221-1229.

[18] Busson, P., Ortegren, J., Ihre, H., Gedde, U. W., Hult, A., Andersson, G., Eriksson, A., Lindgren, M., (2002). "Preparation of Mesogen-Functionalized Dendrimers for Second-Order Nonlinear Optics", Macromolecules, 35: 1663-1671.

[19] Li, J. F., Crandall, K. A., Chu, P., Percec, V., Petschek, R. G., Rosenblatt, C., (1996). "Dendrimeric Liquid Crystals: Isotropic-Nematic Pretransitional Behavior", Macromolecules, 29: 7813-7819.

[20] Antharjanam, P.K.S., Jaseer, M., Ragi, K.N., Prasad, E., (2009). "Intrinsic luminescence properties of ionic liquid crystals based on PAMAM and PPI dendrimers", Journal of Photochemistry and Photobiology A: Chemistry, 203: 50–55.

[21] Canilho, N., Scholl, M., Klok, H.A., Mezzenga, R., (2007). "Thermotropic Ionic Liquid Crystals via Self-Assembly of Cationic Hyperbranched Polypeptides and Anionic Surfactants", Macromolecules, 40: 8374-8383.

[22] Guillon, D., Deschenaux, R., (2002). "Liquid-crystalline dendrimers", Current Opinion in Solid State and Materials Science, 6: 515–525.

[23] Marcos, M., Omenat, A., Serrano, J. L., (2003). "Structure-mesomorphism relationship in terminally functionalised liquid crystal dendrimers", C. R. Chimie, 6: 947–957.

[24] Boiko, N. I., Lysachkov, A. I., Ponomarenko, S. A., Shibaev, V. P., Richardson, R. M., (2005). "Synthesis and comparative studies of carbosilane liquid crystalline dendrimers with chiral terminal mesogenic groups", Colloid and Polymer Science, 283:1155-1162.

[25] Serrano, J.L., Marcos, M., Martin, R., Gonzalez, M., Barbera, J., (2003) "Chiral Codendrimers Derived from Poly(propyleneimine) Dendrimers (DAB)", Chem. Mater., 15: 3866-3872.

[26] Hernandez-Ainsa, S., Marcos, M., Barbera, J., and Serrano, J.L, (2010). "Philic and Phobic Segregation in Liquid-Crystal Ionic Dendrimers: An Enthalpy–Entropy Competition" Angew. Chem. Int. Ed., 49: 1990 –1994.

[27] Fitie, C.F.C., Tomatsu, I., Byelov, D., de Jeu, W.H., Sijbesma, R.P., (2008), "Nanostructured Materials through Orthogonal Self-Assembly in a Columnar Liquid Crystal", Chem. Mater. 20: 2394–2404.

[28] Hernandez-Ainsa, S., Fedeli, E., Barbera, J., Marcos, M., Sierraa T., Serrano, J.L., (2014). "Self-assembly modulation in ionic PAMAM derivatives", Soft Matter, 10: 281–289.

[29] Boiko, N., Zhu, X., Vinokur, R., Rebrov, E., Muzafarov, A., and Shibaev, V., (2000). "New Carbosilane Ferroelectric Liquid Crystalline Dendrimers", Mol. Cryst. and Liq. Crys., 352: 343-350.

[30] Goodby, J.W., (1999). "Mesogenic molecular crystalline materials", Current Opinion in Solid State and Materials Science, 4: 361–368.

[31] Cano, M., Sanchez-Ferrer, A., Serrano, J.L., Gimeno, N., Ros, M.B., (2014). "Supramolecular Architectures from Bent-Core Dendritic Molecules", Angew. Chem. Int. Ed., 53: 13449 –13453.

[32] Hernandez-Ainsa, S., Barbera, J., Marcos, M., Serrano, J.L., (2012). "Liquid Crystalline Ionic Dendrimers Containing Luminescent Oxadiazole Moieties", Macromolecules, 45: 1006−1015.

[33] Shibaev, V. P., (2006). "Intramolecular microsegregation: a driving force of nanostructure formation in liquid-crystalline dendrimers", Liquid Crystals, 33: 1497–1500.

[34] Pegenau, A., Cheng, X.H., Tschierske, C., Goring P., Diele, S., (1999). "Formation of mesophases based on micro-segregation: columnar liquid-crystalline phases of first generation dendrimers with perfuorinated segments", New J. Chem., 23: 465-467.

[35] Boas, U., Christensen, J.B., Heegaard, P.M.H, (2006). “Dendrimers in Medicine and Biotechnology”, 1-24.

[36] Tomalia, D.A., (2005). “Birth of a new macromolecular architecture: dendrimers as quantized building blocks for nanoscale synthetic polymer chemistry”, Progress in Polymer Science, 30: 294-324.

[37] Archut, A., Vogtle, F., (1998). “Functional Cascade Polymers”, Chem. Soc. Rev., 27: 233-240.

[38] Fischer, M., Vogtle, F., (1999). “Dendrimers: From Design to Application-A Progress Report”, Angewandte Chemie Int. Ed., 38: 884-905.

[39] Bosman, A.W., Janssen, H. M., Meijer, E. W., (1999). “About Dendrimers: Structure, Physical Properties, and Applications”, Chem. Rev., 99: 1665-1688.

[40] Tomalia, D.A., Majoros, I., (2003). “Dendrimeric Supramolecular and Supramacromolecular Assemblies”, Journal of Macromolecular Science Part C—Polymer Reviews, C43: 411-477.

[41] Boas, U., Heegaard, P.M.H, (2004). “Dendrimers in Drug Research”, Chem. Soc. Rev., 33: 43-63.

[42] Esfand, R., Tomalia, D.A., (2001). “Poly(amidoamine) (PAMAM) dendrimers: from biomimicry to drug delivery and biomedical applications”, Drug Disc. Today, 6: 427-436.

[43] Newkome, G.R., Yao, Z., Baker, G.R., Gupta, V.K., (1985). “Micelles. Part I. Cascade molecules: a new approach to micelles. A [27]-arborol.”, J. Org. Chem., 50: 2003-2004.

[44] Wörner, C., Mulhapt, R., (1993). “Polynitrile- and Polyamine-Functional Poly(trimethylene imine) Dendrimers” Angewandte Chemie Int. Ed., 32: 1306-1308.

[45] Matthews, O.A., Shipway, A.N., Stoddard J.F., (1998). “Dendrimers-Branching out from Curiosities into New Technologies”, Prog. Poly. Sci., 23: 1-56.

[46] Miller, T.M. and Neenan, T.X., (1990). "Convergent synthesis of monodisperse dendrimers based upon 1,3,5-trisubstituted benzenes", Chemistry of Materials, 2: 346-349.

[47] Hawker, C.J., Frechet, J.M.J., (1990). "Preparation of polymers with controlled molecular architecture. A new convergent approach to dendritic macromolecules", Journal of American Chemical Society, 112: 7638-7647.

[48] Lothian-Tomalia, M. K., Hedstrand, D. M., Tomalia, D.A., Padias, A.B., Hall, H.K., "A Contemporary Survey of Covalent Connectivity and Complexity. The Divergent Synthesis of Poly(thioether) Dendrimers. Amplified Genealogically Directed Synthesis Leading to the de Gennes Dense Packed State", Tetrahedron, 53: 15495-15513.

[49] Sun, F., Chen, F., Fei, W., Sun., Li, Wu, Y., (2012). "A novel strategy for constructing electrochemiluminescence sensor based on CdS-polyamidoamine incorporating gold nanoparticle film and its application", Sensors and Actuators B: Chemical, 166-167: 702-707.

[50] Ning, D., Zhang, H., Zheng, J., (2014). "Electrochemical sensor for sensitive determination of nitrite based on the PAMAM dendrimer-stabilized silver nanoparticles", Journal of Electroanalytical Chemistry, 717-718: 29-33.

[51] Kavosi, B., Hallaj, R., Teymourian, H., Salimi, A., (2014) "Au nanoparticles/PAMAM dendrimer functionalized wired ethyleneamine-violegen as highly efficient interface for ultra-sensitive α-fetoprotein electrochemical immunosensor" Biosensors and Bioelectronics, 59: 389-396.

[52] Fernandes, E.G.R., Vieira, N.C.S., De Queiroz, A.A.A., Guimares, F.E.G., Zucolotto, V., (2010). "Immobilization of Poly(propyleneimine) Dendrimer/Nickel Phtalocyanine as Nanostructured Multilayers Films To Be Used as Gate Membranes for SEGFET pH Sensors", J. Phys. Chem. C, 114: 6478-6483.

[53] Krasteva, N., Guse, B., Besnard, I., Yasuda, A., Vossmeyer, T., (2003). "Gold nanoparticle/PPI-dendrimer based chemiresistors Vapor-sensing properties as a function of the dendrimer size", Sensors and Actuators B, 92: 137-143.

[54] Devarakonda, B., Hill, R.A., Liebenberg, W., Brits, M., De Villiers M.M., (2005). "Comparison of the aqueous solubilization of practically insoluble niclosamide by poliamidoamine (PAMAM) dendrimers and cyclodextrins", International Journal of Pharmaceutics, 304: 193-209.

[55] Jin, Y., Ren, X., Wang, W., Ke, L., Ning, E., Du, L., Bradshaw, J., (2011). "A 5-fluorouracil-loaded pH-responsive dendrimer nanocarrier for tumor targeting", International Journal of Pharmaceutics, 420: 378-384.

[56] Papagiannaros, A., Dimas, K., Papaioannou, G.T., Demetzos C., (2005). "Doxorubicin–PAMAM dendrimer complex attached to liposomes:Cytotoxic studies against human cancer cell lines", International Journal of Pharmaceutics, 302: 29-38.

[57] Nasra, M., Najlah, M., D'Emanuele, A., Elhissi, A., (2014). "PAMAM dendrimers as aerosol drug nanocarriers for pulmonary delivery via nebulization", International Journal of Pharmaceutics, 461: 242-250.

[58] Zhao, Y., Fan, X., Liu, D., Wang Z., (2011). "PEGylated thermo-sensitive poly(amidoamine) dendritic drug delivery systems", International Journal of Pharmaceutics, 409: 229-236.

[59] Balieu, S., Cadiou, C., Martinez, A., Nuzillard, J.-M., Oudart, J.-B., Maquart, F.-X., Chuburu, F., Bouquillon, S., (2013). "Encapsulation of contrast imaging agents by polypropyleneimine-based dendrimers", Journal of Biomedical Materials Research A, 3: 613-621.

[60] Yea, M., Qian, Y., Tang, J., Hu, H., Sui, M., Shen, Y., (2013). "Targeted biodegradable dendritic MRI contrast agent for enhanced tumor imaging", Journal of Controlled Release, 169: 239-245.

[61] Geitner, N.K., Wang, B., Andorfer, R.A., Ladner, D.A., Ke, P.C., Ding, F., (2014). "Structure−Function Relationship of PAMAM Dendrimers as Robust Oil Dispersants" Env. Sci. Technol., 48: 12868-12875.

[62] Diallo, M.S., Christie, S., Swaminathan, P., Johnson, J.H., Goddard, W.A., (2005). "Dendrimer Enhanced Ultrafiltration.1. Recovery of Cu(II) from Aqueous Solutions Using PAMAM Dendrimers with Ethylene Diamine Core and Terminal NH2 Groups", Env. Sci. Technol., 39: 1366-1377.

[63] Hayati, B., Mahmoodi, N.M., Arami, M., Mazaheri F., (2011). “Dye Removal from Colored Textile Wastewater by Poly(propylene imine) Dendrimer: Operational Parameters and Isotherm Studies”, Clean – Soil, Air, Water, 39: 673–679.

[64] Demus, D., One Century Liquid Crystal Chemistry: From Vorlander’s Rods to Disks, Stars and Dendrites”, Molecular Crystals and Liquid Crystals Science and Technology. Section A. Molecular Crystals and Liquid Crystals. 364:25-91.

[65] Chandrasekhar S.F.R.S., (1992). “Liquid Crystals” Second Edition.

[66] Edited by Collyer A.A., (1992). “Liquid Crystal Polymers: From Structures to Applications”.

[67] Hussein, M. A., Abdel-Rahman, M.A., Asiri, A.M., Alamry, K.A., Aly, K.I., (2012) “Review on: liquid crystalline polyazomethines polymers. Basics, syntheses and characterization” Designed Monomers and Polymers, 15: 431-463.

[68] Marcos, M., Martin-Rapun, R., Omenat, A., Serrano, J.L., (2007). “Highly congested liquid crystal structures: dendrimers, dendrons, dendronized and hyperbranched polymers”, Chem. Soc. Rev., 36: 1889-1901.

[69] Donnio, B., Buathong, S., Bury, I., Guillon, D., (2007). “Liquid crystalline dendrimers”, Chem. Soc. Rev., 36: 1495-1513.

[70] Percec, V., Chu, P., Ungar, G., Zhod, J., (1995). “Rational Design of the First Nonspherical Dendrimer Which Displays Calamitic Nematic and Smectic Thermotropic Liquid Crystalline Phases”, J. Am. Chem. Soc., 117: 11441-11454.

[71] Meier, H., Lehmann, M., (1998). “Stilbenoid Dendrimers”, Angew. Chem. Int. Ed. 37: 643-645.

[72] Gehringer, L., Guillon, D., Donnio, B., (2003) “Liquid Crystalline Octopus: An Alternative Class of Mesomorphic Dendrimers”, Macromolecules, 36: 5593-5601.

[73] Baars, M.W.P.L, Söntjens, S.H.M., Fischer, H.M., Peerlings, H. W. I., Meijer, E. W, (1998). “Liquid-Crystalline Properties of Poly(propylene imine) Dendrimers Functionalized with Cyanobiphenyl Mesogens at the Periphery”, Chem.Eur. J., 4: 2456-2466.

[74] Cameron, J.H., Facher, A., Lattermann, G., Diele, S., (1997). “Poly (propy1eneimine) Dendromesogens with Hexagonal Columnar Mesophase”, Adv. Mater., 9: 398-403.

[75] Barbera, J., Marcos, M., Serrano, J.L., (1999). “Dendromesogens: Liquid Crystal Organizations versus Starburst Structures”, Chem. Eur. J., 5: 1834-1840.

[76] Marcos, M., Gimenez, R., Serrano, J.L., Donnio, B., Heinrich, B., Guillon, D., (2001). “Dendromesogens: Liquid Crystal Organizations of Poly(amidoamine) Dendrimers versus Starburst Structures”, Chem. Eur. J., 7: 1006-1013.

[77] Barbera, J., Donnio, B., Gimenez, R., Guillon, D., Marcos, M., Omenat A., Serrano, J.L., (2001). “Molecular morphology and mesomorphism in dendrimers: a competition between rods and discs”, J. Mater. Chem., 11: 2808–2813.

[78] Barbera, J., Gimenez, R, Marcos, M., and Serrano, J.L., (2002). “Dendrimers with laterally grafted mesogens”, Liq. Crys., 29: 309-314.

[79] Rueff, J.M, Barbera, J., Donnio, B., Guillon, D., Marcos, M., Serrano, J.L., (2003). “Lamellar to Columnar Mesophase Evolution in a Series of PAMAM Liquid-Crystalline Codendrimers”, Macromolecules, 36: 8368-8375.

[80] McKenna, M.D., Barbera, J., Marcos, M., Serrano, J.L., (2005). “Discotic Liquid Crystalline Poly(propylene imine) Dendrimers Based on Triphenylene”, J. Am. Chem. Soc., 127: 619-625.

[81] Barrio, J., Tejedor, R.M., Chinelatto, L.S., Sanchez, C., Pinol, M., Orio, L., (2010). “Photocontrol of the Supramolecular Chirality Imposed by Stereocenters in Liquid Crystalline Azodendrimers”, Chem. Mater., 22: 1714–1723.

[82] Chechik, V., Zhao, M., Crooks, R.M., (1999). “Self-Assembled Inverted Micelles Prepared from a Dendrimer Template: Phase Transfer of Encapsulated Guests”, J. Am. Chem. Soc., 121: 4910-4911.

[83] Takahashi, T., Kimura, T., Sakurai, K., (1999) “Structure and liquid crystallinity of the comb-like complexes made of poly(ethylene imine) and some aliphatic carboxylic acids”, Polymer, 40: 5939-5945.

[84] Tsiourvas, D., Felekis, T., Sideratou, Z., Paleos, C.M., (2004). “Ionic liquid crystals derived from the protonation of poly (propylene imine) dendrimers with a cholesterol-based carboxylic acid”, Liquid Crystals, 31: 739-744.

[85] Ujiie, S., Yano, Y., Mori, A., (2004). “Liquid Crystalline Branched Polymer Having Ionic Moieties”, Mol. Cryst. Liq. Cryst., 411:483-489.

[86] Martin-Rapun, R., Marcos, M., Omenat, A., Barbera, J., Romero, P., Serrano, J.L., (2005). “Ionic Thermotropic Liquid Crystal Dendrimers”, J. Am. Chem. Soc., 127: 7397-7403.

[87] Stevelmans, S., van Hest, J. C. M. , Jansen, J. F. G. A., van Boxtel, D. A. F. J.,. de Brabander-van den Berg, E. M. M., Meijer, E. W., (1996). “Synthesis, Characterization, and Guest-Host Properties of Inverted Unimolecular Dendritic Micelles”, J. Am. Chem. Soc., 118: 7398-7399.

[88] Marcos, M., Martin-Rapun, R., Omenat, A., Barbera, J., Serrano, J.L., (2006). “Ionic Liquid Crystal Dendrimers with Mono-, Di- and Trisubstituted Benzoic Acids”, Chem. Mater., 18: 1206-1212.

[89] Cook, A.G., Baumeister, U., Tschierske, C., (2005). “Supramolecular dendrimers: Unusual mesophases of ionic liquid crystals derived from protonation of DAB dendrimers with facial amphiphilic carboxylic acids”, J. Mater. Chem., 15: 1708–1721.

[90] Martin-Rapun, R., Marcos, M., Omenat, A., Serrano, J.L, de Givenchy, E.T., Guittard, F., (2007). “Liquid crystalline semifluorinated ionic dendrimers”, Liq. Crys., 34: 395-400.

[91] Marcos, M., Alcala, R., Barbera, J., Romero, P., Sanchez, C., Serrano, J.L, (2008). “Photosensitive Ionic Nematic Liquid Crystalline Complexes Based on Dendrimers and Hyperbranched Polymers and a Cyanoazobenzene Carboxylic Acid”, Chem. Mater., 20: 5209–5217.

[92] Hernandez-Ainsa, S., Alcala, R., Barbera, J., Marcos, M., Sanchez, C., Serrano, J.L, (2011). “Ionic azo-codendrimers: Influence of the acids contents in the liquid crystalline properties and the photoinduced optical anisotropy”, European Polymer Journal, 47: 311-318.

[93] Hernandez-Ainsa, S.,Barbera, J., Marcos, M., Romero, P., Serrano, J.L., (2012). "Thermotropic Mesomorphism via SelfAssembly of Cationic Dendritic Polymers with an Anionic Polar Carboxylic Acid", Macromol. Chem. Phys., 213: 270-277.

[94] Hernandez-Ainsa, S., Barbera, J., Marcos, M., Serrano, J.L, (2010). "Effect of the Phobic Segregation between Fluorinated and Perhydrogenated Chains on the Supramolecular Organization in Ionic Aromatic Dendrimers", Chem. Mater., 22: 4762–4768.

[95] Vergara, J., Gimeno, N., Cano, M., Barbera, J., Romero, P., Serrano, J.L, Ros, M.B., (2011). "Mesomorphism from Bent-Core Based Ionic Dendritic Macromolecules", Chem. Mater., 23: 4931–4940.

[96] Nguyen, H.H., Serrano, C.V., Lavedan, P., Goudouneche, D., Mingotaud, A.F., de Viguerie, N.L., Marty, J.D., (2014). "Mesomorphic ionic hyperbranched polymers: effect of structural parameters on liquid-crystalline properties and on the formation of gold nanohybrids", Nanoscale, 6: 3599–3610.

[97] Rueff, J.M., Barbera, J., Marcos, M., Omenat, A., Martin-Rapun, R., Donnio, B., Guillon, D., Serrano, J.L, (2006). "PAMAM- and DAB-Derived Dendromesogens: The Plastic Supermolecules", Chemistry of Materials, 18: 249-254.

[98] Tschierske, C., (1998). "Non-conventional liquid crystals—the importance of micro-segregation for self-organisation", J. Mater. Chem., 8(7): 1485–1508

[99] Nishizawa, A., Takanishi, Y., Yamamoto, J., Yoshizawa, A., (2011). "Competition between micro-segregation and anti-parallel alignment of an amphiphilic rod-like liquid crystal", Liq. Crys., 38, 793-801.

[100] Stebani, U., Lattermann, G., Wittenberg M., Wendorff, J.H., (1997). "Liquid crystalline derivatives of oligoethylene-amines and -amino ethers with amide, ester, urea or urethane functions", J. Mater. Chem., 7(4): 607–614.

[101] Hayes, B.L., (2004). "Recent Advances in MicrowaveAssisted Synthesis", Aldrichimica ACTA, 37(2): 66-76.

[102] Lidstrom, P., Tierney, J., Wathey, B., Westman, J., (2001). "Microwave assisted organic synthesis- a review", Tetrahedron, 57: 9225-9283.

[103] Michael, D., Mingos, P., Baghurst, D.R., (1991). "Applications of Microwave Dielectric Heating Effects to Synthetic Problems in Chemistry", Chem. Soc. Rev., 20: 1-47.

[104] Gabriel, C., Gabriel, S., Grant, E.H., Halstead, B. S. J., Mingos, D.M.P., (1998). "Dielectric parameters relevant to microwave dielectric heating", Chem. Soc. Rev., 27: 213-223.

[105] Erturk, A. S., Tulu, M., Bozdogan, A. E., Parali T, (2014). "Microwave assisted synthesis of Jeffamine cored PAMAM dendrimers", European Polymer Journal, 52: 218-226.

[106] Guillevic, M.A., Danks, M.J., Harries, S.K., Collinson, S.R., Pidwell, A.D., Bruce, D.W. (2000) "Structure-property relationships in ortho-metalated imine complexes of Re(I)", Polyhedron, 19: 249-257.

[107] Worl, R., Koster, H., (1999). "Synthesis of New Liquid Phase Carriers for Use in Large Scale Oligonucleotide Synthesis in Solution", Tetrahedron, 55: 2941-2956.

[108] Sawicki, M., Lecercle, D., Grillon, G., Le Gall , B., Serandour , A.L., Poncy , J.L., Bailly, T., Burgada, R., Lecouvey, M., Challeix, V., Leydier , A., Rostaing, S.P., Ansoborlo , E., Taran F., (2008). "Bisphosphonate sequestering agents. Synthesis and preliminary evaluation for in vitro and in vivo uranium(VI) chelation" , European Journal of Medicinal Chemistry, 43: 2768-2777.

APPENDIX-A

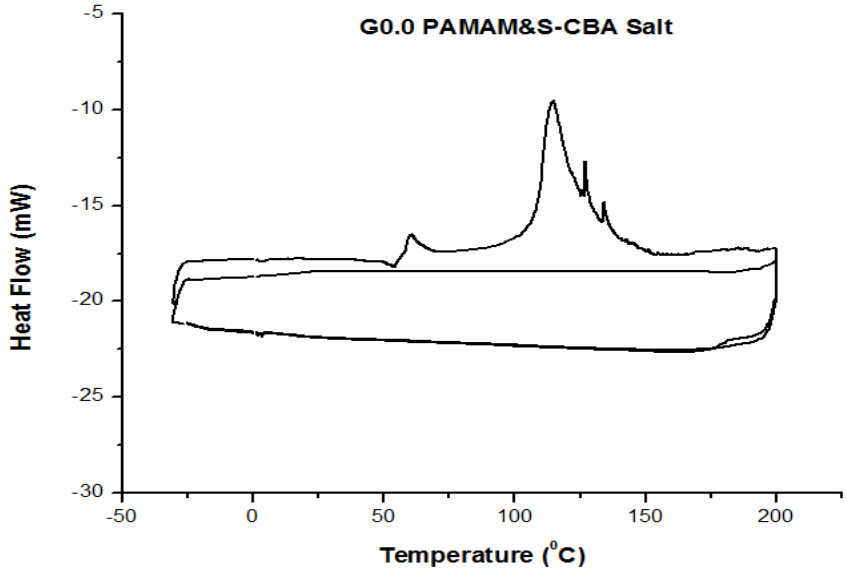
G0.0 PAMAM&S-CBA Salt
Heat Flow (mW)
-5
-10
-15
-20
-25
-30
-50
0
50
100
150
200
Temperature (°C)

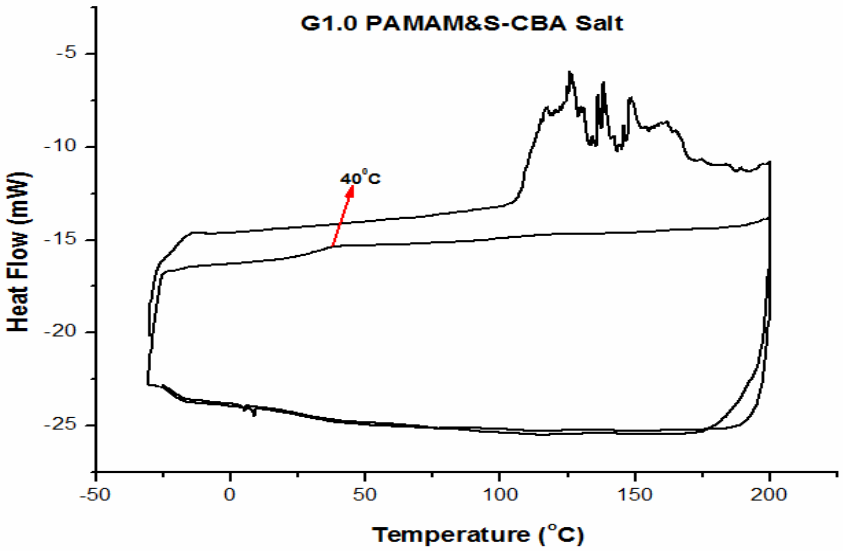
G1.0 PAMAM&S-CBA Salt
Heat Flow (mW)
-5
-10
-15
-20
-25
40°C
-50
0
50
100
150
200
Temperature (°C)

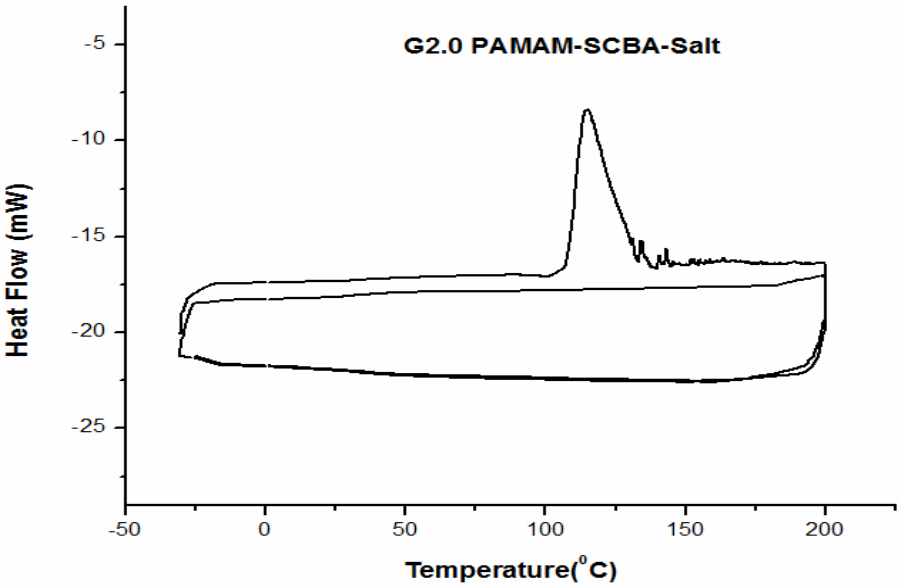
G2.0 PAMAM-SCBA-Salt
Heat Flow (mW)
-5
-10
-15
-20
-25
-50
0
50
100
150
200
Temperature(°C)

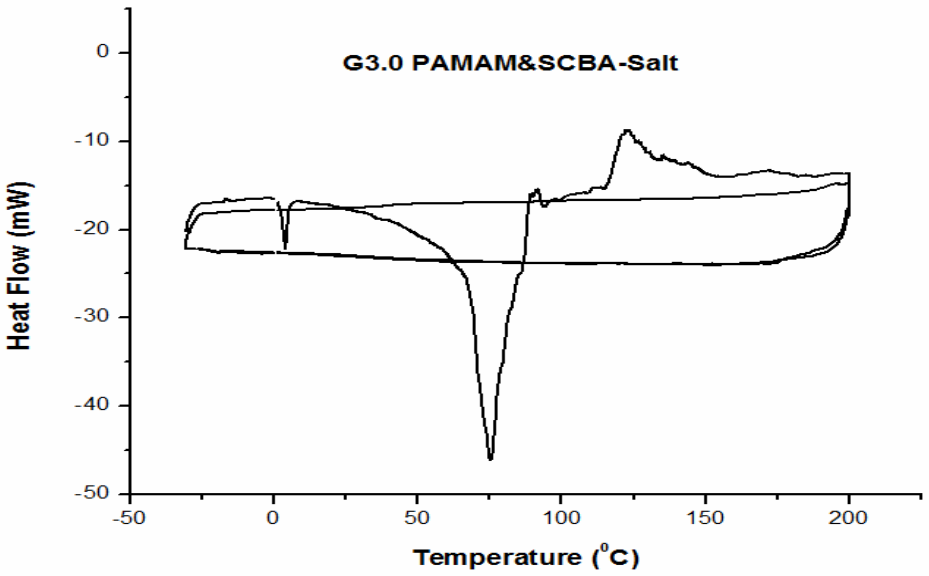
G3.0 PAMAM&SCBA-Salt
Heat Flow (mW)
0
-10
-20
-30
-40
-50
-50
0
50
100
150
200
Temperature (°C)

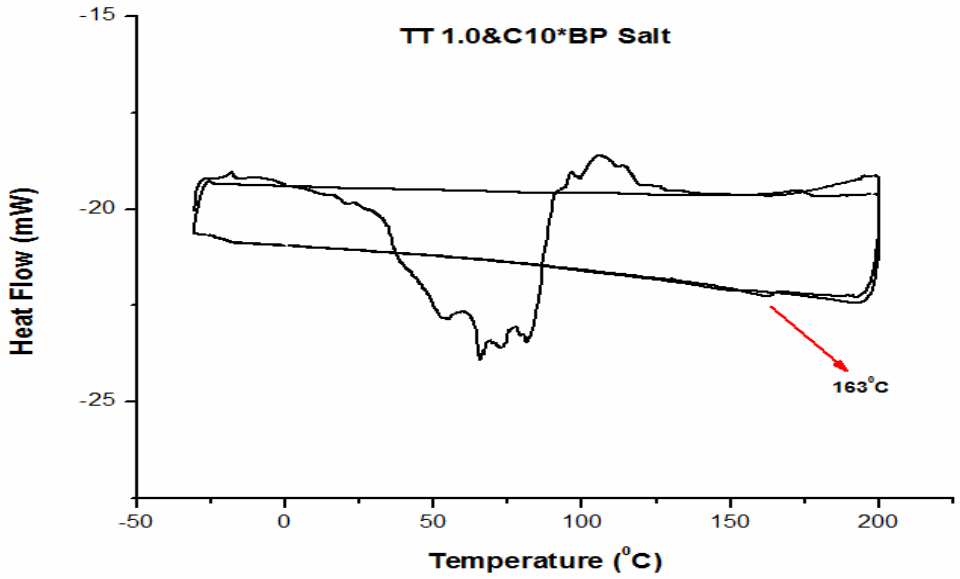
TT 1.0&C10*BP Salt
Heat Flow (mW)
-15
-20
-25
163°C
-50
0
50
100
150
200
Temperature (°C)

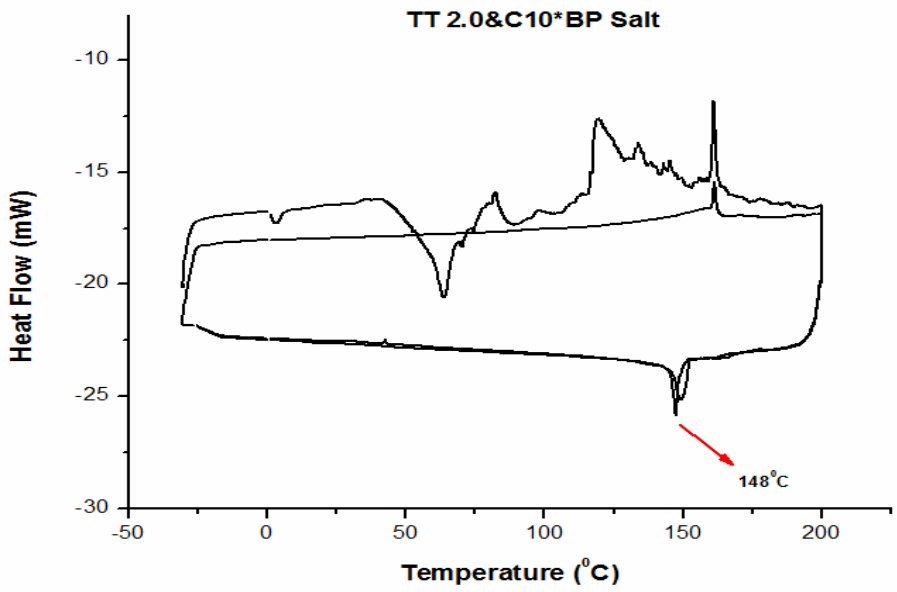
TT 2.0&C10*BP Salt
Heat Flow (mW)
-10
-15
-20
-25
-30
-50
0
50
100
150
200
Temperature (°C)
148°C

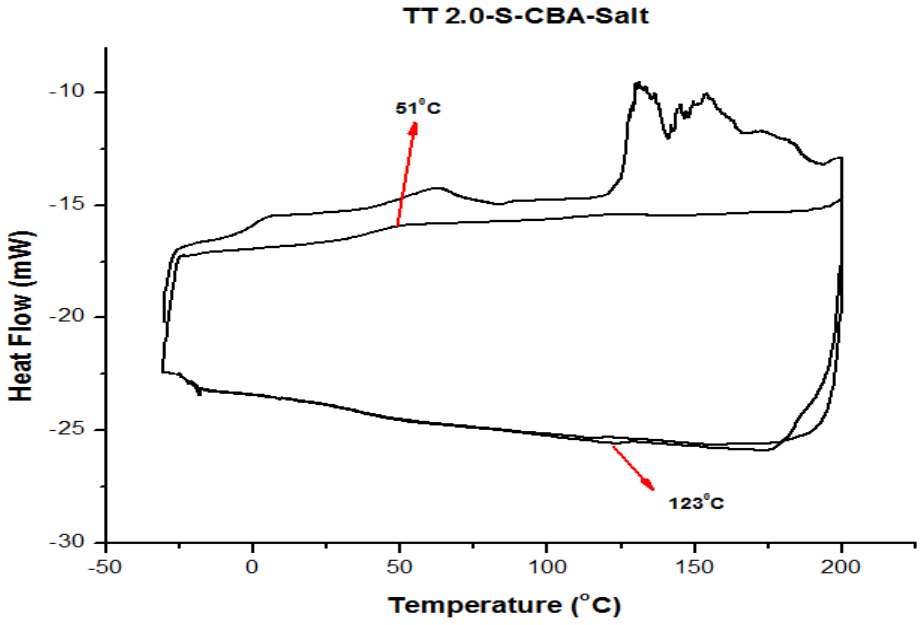
TT 2.0-S-CBA-Salt
Heat Flow (mW)
-10
-15
-20
-25
-30
-50
0
50
100
150
200
Temperature (°C)
51°C
123°C

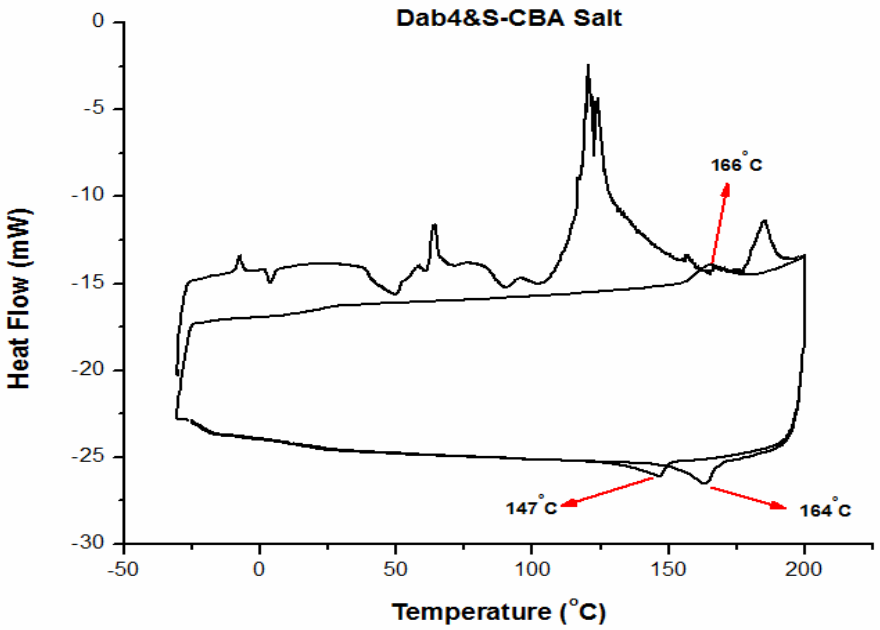
Dab4&S-CBA Salt
Heat Flow (mW)
Temperature (°C)
166°C
147°C
164°C
0
-5
-10
-15
-20
-25
-30
-50
0
50
100
150
200

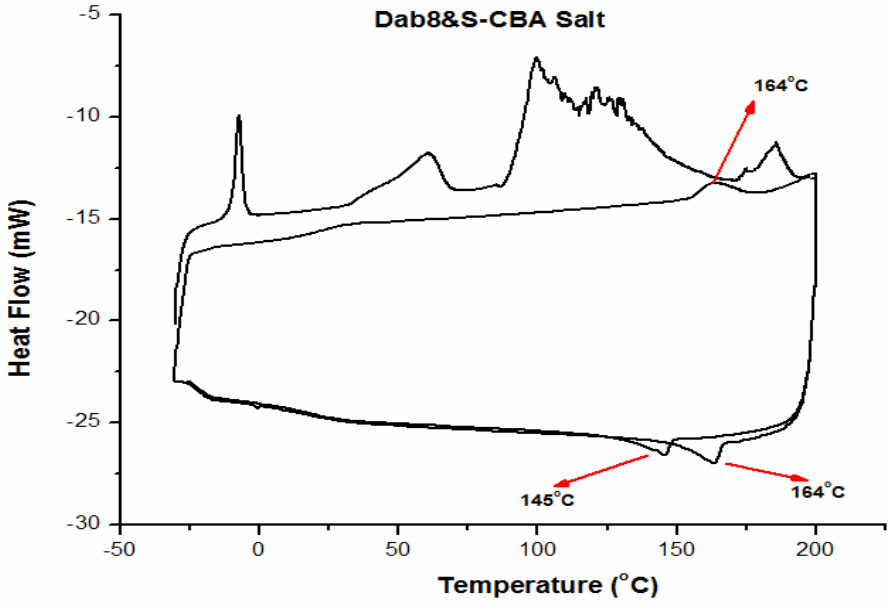
Dab8&S-CBA Salt
Heat Flow (mW)
Temperature (°C)
164°C
145°C
164°C
-5
-10
-15
-20
-25
-30
-50
0
50
100
150
200

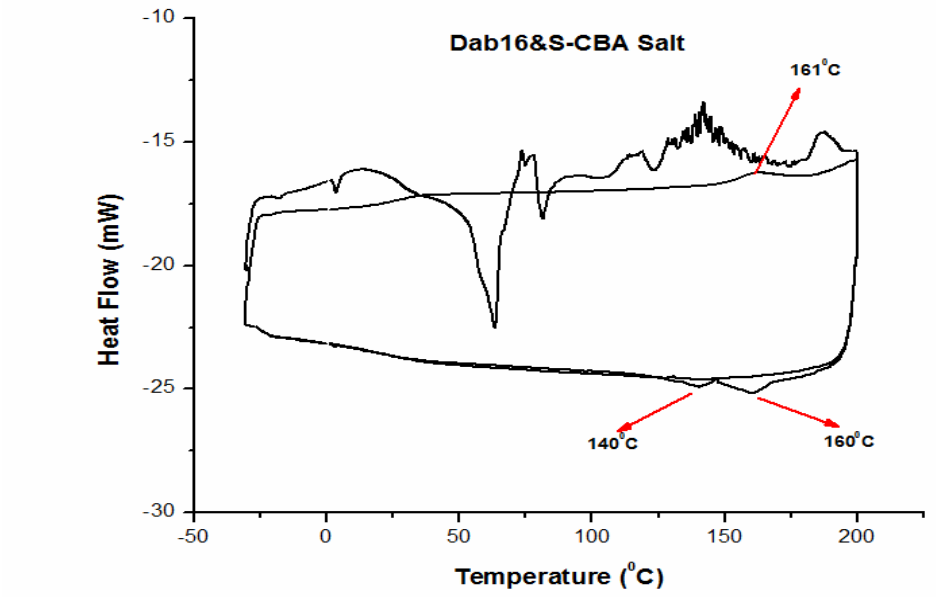
Dab16&S-CBA Salt
161°C
140°C
160°C
Heat Flow (mW)
Temperature (°C)
-10
-15
-20
-25
-30
-50
0
50
100
150
200

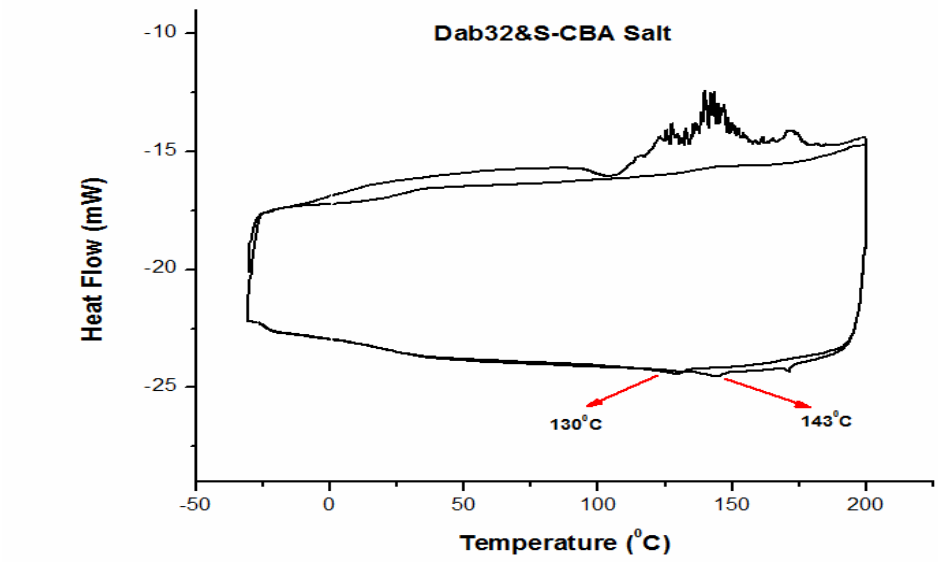
Dab32&S-CBA Salt
130°C
143°C
Heat Flow (mW)
Temperature (°C)
-10
-15
-20
-25
-50
0
50
100
150
200

CURRICULUM VITAE

Personal Info:

Name&Surname: Harun Nezih Türkçü

Date of Birth and Place: 11.11.1980-Korkuteli

E-mail:hnturkcu@gmail.com

Foreign Language: English

Education:

Master: University of Florida -Analytical Chemistry (2005-2008)

Master: Bilkent University - Physical Chemistry (2002-2004)

Undergraduate: Middle East Technical University –Chemistry Department (1997-2002)

Work Experience:

Researcher: Solid Waste Department, Environmental Institute-Marmara Research Center (2012-…)

Researcher: Polyurethane Foam, Akkim Construction Chemicals (2008-2012)

Teaching Assistant: University of Florida (2005-2008)

Teaching Assistant: Bilkent University (2002-2004)

Conference Papers:

1. Harun Nezih Türkçü, Metin Tülü, Hale Ocak, Belkıs Bilgin Eran Poliamidoamine (PAMAM) Dendrimerlere İyonik Sıvı Kristal Özellik Kazandırılması, V. Polimer Bilim ve Teknoloji Kongresi, S12-22, (2014).
2. Harun Nezih Türkçü, Metin Tülü, Hale Ocak, Belkıs Bilgin Eran Polipropilenimine (PPI) Dendrimerlerin Mono-sübstitüte benzoik asit ile iyonik Sıvı Kristal Çalışmaları, V. Polimer Bilim ve Teknoloji Kongresi, P55-117, (2014).